

2024-01-12

# Microwave - Plasma based Thermal Treatment of Asphaltene - derived Carbon Fibres

Chandra, Sharath Krishna

---

Chandra, S. K. (2024). Microwave - plasma based thermal treatment of asphaltene - derived carbon fibres (Master's thesis, University of Calgary, Calgary, Canada). Retrieved from <https://prism.ucalgary.ca>.  
<https://hdl.handle.net/1880/117945>

*Downloaded from PRISM Repository, University of Calgary*

UNIVERSITY OF CALGARY

Microwave - Plasma based Thermal Treatment of Asphaltene - derived Carbon Fibres

by

Sharath Krishna Chandra

A THESIS

SUBMITTED TO THE FACULTY OF GRADUATE STUDIES  
IN PARTIAL FULFILLMENT OF THE REQUIREMENTS FOR THE  
DEGREE OF MASTER OF SCIENCE

GRADUATE PROGRAM IN MECHANICAL ENGINEERING

CALGARY, ALBERTA

JANUARY, 2024

© Sharath Krishna Chandra 2024

## **Abstract**

Asphaltene-based carbon fibres have emerged as a significant and sustainable alternative to conventional Polyacrylonitrile (PAN)-based carbon fibres, owing to their abundant availability, aromatic nature, and high carbon content. This thesis investigates the utilization of asphaltenes, extracted from bitumen in Alberta oilsands, as a valuable precursor for the manufacturing of carbon fibres. The precursor employed in commercial carbon fibre manufacturing accounts for approximately 51% of the total production cost. The utilization of asphaltene as a precursor offers the potential for cost reduction in carbon fibre production. With this reduced cost, carbon fibres, renowned for their exceptional mechanical properties such as high stiffness, remarkable tensile strength, chemical resistance, and capacity to withstand higher temperatures, can find applications across wide range of industries. Moreover, this cost reduction also contributes to the economic viability of converting industrial waste into valuable products. Conventional post-treatment processes in carbon fibre manufacturing, such as furnace stabilization and carbonization, play a crucial role in the production process, demanding considerable time and energy resources. Post-treatment alone, comprising 38% of the overall cost of carbon fibre production, significantly impacts the economic aspects of the manufacturing process.

In this thesis, asphaltenes derived from Alberta oilsands are pretreated with solvents such as pentane and toluene to remove coke residues. Later, these asphaltenes are transformed into fibres through the process of melt spinning using a twin-screw extruder. An innovative approach involving microwave plasma thermal treatment, replacing conventional post-treatment methods, specifically carbonization, is then applied to convert these fibres into carbon fibres. The study of microwave plasma behaviour and its corresponding temperatures is successfully conducted

through the use of Multiphysics Finite Element Analysis (FEA). An experimental optimization study involving the thermal treatment of stabilized fibres under varying power levels and treatment durations using microwave plasma has been conducted. The study successfully implemented microwave plasma techniques to achieve carbonization of asphaltene fibres, resulting in an increase in carbon content and the development of a well-ordered crystalline structure. The Element analysis revealed the dynamic changes in elemental composition, showcasing the effectiveness of microwave plasma in achieving carbonization. X-ray diffraction patterns and Raman spectroscopy provided valuable insights into the structural evolution, highlighting the unique impact of microwave plasma treatment on the development of a layered graphite-like structure and higher graphitic content. However, it is essential to acknowledge limitations, such as the observed surface damage and reduced tensile strength in microwave-plasma treated fibres, emphasizing the need for further optimization of parameters to maximize the benefits of this innovative approach. Overall, this research contributes valuable insights to the field of carbon fibre manufacturing, paving the way for more sustainable and economically feasible production processes with the utilization of asphaltene-based precursors and microwave plasma techniques.

## **Acknowledgements**

I am grateful to my supervisor, Dr. Simon Park, for giving me the opportunity to work on this fascinating project and for providing valuable support and guidance throughout. His wealth of experience has inspired me throughout my studies. I would like to express my gratitude to Dr. Allen Sandwell, Dr. Lin Ge, and Talha Zafar for their unwavering support during my research journey. Additionally, I extend a heartfelt thank you to everyone in the MEDAL group for their generosity and support. I would also like to thank Geetha and my family who have been there for me emotionally as I pursued my studies. I would also like to acknowledge the time and effort given by the examination committee members, Dr. Simon Li and Dr. Josephine Hill.

## Table of Contents

<b>Abstract.....</b>	<b>i</b>
<b>Acknowledgements .....</b>	<b>iii</b>
<b>Table of Contents .....</b>	<b>iv</b>
<b>List of Figures.....</b>	<b>vii</b>
<b>List of Tables .....</b>	<b>x</b>
<b>List of Symbols, Abbreviations, and Nomenclature .....</b>	<b>xi</b>
<b>CHAPTER 1. INTRODUCTION .....</b>	<b>1</b>
1.1 Motivations and Problem Statement .....	5
1.2 Objectives.....	7
1.2.1 <i>Manufacturing of Carbon Fibres</i> .....	8
1.2.2 <i>Comprehensive Modelling of Microwave Plasma</i> .....	9
1.2.3 <i>Microwave Plasma Heat Treatments</i> .....	9
1.3 Organization of Thesis .....	10
<b>CHAPTER 2. LITERATURE REVIEW .....</b>	<b>12</b>
2.1 Precursor materials and processing .....	13
2.1.1 <i>Polyacrylonitrile (PAN)</i> .....	13
2.1.2 <i>Pitch</i> .....	16
2.1.3 <i>Rayon</i> .....	18
2.1.4 <i>Asphaltenes</i> .....	20
2.2 Spinning .....	24
2.3 Post-treatment.....	27
2.3.1 <i>Conventional Stabilization</i> .....	27
2.3.2 <i>Conventional Carbonization</i> .....	30
2.3.3 <i>Conventional Graphitization</i> .....	33

2.3.4 Microwave-based Carbonization .....	35
2.3.5 Microwave Plasma Carbonization .....	41
2.4 Modelling of Microwave Plasma .....	44
2.5 Applications .....	46
2.6 Summary .....	47
<b>CHAPTER 3. MICROWAVE PLASMA MODELLING .....</b>	<b>49</b>
3.1 Geometric description .....	50
3.2 Theory of the model .....	52
3.2.1 Electromagnetic Wave Equations.....	53
3.2.2 Plasma Equations .....	55
3.2.3 Plasma Chemistry.....	57
3.2.4 Modelling Parameters .....	59
3.3 Simulations.....	60
3.4 Validation .....	64
3.5 Summary .....	67
<b>CHAPTER 4. EXPERIMENTS.....</b>	<b>68</b>
4.1 Materials.....	68
4.2 Processing of Asphaltene Fibres .....	69
4.2.1 Pre-treatment.....	69
4.2.2 Melt-spinning.....	71
4.2.3 Conventional Stabilization .....	72
4.3 Microwave Plasma Carbonization .....	73
4.4 Testing Conditions .....	76
4.4.1 Element Analysis and SEM.....	76
4.4.2 Spectroscopic and Crystallographic Properties .....	77

4.4.3 Mechanical Properties .....	78
4.5 Summary .....	79
<b>CHAPTER 5. RESULTS AND DISCUSSIONS .....</b>	<b>80</b>
5.1 Element Analysis.....	80
5.2 Morphological Properties .....	82
5.3 Spectroscopic and Crystallographic Properties .....	86
5.3.1 XRD Analysis.....	86
5.3.2 Raman Spectroscopy .....	89
5.4 Thermal Analysis .....	92
5.5 Mechanical Properties .....	95
5.6 Mechanism of Microwave and Microwave Plasma .....	101
5.7 Summary .....	103
<b>CHAPTER 6. CONCLUSIONS.....</b>	<b>105</b>
6.1 Novel Scientific Contributions.....	106
6.2 Assumptions and Limitations.....	107
6.3 Future Work .....	108
<b>REFERENCES.....</b>	<b>112</b>
<b>APPENDIX A: REPRINT PERMISSIONS .....</b>	<b>120</b>
<b>APPENDIX B: CHARACTERIZATION DATA .....</b>	<b>132</b>



## List of Figures

Figure 1.1: Cost distribution for the production of PAN based carbon fibres [Mainka et al. 2015]	2
Figure 2.1: Processing steps of PAN-based carbon fibres [Bisheh & Abdin 2023]	15
Figure 2.2: Structure of typical pitch precursor [Frank et al. 2014]	17
Figure 2.3: Chemical structure of cellulose polymer chain [Park 2018]	19
Figure 2.4: Asphaltene structure a) Archipelago model [adapted from Tukhvatullina 2013] b) Island structure [Mullins 2010]	21
Figure 2.5: Schematic diagram of asphaltene-based carbon fibre production	22
Figure 2.6: TGA curves of asphaltenes in air and nitrogen atmosphere [Trejo et al. 2010]	24
Figure 2.7: Schematic of melt-spinning process to produce mesophase pitch fibres [Delhaes 2003]	25
Figure 2.8: Different die designs and the effect on resultant fibre structure and properties [Bhat 2016]	26
Figure 2.9: Chemical reactions during the stabilization of PAN based carbon fibres [Frank et al. 2017]	29
Figure 2.10: Schematic of carbon fibre post-treatment [Wyatt et al. 1994]	30
Figure 2.11: Carbonization reaction path of PAN-based carbon fibres [Frank et al. 2017]	32
Figure 2.12: Fundamental reaction path for carbonization of a mesophase pitch precursor [Frank et al. 2014]	33
Figure 2.13: Raman spectra taken from surface of PAN-based carbon fibres graphitized at different temperatures (1800 to 2000°C) [Liu et al. 2008]	34
Figure 2.14: Electric and magnetic field components in microwaves [Kappe et al. 2013]	37
Figure 2.15: Schematic of multi-mode microwave adapted from [Cundy 1998]	39
Figure 2.16: Schematic of single-mode microwave adapted from [Cundy 1998]	40

Figure 2.17: Microwave plasma system for the carbonization process [Kim et al. 2015] .....	43
Figure 2.18: 2D plot of the gas temperature distribution in the computational domain [Baeva et al. 2012] .....	45
Figure 2.19: a) Cutaway view of the microwave plasma torch b) slice plots of the distribution of the electron density ( $m^{-3}$ ) inside the quartz tube [Shen et al. 2020] .....	46
Figure 3.1: Schematic of microwave plasma experimental arrangement .....	50
Figure 3.2: Simplified geometry of the experimental setup for modelling in COMSOL™ Multiphysics .....	51
Figure 3.3: Fine mesh defined within the quartz tube .....	52
Figure 3.4: Contour temperature plots of plasma temperatures in quartz tube at a) 1E-7 seconds b) 1E-6 seconds .....	60
Figure 3.5: Temperature in quartz tube progressing over the time (1000 W, 700 W) .....	61
Figure 3.6: Electric field norm dynamics at a) 1E-7 seconds b) 1E-6 seconds .....	63
Figure 3.7: Electron potential distribution in the quartz tube .....	64
Figure 3.8: a) Arrangement of pyrometer in the setup b) Temperature-plot measurement .....	65
Figure 4.1: Pre-treatment process of Alberta Oilsands Asphaltenes (AOA) .....	70
Figure 4.2: Twin-screw extruder setup with godet system .....	72
Figure 4.3: a) Tube furnace setup for stabilization process b) Sample prepared on ceramic plate for stabilization process .....	73
Figure 4.4: a) Schematic diagram of microwave plasma setup b) Quartz tube setup housed in conventional microwave oven .....	75
Figure 4.5: a) Schematic diagram of fibre prepared for tensile testing .....	79
Figure 5.1: SEM image of furnace stabilized asphaltene fibres .....	83
Figure 5.2: SEM image of conventionally carbonized asphaltene fibres .....	84
Figure 5.3: SEM images of microwave plasma treated asphaltene fibres at 1000 W (a-b) 5 min, (c-d) 7 min, (e-f) 9 min .....	85

Figure 5.4: Comparative XRD analysis of conventionally carbonized fibres and microwave plasma treated fibres at 1000 W at various durations (5 min, 7 min, 9 min).....	87
Figure 5.5: Raman spectra of asphaltene carbon fibres after microwave plasma treatment (1000 W) at various durations (5 min, 7 min, 9 min) .....	90
Figure 5.6: Temperature measurement at different power levels from the Pyrometer: a) 1000 W b) 700 W .....	92
Figure 5.7: Comparison of average tensile strength and elastic modulus in stabilized, conventionally carbonized and microwave plasma treated fibres .....	96
Figure 5.8: Elemental mapping of the Conventional Stabilized Fibres [Liu et al. 2018] .....	99
Figure 5.9: Schematic diagram of PAN fibres stabilized by conventional and microwave heating [Liu et al. 2018] .....	101
Figure 5.10: Schematic diagram of generation of microwave plasma .....	103
Figure 6.1: Schematic diagram of plasma assisted stabilization mechanism [Lee et al. 2013] ..	110

## List of Tables

Table 2.1: Comparison of different carbon fibre precursors, their yields and strengths [Kaur et al. 2016] .....	14
Table 3.1: Primary chemical reactions and collision mechanisms during argon discharge [Shen et al. 2020; Yadav et al. 2021] .....	58
Table 3.2: Variable parameters implemented in the model .....	60
Table 3.3: Comparison of simulation temperature with existing literature .....	66
Table 4.1: Sample-data obtained from Asphaltene sample bank [Alberta Innovates 2018] .....	68
Table 5.1: Comparison of Element analysis of samples .....	81
Table 5.2: The average interplanar spacing (d), the crystalline thickness ( $L_c$ ), and layer plane length ( $L_a$ ) of conventionally carbonized fibres and microwave plasma treated fibres (1000 W) .....	89
Table 5.3: Parameters calculated from obtained Raman peaks of conventionally carbonized and microwave plasma (1000 W) treated .....	91
Table 5.4: Temperature comparison between experiment, simulation, and literature .....	94
Table 5.5: Comparative analysis of mechanical properties of different microwave plasma treated carbon fibres .....	98
Table 5.6: Comparative analysis of mechanical properties of asphaltene-derived carbon fibres using conventional heating techniques .....	100
Table 5.7: Dielectric constants of materials at 20 °C .....	102

## List of Symbols, Abbreviations, and Nomenclature

$\omega$	Angular Wave Frequency	$rad/s$
$\mu$	Dynamic Viscosity	$Pa.s$
$E$	Electric Field Strength	$V/m$
$n_e$	Electron Density	$e/m^3$
$D_e$	Electron Diffusion Coefficient	$m^2/s$
$\nu$	Electron Elastic Collision Frequency	$Hz$
$\mu_\varepsilon$	Electron Energy Density	$V/m^3$
$\Gamma_e$	Electron Energy Flux	$W/m^2$
$n_\varepsilon$	Electron Energy Mobility	
$\Gamma_\varepsilon$	Electron Flux	
$m_e$	Electron Mass	$kg$
$\mu_e$	Electron Mobility	$m^2/(V.s)$
$\sigma$	Electronic Conductivity	$S/m$
$D_\varepsilon$	Energy Diffusivity	$m^2/s$
$Q_{el}$	Energy gain due to elastic collisions between heavy particles and electrons	$eV$
$R_\varepsilon$	Energy gain or loss due to inelastic collisions	$eV$
$e$	Fundamental Charge	<i>Coulomb (C)</i>
$Q_W$	Heat released due to non-elastic collisions	$eV$
$i$	Imaginary number	
$F$	Lorentz force	$N$
$H$	Magnetic Field Strength	$A/m$
$\rho$	Mass Density	$kg/m^3$
$\mu_0$	Permeability of Vacuum	$H/m$
$\varepsilon_0$	Permittivity of Vacuum	$F/m$
$\omega_p$	Plasma Frequency	$Hz$
$P$	Pressure	$Pa$
$R_e$	Rate of change of Electron Density	$s^{-1}$
$\varepsilon_r$	Relative Electric Permittivity of Vacuum	
$C_P$	Specific heat capacity	$J/g.K$
$\sigma_K$	Thermal Conductivity	$W/m.K$

$I$	Unit Tensor	
$u$	Vector Velocity of the fluid	$m/s$
$k_0$	Wave Number	$m^{-1}$
<i>AOA</i>	Alberta Oilsands Asphaltenes	
<i>AC</i>	Alternating Current	
<i>CO<sub>2</sub></i>	Carbon dioxide	
<i>DC</i>	Direct Current	
<i>GHz</i>	Gigahertz	
<i>GHG</i>	Greenhouse Gas Emissions	
<i>PAN</i>	Polyacrylonitrile	
<i>RF</i>	Radio Frequency	
<i>SEM</i>	Scanning Electron Microscope	
<i>TGA</i>	Thermogravimetric Analysis	
<i>2D</i>	Two-dimensional	
<i>XRD</i>	X-ray Diffraction	

## CHAPTER 1. INTRODUCTION

In recent years, the demand for lightweight materials has witnessed a significant surge, mainly driven by the growing need for lightweight components in the automobile and aerospace industries. Addressing this demand, carbon fibres have emerged as one of the premier choices, offering the ideal balance of reduced weight without compromising strength and durability. Carbon fibres are defined as fibres that consist of at least 92% carbon by weight [Chung et al. 2012]. Carbon fibres, which are referred to as a ‘material of the 21<sup>st</sup> century’, have found their place in numerous industries due to their exceptional stiffness, high tensile strength, remarkable chemical resistance, and capacity to endure high temperatures while exhibiting minimal thermal expansion, all while retaining their lightweight properties [Stantec 2018]. These distinctive features make carbon fibres widely applicable in sectors such as aerospace, military, turbine blades, construction, lightweight cylinders and pressure vessels, medical, automobile, and sporting goods.

Carbon fibres are manufactured by the controlled pyrolysis of fibrous carbonaceous materials. The characteristics of carbon fibres are closely related to the selection of the precursor material and the processing methods applied [Edie 1998]. Substantial research efforts have been dedicated to studying various precursor materials, aiming to optimize the production of carbon fibres. Different precursor materials like polyacrylonitrile (PAN), rayon, pitch, polyolefins, and bio-based precursor polymers are employed to manufacture carbon fibres. Among these, the notable precursor materials used were PAN, pitch, and rayon.

At present, PAN is widely regarded as the most suitable precursor for carbon fibre production. PAN-based precursor fibres account for over 90% of the current carbon fibres manufacturing due to their ability to produce high-performance carbon fibres characterized by

exceptional strength, modulus, and toughness [Kaur et al. 2016]. While the global production of carbon fibres has experienced rapid growth, their extensive application is limited by the high production costs and strong demand. The overall challenge revolves around the combination of precursor cost, yield, processing cost, and similar factors [Park 2018].

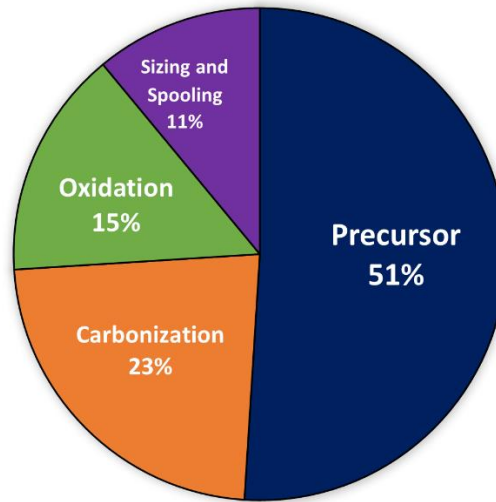


Figure 1.1: Cost distribution for the production of PAN based carbon fibres [Mainka et al. 2015]

Producing carbon fibres of commercial quality from pitch and PAN precursors incurs significant costs, primarily attributed to the expensive raw materials and intricate processing procedures with pitch-based carbon fibres [Dunham & Edie 1989]. The conventional methods of carbon fibre production, predominantly relying on polyacrylonitrile (PAN), pose limitations in terms of energy consumption, cost, and environmental impact. When evaluating the expenses associated with carbon fibre manufacturing, it becomes evident that over 50% of the costs pertain to precursor production, with 38% linked to the post-treatment process, as shown in Figure 1.1 [Mainka et al. 2015]. The transformation of precursors into carbon fibres is extremely energy and cost intensive, causing significant CO<sub>2</sub> emissions. The high cost of carbon fibres makes it unfeasible for widespread application in cost-sensitive markets, such as the building construction



industry [Arnold et al. 2018]. To address these challenges and promote the sustainable production of carbon fibres, researchers and industries are actively investigating alternative carbon sources and innovative manufacturing methods.

In seeking cost-effective and abundant sustainable carbon sources, attention has turned to Alberta Oilsands Asphaltenes (AOA). The northern region of Alberta is renowned for its large reserves of Oilsands. Oil sand can be described as a naturally occurring blend containing sand, clay, or various minerals, along with water and bitumen, a dense and highly viscous form of oil [Alberta Innovates 2018]. The viscosity of Alberta's oil sands bitumen is often associated with its asphaltene and resin content. Its high viscosity, ranging from 105 to 106 mPa.s, hinders flow at typical reservoir conditions. Various solvent deasphalting techniques are employed to reduce the asphaltene content, enabling smoother transportation and processability. For every million barrels of bitumen utilized, approximately 470,000 barrels of heavy fraction bitumen containing asphaltenes are generated [Zhou et al. 2021].

The definition of asphaltene relies more on its solubility characteristics rather than its chemical composition. Asphaltenes refers to the fraction that is insoluble in n-alkanes with low carbon number (n-hexane, n-heptane, or n-pentane) but soluble in light aromatic hydrocarbons like toluene and benzene [Zuo et al. 2019]. The inherent properties of asphaltenes, including their high carbon content, aromaticity, presence of hetero atoms, and polar functional groups, make them valuable candidates for the synthesis and development of functional carbonaceous materials and structures [Zhang et al. 2014]. These asphaltenes can serve as a sustainable precursor for carbon fibres, potentially contributing to significant cost reduction.

Precursors can be processed into filaments through a variety of methods, including melt spinning. Melt spinning includes a three-step process: melting the precursor, extrusion through a

spinneret, and drawing the fibres as they cool [Edie 1998]. These fibres require a series of post-treatment processes to transform into carbon fibres. The precursor fibres undergo an initial phase of stabilization and stretching within the temperature range of 200-400 °C in an oxidizing environment, a process significantly influenced by the inherent chemistry of the precursor material. Later, during the carbonization process, the stabilized fibres are subjected to elevated temperatures ranging from 800 °C to 1600 °C in an inert atmosphere. This thermal treatment eliminates non-carbon impurities, including hydrogen, oxygen, nitrogen, and other noncarbon elements [Park 2018].

As stated in a study by Mainka et al., Conventional post-treatment procedures, including both stabilization and carbonization, constitute 38% of the total cost and demand substantial energy consumption. This problem can be mitigated through the utilization of one of the most effective electromagnetic methods, Microwave plasma. Plasma is a distinctive state of matter, often referred to as the fourth state, characterized by the ionization of its constituent atoms and molecules, resulting in a mixture of positively and negatively charged particles. The generation of plasmas can vary depending on the voltage source employed to excite the carrier gas. This gas can be air, oxygen, nitrogen, or an inert gas like argon, depending on the specific conditions required [Breeze 2018]. To initiate plasma formation, voltage sources, including Alternating Current (AC), Direct Current (DC), Radio Frequency (RF), or microwave can be utilized [Wu 2004]. In this study, microwave energy has been employed as the power source to excite the carrier gas, leading to the generation of plasma, which is used for the thermal treatment of asphaltene-based carbon fibres. This technique combines the advantages of microwave energy and plasma fields to rapidly heat and transform asphaltene precursors into carbon fibres.

## 1.1 Motivations and Problem Statement

The utilization of carbon fibres in various industries has witnessed remarkable growth over recent decades. These lightweight, high-strength materials have revolutionized sectors such as aerospace, automotive, renewable energy, construction, and sporting goods [Bisheh & Abdin 2023]. Their exceptional mechanical properties, coupled with a low-density profile, make them an invaluable resource for creating sustainable, efficient, and advanced engineering solutions. However, the utilization of carbon fibres across diverse industries has been constrained primarily because of their increased cost. The ability to overcome these cost-related challenges is paramount to fully unlocking the potential of carbon fibres. The cost of carbon fibres is highly influenced by the choice of precursor material. Thus, a cost-effective precursor is required to reduce approximately 51% of the overall carbon fibre cost associated with the PAN precursor.

The post-treatment phase, encompassing both stabilization and carbonization, demands a substantial amount of energy [Park 2018]. According to findings in the study by Mainka et al., the post-treatment phase alone constitutes 38% of the overall cost incurred in carbon fibre production. Besides these considerations, the amount of GHG emissions associated with carbon fibre manufacturing presents a concern demanding our attention and resolution. To manufacture carbon fibres from PAN, the predominant raw material in carbon fibre production, the associated environmental footprint is estimated to be approximately 24 kg-CO<sub>2</sub> equivalent per one kilogram of carbon fibre manufactured [Kawajiri & Sakamoto 2021]. Studies conducted by [Das 2011] reveal that a substantial share of GHG emissions originates from the PAN precursor and post-treatment stages in the carbon fibre production process. This metric highlights the significance of exploring environmentally friendly alternatives in carbon fibre production. Amidst global concerns regarding climate change and the need to mitigate GHG emissions, governments and

companies worldwide are actively seeking environmentally sustainable solutions. In the carbon fibre manufacturing industry, the reduction of GHG emissions emerges as a critical challenge that needs to be addressed immediately.

Asphaltenes possesses notable attributes such as high carbon content, carbon yield, and substantial aromaticity [Zuo et al. 2019], rendering it as a promising and sustainable precursor for carbon fibre production. Examining the cost structure of carbon fibre manufacturing, a study by Mainka et al. (2015) highlights that, historically, over 50% of the total costs are attributed to the production of the precursor material PAN. The oxidation process accounts for approximately 15%, and the subsequent carbonization process represents around 23% of the total costs. In line with this, it is observed that from the remaining 49% of the manufacturing costs, approximately 38% is associated with the stabilization and carbonization processes. Conventional post-treatment methods, often conducted in furnaces, necessitate temperatures exceeding 1000 °C, resulting in significant time, energy, and financial expenditures that ultimately hinder the efficiency of carbon fibre manufacturing [Galos 2020].

In this thesis, Alberta Oilsands Asphaltenes (AOA) is utilized as a precursor for carbon fibre manufacturing. A twin-screw extruder, designed with a spinneret, heat chamber, and godet, is employed to apply the melt spinning technique for fibre production. Microwave plasma carbonization has been adopted to convert stabilized fibres into carbonized fibres. The chemical structures are analyzed using techniques such as X-ray Diffraction (XRD), Raman spectroscopy, and elemental analysis (CHNS). Furthermore, the morphological and mechanical properties have been investigated through Scanning Electron Microscopy (SEM) and Tensile testing, respectively. These fibres properties are compared to those of the conventionally manufactured asphaltene-carbon fibres, which were processed using traditional tube furnaces.

This thesis addresses the manufacturing of carbon fibres, proposing an innovative and sustainable approach by leveraging asphaltene-derived materials. The study initiates with the pretreatment of asphaltenes, efficiently removing coke residues using solvents like pentane and toluene. An experimental study, involving varied power levels and treatment durations, demonstrates the efficacy of microwave plasma treatments in carbonizing asphaltene-based fibres. The comprehensive suite of analyses conducted in this study serves as a fundamental pillar in unraveling the intricate dynamics of asphaltene-derived carbon fibres subjected to innovative manufacturing processes. Collectively, these analyses aim to achieve a nuanced understanding, working towards the overarching goal of studying effect of process parameters.

## **1.2 Objectives**

This work addresses the challenges associated with the transforming of carbon-rich abundant AOA, with the goal of transforming these carbon-rich waste materials into high-value carbon fibres. Utilizing microwave plasma technology, the study aims to understand the influence of different treatment durations and power levels on the resulting material properties. Additionally, the research seeks to develop a comprehensive model and simulation for microwave plasma temperatures, providing insights into the transformation process. Through systematic experimentation and analysis, the study aims to contribute valuable insights into the manufacturing processes for asphaltene-derived carbon fibres. To accomplish this, the following objectives have been defined:

### *1.2.1 Manufacturing of Carbon Fibres*

The first objective is to develop a processing method for carbon fibres using asphaltene-based precursors extracted from Alberta oilsands. The asphaltene sample contains various impurities, including resins and light hydrocarbons. To purify the sample, a Soxhlet extraction setup using n-pentane has been used to remove light hydrocarbons, followed by a toluene treatment to eliminate coke residues. This pretreatment process significantly enhances spinnability and processability. After undergoing the pretreatment process, the asphaltenes will be further processed through melt spinning. This operation will take place in a twin-screw extruder at temperatures ranging from 220-250 °C. The extruded material will then be drawn through a spinneret to create continuous filaments, commonly referred to as spun fibres.

The spun fibres will be heated to 350 °C within a controlled oxidizing atmosphere, carefully chosen to avoid combustion. This temperature is below the fibre softening point, aligning with established practices for oxidative stabilization. The controlled oxidation process, conducted at temperatures between 250–350 °C, introduces functional groups and enhances hydrogen bonding, which is crucial for three-dimensional cross-linking without hindering crystallite growth [Park 2018]. This process converts them from a thermoplastic to a thermoset, creating a thermally stable structure. This oxidative stabilization process is commonly carried out in a tube furnace, where the molecular bonds within the fibres undergo a restructuring, resulting in an enhancement of their overall strength. These stabilized fibres are evaluated for their properties and undergo further processing steps involved in carbon fibre manufacturing.

### *1.2.2. Comprehensive Modelling of Microwave Plasma*

The carbonization process requires higher temperatures to remove non-carbon elements and convert precursor materials into carbonaceous materials. In this study, microwave plasma is used for thermal treatment of the fibres. To investigate the behaviour of microwave plasma in the system, a comprehensive modelling approach using COMSOL™ Multiphysics software is employed. This model will be based on principles of electromagnetic wave propagation and plasma physics, considering the factors such as microwave power, chamber geometry, and pressure in the system.

The purpose of this simulation study is to analyze the temperature distribution within the system, propagation of electric fields, and the impact of microwave power on plasma temperature. These investigations will be conducted to examine how process parameters affect microwave plasma behaviour in order to optimize conditions for achieving uniform and controlled carbonization of asphaltene fibres. The goal is to bridge the gap between theoretical understanding and practical application in carbon fibre manufacturing using microwave plasma. The simulated temperature results from this model will be compared with experimental data and existing literature to validate its accuracy and effectiveness.

### *1.2.3 Microwave Plasma Heat Treatments*

The furnace-stabilized fibres will undergo microwave plasma treatments in a custom-designed quartz tube setup housed within a conventional microwave, with argon gas flowing at atmospheric pressure. The focus of the experiments will be on determining the most effective process parameters for carbonization, such as power, gas flow rate, pressure, and treatment duration.

The resultant carbon fibres will undergo a comprehensive characterization providing valuable insights into their providing morphological properties, crystallographic structure, and chemical composition. The experimental temperatures will be compared with numerical simulations to validate the developed model and further optimize processing conditions with the goal of effectively carbonizing the asphaltene fibres. A comparison between microwave plasma treated fibres and conventionally carbonized fibres will be conducted to evaluate their respective properties.

### **1.3 Organization of Thesis**

This thesis is organized into six chapters. Chapter Two provides a comprehensive discussion of commonly utilized precursors and methodologies for carbon fibre manufacturing. This chapter includes various manufacturing processes, such as spinning techniques, stabilization, carbonization, and graphitization, offering a comprehensive exploration of each. Additionally, different approaches for post-treatment, including a review of microwave plasma techniques and previous attempts at modeling the microwave-plasma process have been explored. Chapter Three presents the results of the simulation of microwave plasma using COMSOL™ Multiphysics, carried out in this work. This simulation work yields insights into temperature distribution and plasma behaviour. In Chapter Four, a comprehensive description of the experimental setup has been presented, which includes a twin-screw extruder employed in fibre production and a custom-designed quartz tube housed within a conventional microwave oven equipped with a pyrometer for temperature measurement. Chapter Five presents the characterization results of the microwave plasma carbonization process. This section includes the analysis of chemical, morphological, spectroscopic, crystallographic and mechanical properties, with comparative evaluations against



conventional manufacturing processes. Chapter Six concludes the thesis by providing an overview of the novel scientific contributions, assumptions, limitations and indicating directions for future work.

## **CHAPTER 2. LITERATURE REVIEW**

The exploration of alternative precursors and advancements in stabilization and carbonization techniques have gained the attention of numerous researchers in the field of carbon fibre manufacturing. While mesophase pitch ranks as the second most widely used precursor, there is a growing interest in utilizing petroleum residues and coal tar to expand the range of carbon fibre precursors [Chung 2014].

Recent research has increasingly emphasized the utilization of naturally abundant carbonaceous materials, with a notable focus on asphaltenes. Despite their abundant presence in Alberta's oilsands, asphaltene research remains relatively limited. Traditionally, oxidative stabilization and carbonization in the carbon fibre manufacturing process have been accomplished through thermal treatment in furnaces, a method known as conventional heat treatment. However, alternative techniques are emerging in this field. One such innovation is microwave plasma, which gained recognition for its capacity to subject samples to high temperatures, shorten treatment durations, reduce energy consumption, and lower costs. The novelty of these processes presents challenges, which demand experimentation with various process parameters and modelling to understand the potential and limitations of these innovative approaches.

## 2.1 Precursor materials and processing

Carbon fibres are materials known for their superior strength and stiffness, made primarily of carbon atoms. These fibres are produced through a multi-step process involving the heating and chemical treatment of synthetic polymer fibres, resulting in the removal of non-carbon elements and the formation of a highly ordered carbon structure. Carbon fibres were first used commercially for incandescent lamp filaments made from carbonized cotton and bamboo fibres. In 1879, Thomas Alva Edison experimented with carbon fibre filaments for his incandescent light bulb, which glowed when heated by electricity. This marks the earliest known commercial use of carbon fibres. Pitch-based and PAN-based carbon fibres were subsequently produced starting in 1963 and 1971, respectively [Park 2018].

At present, numerous companies supply carbon fibre products in commercial markets, with annual production exceeding 10,000 tons. The predominant source for these carbon fibres is Polyacrylonitrile (PAN), accounting for more than 90% of the total production, while the remaining fraction is crafted from pitch-based precursors. [Choi et al. 2019]. This section covers the production process of carbon fibres using PAN, rayon, and pitch as precursor materials. In addition, a discussion of the potential use of asphaltenes in carbon fibre production has been explored.

### 2.1.1 Polyacrylonitrile (PAN)

Polyacrylonitrile (PAN) stands out as the optimal precursor for carbon fibres due to their unique blend of tensile and compressive properties, coupled with impressive carbon yield. This preference of PAN-based fibres traces its origins back to the 1940s when DuPont initially developed them for textile applications. The thermal stability exhibited by PAN-based fibres

played a crucial role in broadening their utility, spurring further exploration into heat treatment processes. In the early 1960s, a significant breakthrough occurred when Shindo, working at the Government Industrial Research Institute in Osaka, Japan, achieved the carbonization and graphitization of PAN-based fibres. The tensile strength of the PAN-based carbon fibres is in the range of 4.0 – 6.6 GPa depending on maximum carbonization temperature [Park 2018].

Table 2.1. Comparison of different carbon fibre precursors, their yields and strengths [Kaur et al. 2016]

<b>Precursors</b>	<b>Average tensile strength (GPa)</b>	<b>Yield (%)</b>
Polyacrylonitrile (PAN)	6.6	>50
Rayon	0.4	10
Pitch, mesophase pitch	0.6,3.5	60-80

Despite its high cost, PAN serves as the precursor polymer of choice for 90% of global carbon fibre production. The preference is attributed to the superior properties it imparts to carbon fibres, as shown in Table 2.1, making it the preferred option over alternative precursor polymers like rayon and pitch. These characteristics are inherent to PAN, owing to its molecular structure that incorporates highly polar nitrile groups. These groups result in durable interactions, preserving the orientation of polymer chains at high temperatures [Kaur et al. 2016]. Nowadays, commercial carbon fibres derived from PAN are widely utilized in the aerospace industry due to their exceptional mechanical properties.

While PAN-based fibres can be generated through wet or dry spinning processes, the vast majority of precursor fibres employed in commercial PAN based carbon fibre production relies on wet spinning techniques. The fundamental steps involved in processing PAN-based precursor fibres are illustrated in Figure 2.1. The production of PAN-based carbon fibres typically begins with precursor synthesis, which involves a polymerization process followed by fibre spinning. The selection of the comonomer and its quantity, as well as the polymerization method, are carefully determined based on the intended application of the resulting carbon fibres [Park 2018]. After the polymerization process, the resulting polymer is then subjected to spinning to create the desired fibrous shape. Due to the tendency of PAN to undergo thermally induced cyclization reaction before melting the solution spinning method is employed instead of melt spinning [Chung 2014].

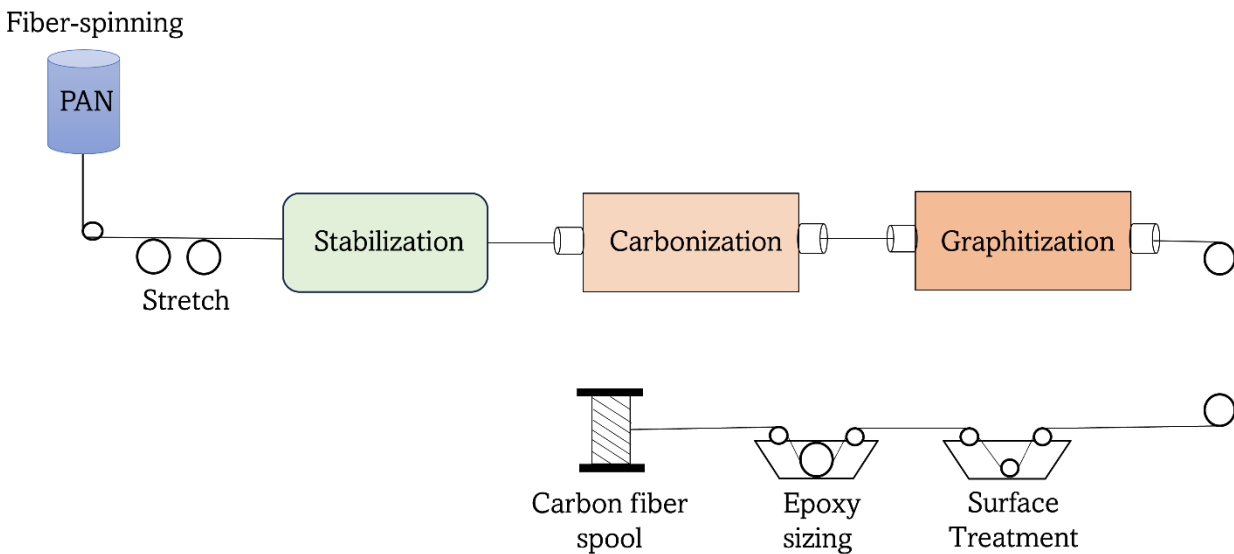


Figure 2.1: Processing steps of PAN-based carbon fibres [Bisheh & Abdin 2023]

Following the fibre spinning process, the fibres are then stabilized through a heat treatment process typically performed in air at temperatures between 200 and 300 °C. Often, the fibres are

subjected to stretching to apply tension during this step. The stabilization process involves three concurrent reactions: cyclization, incorporation of O-containing groups, and dehydrogenation. These reactions work together to convert thermoplastic PAN precursor material into a thermoset compound [Chung 2014]. After stabilization, the fibres are carbonized through exposure to high temperatures of 1000 to 1500 °C in an inert atmosphere. This process converts the stabilization fibres into carbon fibres. Additionally, a further heat treatment process called ‘graphitization’ can be carried out to produce high-modulus carbon fibres. Surface treatment in carbon fibre manufacturing involves chemical modifications to enhance adhesion. Epoxy sizing, a resin coating, is then applied for protection and improved bonding. Both processes contribute to the fibre’s performance in composite materials [Bisheh & Abdin 2023].

### *2.1.2. Pitch*

Another widely adopted precursor in carbon fibre manufacturing following PAN is pitch. Pitch-based carbon fibres dominate the remaining 10% share of the carbon fibre market. Similar to PAN-based carbon fibres, the distinctive properties of pitch-based fibres are the direct result from both the precursor material and the specific fibre conversion process [Edie 1998]. In the case of pitch-based fibres, the precursor is mesophase pitch, characterized by its composition of substantial polynuclear aromatic hydrocarbons in a liquid crystalline form [Delhaes 2003]. A pitch is typically distinguished by its softening point. Irrespective of the source, pitch comprises a diverse array of molecular species with different molecular weights.

Pitch predominantly originates from coal tar and residues of petroleum distillation processes, although it can also be manufactured using diverse sources, including naphthalene, anthracene, and shale tars. The term “pitch” carries a versatile definition, often referring to a tar-

like substance obtained from a wide range of natural (petroleum fraction, coal hydration, asphalt) and synthetic precursor materials (pyrolysis of polyaromatic compounds and polymers) [Frank et al. 2014]. Pitch is characterized as a substance of relatively low molecular weight, displaying heterogeneity in its composition.

A typical pitch precursor molecule, as shown in Figure 2.2 tends to have molecular weights approximately in the range of 1000 g/mol. Pitch comprises numerous distinct species, primarily polyaromatic in nature, often featuring methyl side groups. In most cases, high aromaticity levels correlate with high quality carbon fibres [Riggs et al. 1982]. Manufacturing carbon fibres from pitch precursors involves a series of steps, similar to the process followed with PAN-based materials.

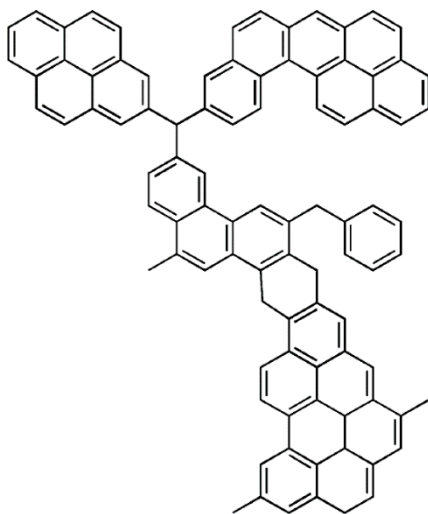


Figure 2.2: Structure of typical mesophase pitch precursor [Frank et al. 2014]

Union Carbide pioneered the production of initial commercial mesophase precursors through a thermal polymerization method. The original process yielded a combination of both isotropic and mesophase pitch, as documented in patents [Singer 1981]. These early patents

asserted that minor quantities of isotropic pitch were essential to lower the viscosity of the polymerized mesophase, consequently reducing the required spinning temperature. Mesophase pitch possesses a softening point and flow behaviour considerably below their degradation temperature. This distinctive property enables them to undergo the melt spinning process, transforming them into fibre form with ease by using melt-spinning technique [Edie 1998].

After the fibre-spinning process, the precursor fibres are subjected to heat-treatment. The primary objective of oxidative stabilization is to create crosslinks within the spun fibres, involving a process that combines both diffusion and chemical reactions. Unlike PAN, mesophase precursor fibres already possess a highly oriented structure after the spinning process. Therefore, there is no need to apply tension during stabilization. Typically, the mesophase fibres can achieve stabilization by exposure to air within a temperature range of 230 to 280 °C. After stabilization, the pitch fibre undergoes carbonization within a temperature range of 1500 to 3000 °C, conducted in an inert atmosphere [Delhaes 2003]. During this stage, the majority of non-carbon elements present in the fibre are vaporized in the form of various gases. Mesophase precursor results in a notably higher yield pitch-based carbon fibre process, ranging from 70 to 80% [Park 2018]. This yield is substantially higher compared to the PAN-based process.

### *2.1.3 Rayon*

In 1959, the National Carbon Company (a division of Union Carbide) began producing carbon cloth made from rayon precursor, followed by carbon yarn in 1961, and finally carbon fibres in 1965 [Riggs et al. 1982]. Rayon fibres, which are manufactured textile fibres and filaments composed of regenerated cellulose, have various types and grades available on the market, with the majority used for textile applications. However, in 1978, the production of carbon



fibres from rayon precursors was stopped by most manufacturers and replaced with PAN and pitch-based carbon fibres due to the superior properties offered by PAN precursors. Besides, a few manufacturers have continued to cater to the niche market for carbon fibres from cellulosic precursors. Rayon-based carbon fibres find common applications as ablative shields and high-temperature packing materials [Riggs et al. 1982].

Rayon undergoes a series of intricate chemical and physical processes to transform into a suitable fibre form. These processes play a crucial role in converting the rayon precursor material into fibres with the desired properties and characteristics. Regarding chemical and mechanical properties, the stabilization of the precursor fibres is important to produce stable carbon fibres through the subsequent carbonization process. Cellulose is a glucose-based linear polymer connected by  $\beta$ -(1-4) glycosidic linkages, as shown in Figure 2.3. These hydroxyl groups readily engage in both intra- and intermolecular hydrogen bonding within the cellulose framework, resulting in a variety of well-ordered crystalline configurations [Donnet & Bansal 1998]. The molecular stoichiometry implies a theoretical carbon yield of 44.4% during the carbonization process of cellulose. However, the actual carbon yield falls significantly in practice, ranging from 10% to 30%. This difference arises from the depolymerization of the macromolecular chains and the removal of carbon through various reactions [Park 2018].

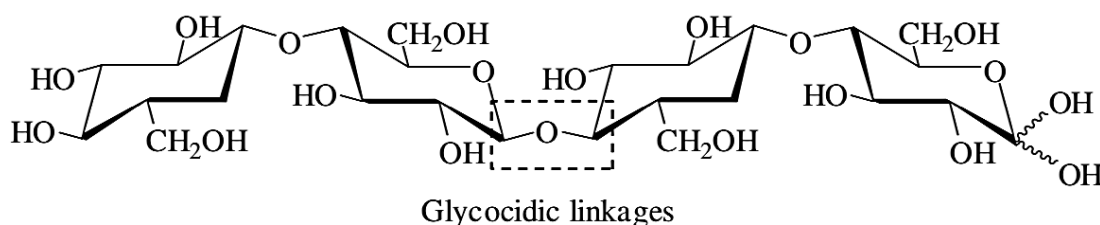


Figure 2.3: Chemical structure of cellulose polymer chain [Park 2018]

Figure 2.3 shows the chemical structure of the cellulose polymer chain where cellulose is a glucose-based, linear polymer connected by  $\beta$ -(1-4) glycosidic linkages. The pyrolysis of cellulose primarily revolves around two key reactions, dehydration and depolymerization. During the dehydration process at 300 °C, the removal of dihydroxyl groups results in the formation of conjugated double bonds. Eventually, the dehydrated cellulose structure takes on a more aromatic form. This phase is crucial for preserving the structural integrity of cellulose and preparing it for subsequent carbonization steps [Park 2018].

Carbonization of the uniformly heat-treated rayon can be carried out under inert atmosphere in the temperatures usually ranging from 1000 to 1500 °C in a significantly brief time, typically less than 1 min. Investigators have also used various reactive atmospheres to carbonize the rayon fibre like hydrochloric acid, ammonia and alkylamines [Donnet & Bansal 1998]. The use of tension during the carbonization of heat-treated rayon increases the degree of preferred orientation and hence an improvement in fibre mechanical properties [Edie 1998].

#### *2.1.4 Asphaltenes:*

Asphaltenes, a complex aromatic mixture, are commonly found in crude oil and the residues from petroleum and coal processing. The term “asphaltene” was initially coined in 1837 to describe the distillation residue of bitumen. Fundamental knowledge of asphaltene is gradually enriched due to the development of separation and identification techniques. However, challenges persist in accurately determining their molecular structure, constituents, and the relationships between structure and behaviour [Zuo et al. 2019]. Asphaltenes are defined as the fraction of bitumen that is insoluble in n-alkanes with low carbon number (n-hexane, n-heptane or n-pentane) but soluble in light aromatic hydrocarbons (toluene and benzene). However, suggestions have been

made that the presence of cyclic terpenoids, pigments, alkanolic-derived hydrocarbons and heterocycles help to define asphaltenes [Strausz & Lown 2003].

To comprehend the origin and processing of petroleum asphaltenes, a thorough understanding of their molecular structure is essential. Two primary structural patterns have been proposed for asphaltene molecules: the "archipelago" model, consisting of alkyl-bridged aromatic and cycloalkyl groups, and the "Island" model, which are alkylated condensed polycyclic aromatics, as shown in the Figure 2.9.

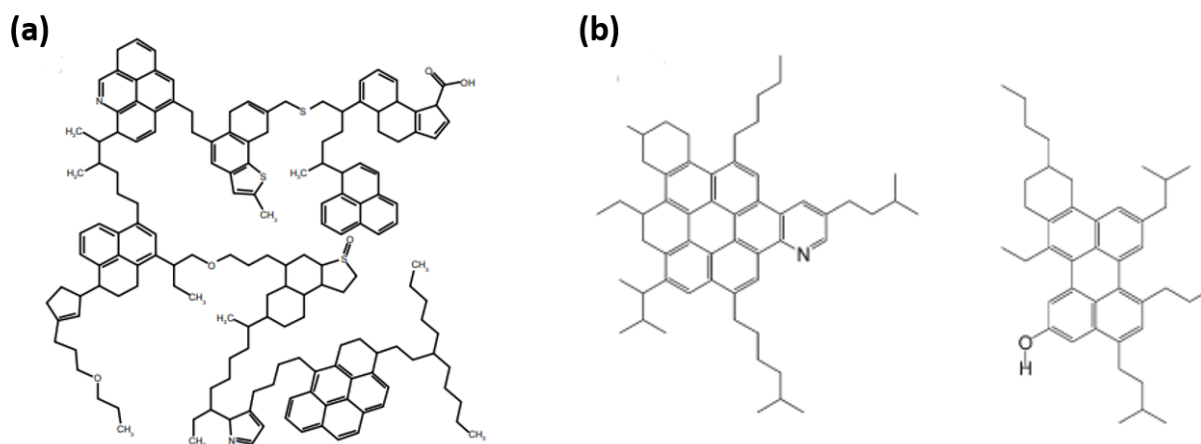


Figure 2.4: a) Asphaltene structure - archipelago model [adapted from Tukhvatullina 2013] b) Island structure [Mullins 2010]

Asphaltenes possess the potential to serve as an excellent precursor for carbon fibre production due to their favorable H to C ratios (ranging from 1:1 to 1.2:1), high carbon content, complex molecular structure composed of polycyclic aromatic hydrocarbons (PAHs) with alkyl side chains and heteroatoms, cost-effectiveness, and widespread availability [Bohnert et al. 2012].

Asphaltenes are abundant in the northern region of Alberta, primarily in the oil sands. They are separated from bitumen and heavy oils to reduce viscosity which will facilitate their smooth

transportation. In addition, the use of asphaltenes as a precursor for carbon fibre production can help address the environmental concerns associated with the disposal of asphaltene as a waste. Consequently, the utilization of asphaltene precursors in carbon fibre production could pave the way for the manufacturing of high-performance, cost-efficient carbon fibres, thereby expanding the application of carbon fibre-based components [Zuo et al. 2021].

The manufacturing of carbon fibres from asphaltenes follows a processing path similar to that of other precursor materials, as shown in Figure 2.5. The process of converting asphaltenes into carbon fibres includes several key steps. Initially, melt-spinning is employed to transform the asphaltenes into a fibrous form. Later, the precursor fibres undergo oxidative stabilization to turn them into thermo-set, preparing them for the final carbonization step. In this step, the fibres are exposed to high temperatures within an inert atmosphere. Prior to the melt-spinning process, asphaltenes require pre-treatment to improve their softening temperature, thus enhancing the melt spinning procedure. One effective method for achieving this is through solvent deasphalting.

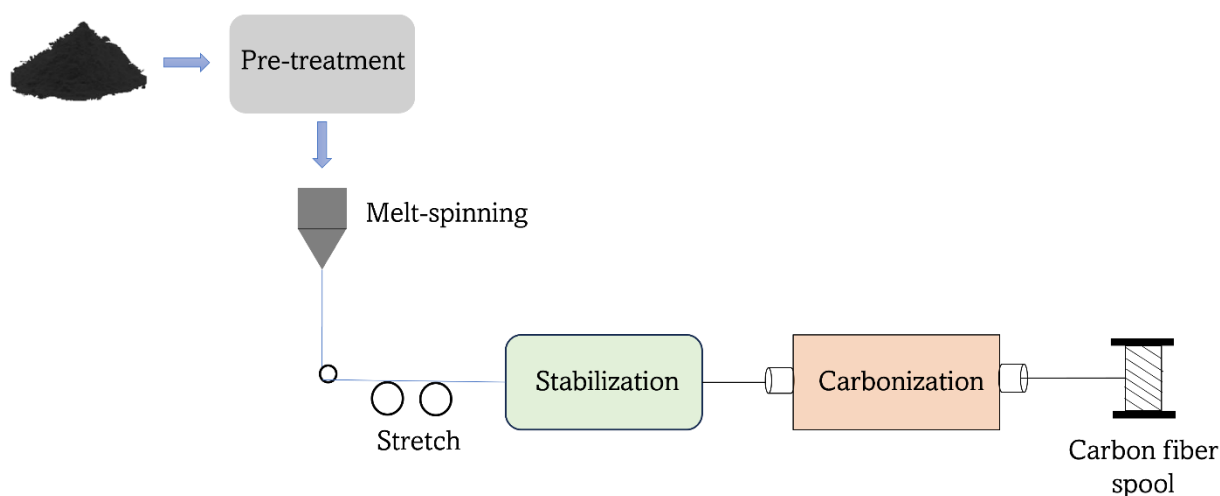


Figure 2.5: Schematic diagram of asphaltene-based carbon fibre production

Asphaltene pre-treatment is a critical step in preparing asphaltene for its role in the carbon fibre production process. This process involves a series of controlled steps to ensure the asphaltene is in a suitable state for subsequent melt spinning [Leistenschneider et al. 2021]. Thermal pretreatment has been utilized following solvent de-asphalting as a method to improve the mechanical properties of carbon fibres derived from asphaltenes [Zuo et al. 2021].

The melt spinning technique is the preferred method for precursors with a softening point below 400 °C, primarily due to its simplicity, cost-effectiveness, and the absence of solvent usage [Kim et al. 2015]. This process involves melting the precursor, followed by extrusion to form fibres. Subsequently, these fibres undergo a series of treatments, including oxidative stabilization and carbonization, to ultimately become carbon fibres. During oxidative stabilization, also referred to as the stabilization step, the green fibres are exposed to air at temperatures typically lower than the precursor's softening point, with temperatures reaching up to 300 °C. This phase initiates oxidative cross-linking reactions involving heteroatom-containing groups, resulting in the stabilization of the fibre structure [Leistenschneider et al. 2021].

The temperature for oxidative stabilization depends largely on the nature of the sample. As observed in the thermogravimetric analysis (TGA) curves presented in Figure 2.6, asphaltene samples did not exhibit any significant weight change until reaching 230 °C. However, between 230 °C and 390 °C, a gradual and steady reduction in weight occurs, followed by a relatively rapid weight loss within a narrow temperature range of 390 °C to 470 °C. Subsequently, decomposition of the asphaltenes becomes evident. These TGA curves provide valuable insights for determining melt-spinning and stabilization temperatures. The precise control of temperature during these critical stages is essential to ensure the successful transformation of asphaltenes into high-performance carbon fibres with desirable mechanical properties.

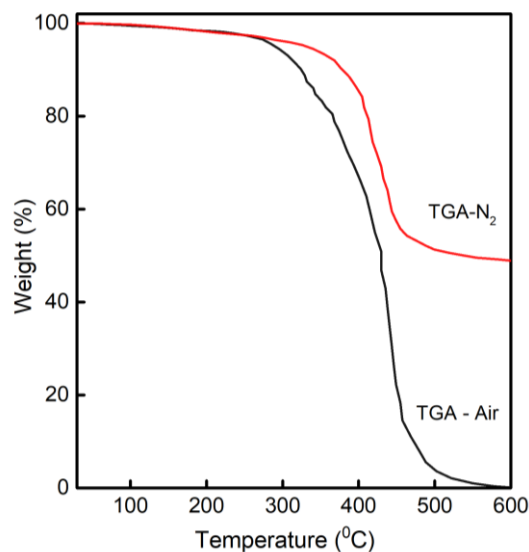


Figure 2.6: TGA-curves of asphaltenes in air and nitrogen atmosphere [Trejo et al. 2010]

## 2.2. Spinning

In the process of carbon fibre production, a crucial stage involves the transformation of precursor materials, typically in powder or pellet form, into continuous, elongated filaments through a process known as spinning. This process plays a pivotal role in determining the characteristics and properties of the eventual carbon fibres [Morgan 2005]. Currently, the industry primarily employs three main spinning techniques: melt spinning, wet spinning, and dry spinning. The choice of which spinning technique to employ is contingent upon both the inherent nature of the precursor material and the specific end properties desired for the resulting carbon fibres [Park 2018].

Melt spinning is an economically efficient technique that significantly reduces the production costs of precursor fibres, thereby benefiting the carbon fibre manufacturing process. This method finds extensive use in producing textile fibres for a wide range of applications. Melt spinning involves the extrusion of molten polymers through small orifices, where the extruded

material cools in the ambient air and solidifies into fibres. During the cooling process, the fibres undergo a reduction in diameter, enhancing molecular alignment [Brown et al. 2022]. Additional drawing processes may be applied to further decrease fibre diameter and improve mechanical properties, as depicted in Figure 2.7.

This fibre formation process offers a high degree of control through various parameters and is well-established. An essential aspect contributing to the cost reduction in carbon fibre production is that the throughput of melt spinning greatly surpasses that of solution spinning, and it eliminates the need for handling and disposing of substantial quantities of solvents [Delhaes 2003]. Melt spinning accommodates a wide range of natural and synthetic materials, many of which have been demonstrated as suitable precursors for carbon fibres. Four primary categories of melt-spinnable carbon fibre precursors have emerged, including melt-processible PAN, mesophase pitch, biomaterials like lignin and cellulose, and synthetic polymers [Brown et al. 2022].

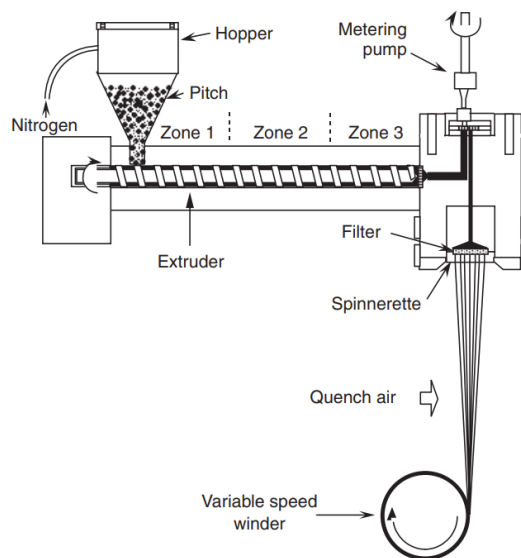


Figure 2.7: Schematic of melt-spinning process to produce mesophase pitch fibres [Delhaes 2003]

The schematic of a typical melt-spinning process, employed in the production of mesophase pitch precursor fibres [Delhaes 2003], is presented in Figure 2.7. The process begins with solid chips from mesophase pitch loaded into the extruder's feed hopper. The rotating screw inside the extruder transports and heats the chips, turning them into a highly viscous melt. This molten precursor then moves to the pumping section of the extruder, where fluid pressure increases due to narrowing channels. After exiting the extruder, it enters a transfer manifold before being propelled into a spin pack with a filter for removing small solid particles from the molten precursor. Finally, as it exits the pack, it passes through a plate containing numerous fine holes called spinneret [Delhaes 2003].

Carbon fibres derived from melt-spun PAN copolymers underperform conventionally produced carbon fibres because of the limitation of cyclization groups, which is critical to proper stabilization and the development of mechanical properties in carbon fibres [Huang 2009]. On the other hand, melt spinning pitch fibres is notoriously challenging because the material properties are highly sensitive to its processing conditions.

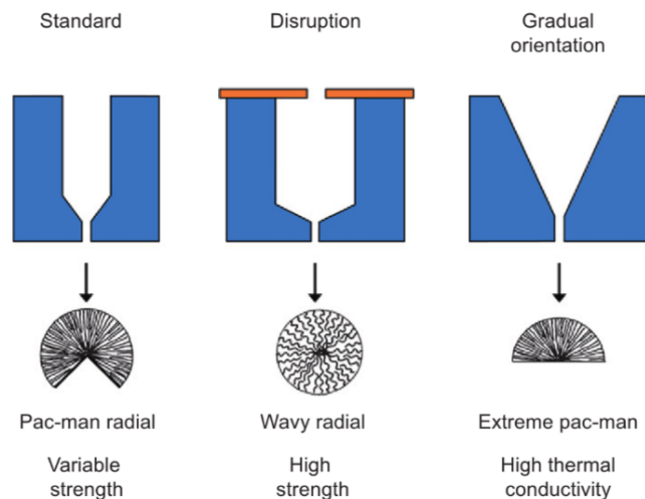


Figure 2.8: Different die designs and the effect on resultant fibre structure and properties [Bhat 2016]



The minor variations in the spinning temperature, capillary design, and die geometry can induce vastly different and heterogeneous microstructures, significantly affecting the fibre's properties, as shown in the Figure 2.8 [Bhat 2016]. The viscosity of the melt is one of the main factors for successfully spinning, and it is affected by the nature of the raw material, temperature, flow rate, molecular weight, and mesophase content. The stress profile on the fibre as a consequence of spinning and drawing influences the morphology of the mesophase of fibres which influences the final properties of fibres [Edie 1998].

### **2.3. Post-treatment**

After the spinning process, the spun fibres are subjected to various post-treatment steps to convert the precursor material into carbon fibres. These post-treatment procedures involve several heating stages, including stabilization, carbonization, and graphitization.

#### *2.3.1 Conventional Stabilization*

Achieving high-performance carbon fibre often requires a crucial step known as stabilization, which involves heating the fibres above their glass transition temperature ( $T_g$ ). This process is essential as it helps prevent the loss of fibre structure and avoids softening prior to the subsequent high-temperature carbonization stage. Stabilization plays a significant role in promoting cross-linking within the fibre, ensuring its overall strength and performance. During this particular stage of the process, the fibres are subjected to heat treatment while being held under tension at relatively lower temperatures (200 – 300 °C) [Liu et al. 2018]. Researchers have conducted reviews on the stabilization process in various materials and have observed that although they share similarities, they tend to follow slightly different pathways.

Careful control of the exothermic reactions within the oven relies on maintaining a uniform temperature distribution, ensuring that overheating is avoided. The optimum airflow heats the fibre, providing the required oxygen for the reaction, and removes exhaust components and excess heat reaction from the fibres. Furthermore, the process is typically carried out under tension or even by applying drawing to prevent shrinkage of the elements [Morgan 2005].

During the stabilization process polyacrylonitrile based green fibres, the PAN molecules undergo cyclization, transforming into a non-meltable ladder structure. Stabilization in an oxygen-rich atmosphere yields fibres with superior mechanical properties and higher carbon yield. This is due to the formation of stable structures with cross-linking generated by oxygen groups in the polymer backbone [Frank et al. 2017].

Concurrent dehydrogenation and cyclization processes can occur during stabilization, as shown in Figure 2.9. The diffusion rate of these reactions is controlled, depending on factors such as fibre diameter, precursor composition, temperature, and oxygen concentration in the stabilization environment. Furthermore, the fusion of oxygen-containing groups within the polymer backbone enhances the ladder polymer's stability, enabling it to withstand high-temperature carbonization process [Morgan 2005].

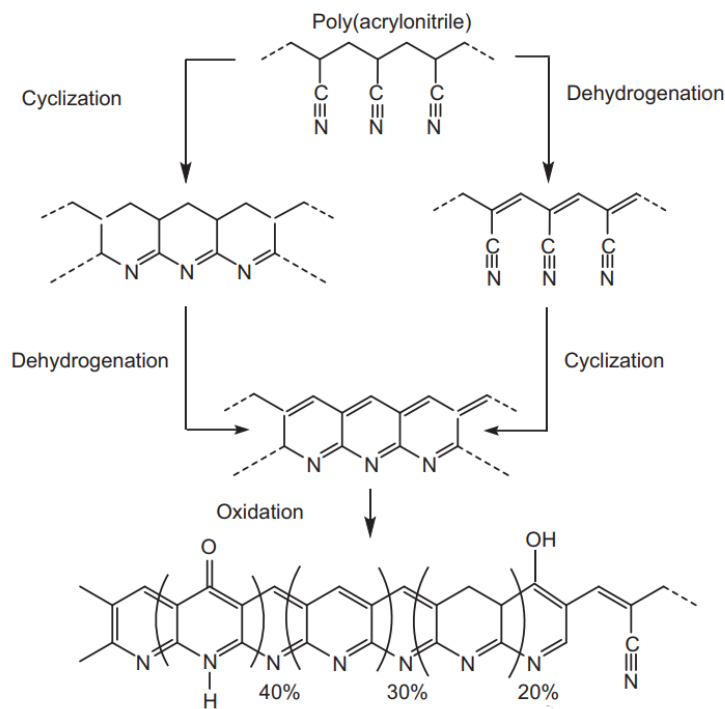


Figure 2.9: Chemical reactions during the stabilization of PAN based carbon fibres [Frank et al. 2017]

During the oxidation stage, the density of PAN-based fibres undergoes a transformation, increasing density from 1.18 to 1.36-1.38 g/cm<sup>3</sup>. In this oxidized state, the fibres typically contain 62-70 wt.% carbon, 20-24 wt.% nitrogen, 5-10 wt.% oxygen, and 2-4 wt.% hydrogen [Frank et al. 2017]. In the oxidation process, the polymer chains are converted into heteroaromatic structure, which shares some similarities with the subsequent carbon phase. Various models have been suggested to explain the cyclization of PAN molecules, and the intricate mechanisms behind the formation of the ladder structure involves a complex series of chemical reactions that have been the subject of extensive research in recent decades [Frank et al. 2014].

Subjecting PAN-based precursors to heat treatment under tension in an oxidizing atmosphere at temperatures exceeding 200 °C triggers a range of thermally activated processes.

These processes entail significant reorganization of the polymer chains and cross-linking of the molecular chains by oxygen bonds [Donnet & Bansal 1998]. These interactions maintain the aligned supramolecular structure even after the release of tension, ensuring its prevention for subsequent processing steps. The ideal oxygen absorption during the oxidation treatment typically falls within the 8-10% range [Fitzer & Manocha 1998]. Figure 2.4 illustrates a schematic diagram of the stabilization and carbonization process in an industrial template.

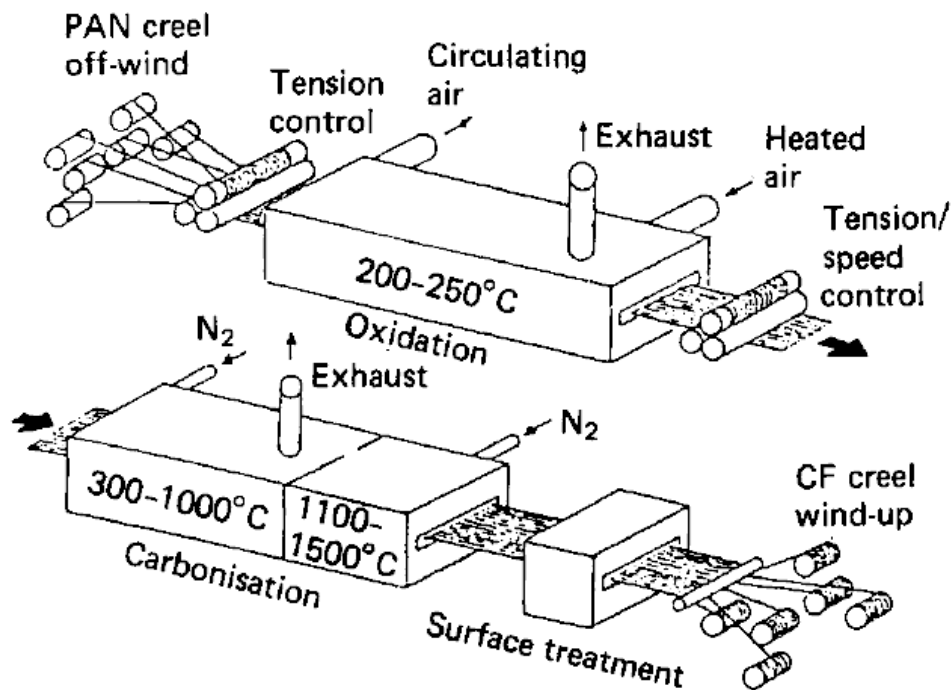


Figure 2.10: Schematic of carbon fibre post-treatment [Wyatt et al. 1994]

### 2.3.2 Conventional Carbonization

The stabilized precursor fibres, which are capable of enduring elevated temperatures, undergo thermal pyrolysis in an inert atmosphere, resulting in their transformation into carbon fibres. This process entails the elimination of volatile compounds, yielding carbon fibres with a

carbon content of approximately 50 wt.% relative to the initial precursor [Frank et al. 2017]. The final phase plays a pivotal role in achieving the desired microstructural configuration, where carbon atoms align themselves to a graphene-like structure, exhibiting coplanar orientation. The structure exhibits a stacked and ordered arrangement, with each stack featuring a specific crystal thickness. The fibre's crystalline characteristics can be refined by controlling the pyrolysis temperature and the duration of processing. Notable transformations occur at distinct temperature ranges, such as the liberation of nitrogen and sulfur-containing compounds, observed between 900 and 1200 °C. The release of these compounds leads to the formation of pores within the fibre material, highlighting the temperature's critical role in the carbonization process [Banerjee et al. 2021].

Concerning PAN-based fibres, the initial phase of the carbonization process typically involves a slow rate of heating to ensure that the release of gaseous decomposition compounds does not harm the fibre. Within the temperature range of 400 to 500 °C, the hydroxyl groups in the oxidized PAN-based fibres engage in crosslinking condensation reactions, leading to the reorganization and merging of the cyclized sections [Huang 2009]. Intramolecular dehydrogenation occurs between 400 °C and 600 °C, followed by denitrogenation and formation of plain graphite layers at higher temperatures, as shown in Figure 2.11. Increased heating rates during the carbonization process can introduce imperfections into the carbon fibres, whereas slower carbonization rates lead to the early release of significant nitrogen quantities in the process, a condition preferred for achieving carbon fibres with high tensile strength [Frank et al. 2017].

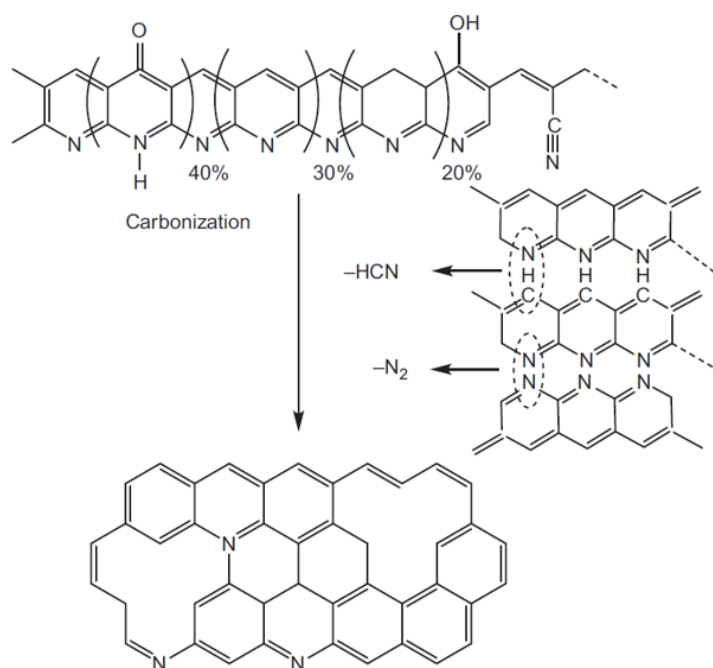


Figure 2.11: Carbonization reaction path of PAN-based carbon fibres [Frank et al. 2017]

The transformation of mesophase pitch precursor fibres into carbon fibres also includes carbonization and graphitization. To attain desirable tensile strengths and high Young's moduli, the final heat treatment temperature typically ranges from 2000 to 3000 °C. In the carbonization reaction of pitch, as shown in Figure 2.12, temperatures exceeding 350 °C induce a condensation reaction that eliminates hydrogen and forms additional covalent bonds. Beyond 1500 °C, the structure eliminates more hydrogen, and in the case of pitch derived from natural sources, nitrogen and oxygen are also removed [Frank et al. 2014].

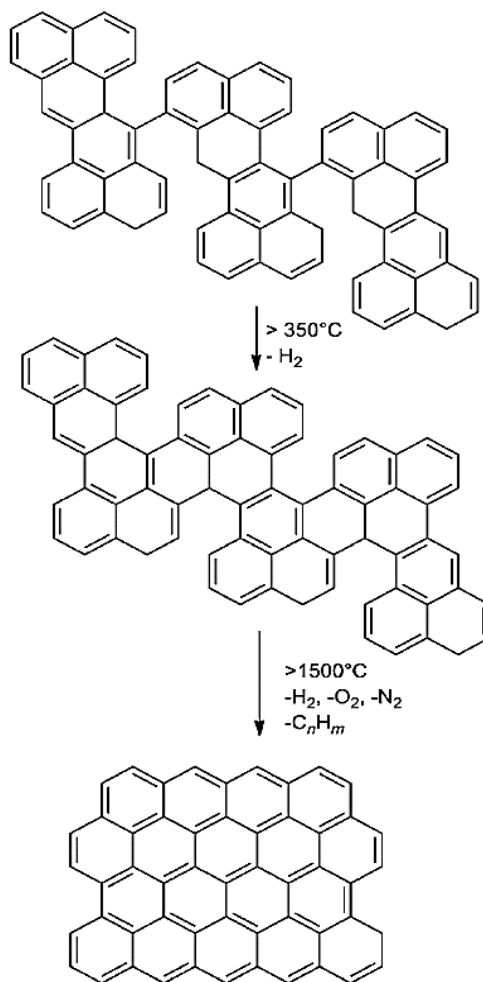


Figure 2.12: Fundamental reaction path for carbonization of a mesophase pitch precursor [Frank et al. 2014]

### 2.3.3 Conventional Graphitization

The last stage of the heat treatment process for carbon fibres, conducted at temperatures reaching up to  $3000^{\circ}\text{C}$ , is known as graphitization [Park 2018]. During this process, the small turbostratic crystallites within the fibres align and orient themselves along the fibre axis. This alignment results in a higher Young's modulus, which measures stiffness, but it also simultaneously decreases the tensile strength of the final carbon fibre product. To facilitate this

high-temperature process, a specialized furnace with a graphite muffle is employed, operating within a meticulously controlled inert atmosphere. It is imperative to maintain undisturbed conditions throughout the duration of the process [Liu et al. 2008].

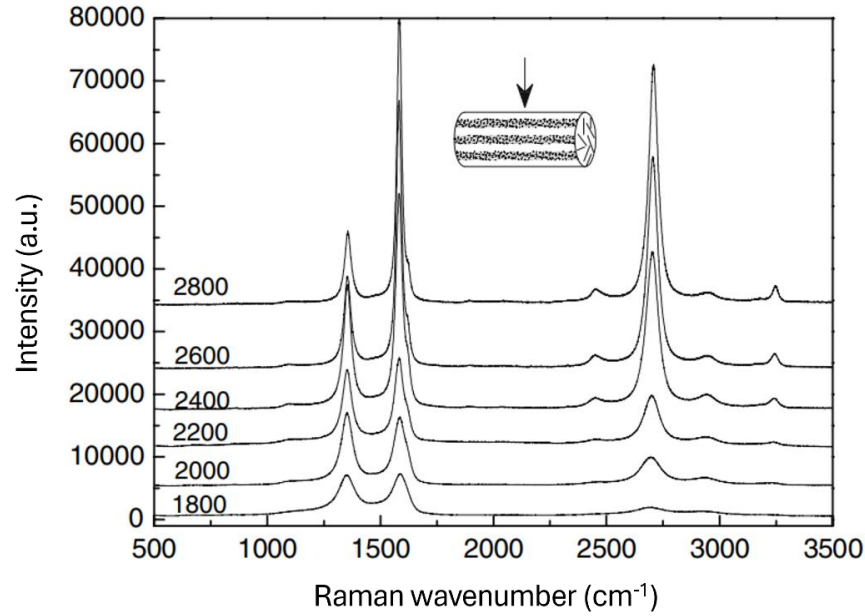


Figure 2.13: Raman spectra taken from surface of PAN-based carbon fibres graphitized at different temperatures (1800 to 2000 °C) [Liu et al. 2008]

It is found that with increasing temperature, there is a noticeable increase in Raman intensity and a narrowing of spectral lines in the first-order spectrum (1000-2000  $\text{cm}^{-1}$ ) as shown in Figure 2.13. At a heat treatment temperature of 2000 °C, a distinct new peak emerges at 1620  $\text{cm}^{-1}$ , indicating the realignment of crystallites along the fibre axis. These observed alterations in the Raman spectra during the graphitization process provide valuable insights into the evolving structural properties of carbon fibres, thereby contributing crucial information for their diverse applications [Liu et al. 2008].



#### *2.3.4 Microwave-based Carbonization*

In a study by Nabais et al., the microwave-based carbonization process for activated carbon fibres (ACF) was examined. They have demonstrated that microwave treatment significantly influences ACF porosity, leading to a reduction in micropore volume and size. Importantly, the study revealed that microwave treatment is highly effective in modifying the surface chemistry of ACFs. The research findings indicate that microwave heating is a rapid, cost-efficient method for altering both porosity and surface chemistry in ACFs. It achieves the removal of surface groups without eliminating oxygen and nitrogen atoms bonded within pseudographitic planes. The study highlights the advantages of using a microwave furnace for modifying carbon materials, emphasizing its rapidity, cost-effectiveness, and efficiency compared to conventional furnaces. The research also suggests potential applications, such as acid gas adsorption and catalyst development, stemming from the reactive state maintained on the surfaces of carbon materials after microwave treatment.

Jin et al. explored the microwave-based carbonization process for pre-oxidized PAN fibres, comparing it with conventional heating methods. The study revealed that microwave carbonized fibres (MCFs) produced at temperatures between 750 and 1000 °C exhibited higher carbon content, larger crystallite dimensions ( $L_a$  and  $L_c$ ), increased porosity, and a more uniform cross-sectional structure compared to conventionally carbonized fibres (CCFs) at the same temperature. However, beyond 1000 °C, the crystallite sizes of MCFs became smaller than those of CCFs at equivalent temperatures, and the skin-core difference in structure increased with rising temperatures for MCFs. Tensile strength and modulus of MCFs were superior to those of CCFs in the 750–1000 °C range, while both types showed similar mechanical properties above 1000 °C. This behaviour was attributed to the temperature-dependent microwave adsorption ability of the carbonized fibres. The

study emphasizes the importance of understanding the dielectric properties of fibres in relation to frequency and temperature for predicting heating efficiency, selectivity, and heat distribution in microwave-based carbonization processes.

Zhao et al. focused on the preparation of PAN precursor through a one-step method involving polymerization and spinning. Following conventional pre-oxidation at 180–280 °C in air, the polyacrylonitrile pre-oxidized fibre underwent carbonization at 600–1000 °C using both microwave heating and conventional heating in a nitrogen atmosphere. Real-time surface temperature monitoring was accomplished with an infrared thermometer. In comparison to CCF-700, MCF-700 exhibited a remarkable 10.06% increase in tensile strength. Notably, the microwave carbonization method achieved superior carbon fibre tensile strength at a temperature 200 °C lower than conventional carbonization. Furthermore, MCF-700 displayed a significantly higher initial modulus, surpassing that of CCF-700 by 51.33%. The conclusion highlights the PAN precursor's pre-oxidation and subsequent carbonization under varying conditions, emphasizing the utilization of infrared thermometry for real-time temperature monitoring and online mass spectrometry for analyzing pyrolysis product composition.

Microwaves fall within the electromagnetic spectrum as a type of electromagnetic radiation, encompassing frequencies that range from 0.3 to 30 GHz and wavelengths spanning from 1 mm to 1 m. In domestic and commercial microwave applications, the microwave applicator typically operates at a frequency of 2.45 GHz, corresponding to a wavelength of 12.25 cm. Microwaves consist of two components: electric waves and magnetic waves, as illustrated in Figure 2.14 [Kappe et al. 2013].

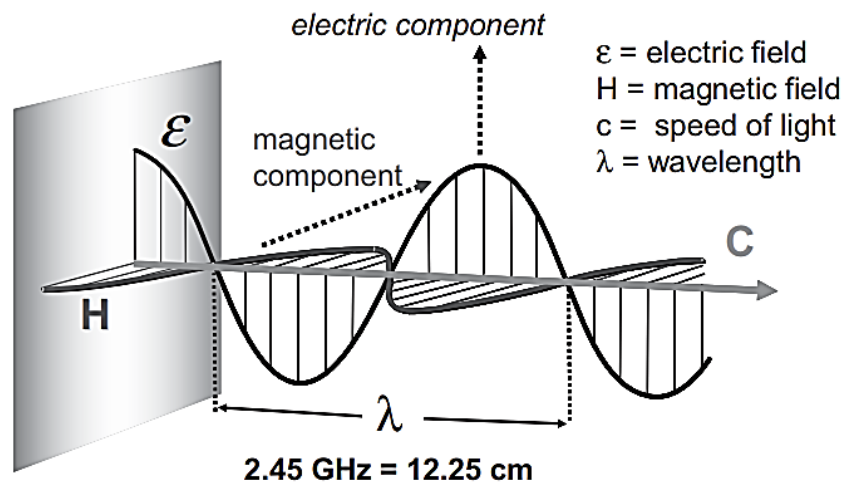


Figure 2.14: Electric and magnetic field components in microwaves [Kappe et al. 2013]

The electric component of a microwave plays a significant role in heating through two primary mechanisms: dipolar polarization and ionic conduction. Microwave heating occurs through the alignment of dipoles in a substance exposed to microwaves. When a material with a dipole moment is irradiated with microwaves, its dipoles align with the applied electric field. As the field oscillates, the dipole field tries to realign with the alternating electric field, resulting in the loss of energy as heat through molecular friction and dielectric loss. At the frequency of 2.45 GHz commonly used in commercial systems, there is enough time for dipole rearrangement, leading to the conversion of electrical energy into thermal energy [Kappe et al. 2013].

Ionic conduction serves as the second significant heating mechanism. Within this mechanism, charged particles, typically ions, present in a sample undergo oscillation due to the influence of the microwave field. As they oscillate back and forth, these charged particles collide with neighboring molecules or atoms, resulting in agitation and motion. These collisions generate heat through the conversion of kinetic energy, contributing to the overall heating process [Kappe et al. 2013].

Microwave radiation generates heat in materials through the mechanism of dielectric loss, which involves the absorption and conversion of electromagnetic energy into thermal energy. The classification of materials based on their microwave interaction includes three main groups: conductors (metals and alloys), insulators (fused quartz, glasses, ceramics, Teflon, and polypropylene), and absorbers (aqueous solutions and polar solvents) [Li & Yang 2008]. Microwave absorption performance can be evaluated based on four characteristic parameters, namely dielectric constant ( $\epsilon'$ ), dielectric loss ( $\epsilon''$ ), tangent loss ( $\delta$ ), and penetration depth [Issa et al. 2015]. These parameters provide valuable insights into the efficiency and effectiveness of a material or substance in absorbing microwave radiation.

In carbon fibre synthesis, the formation of a core-shell structure can be problematic, particularly at high heating rates in traditional furnaces. However, microwave heating offers a solution by enabling heat to propagate from the core to the shell [Liu et al. 2018]. Within academic research, the microwave mode of treatment is increasingly preferred over conventional methods due to its numerous advantages. These include rapid internal heating, efficient direct energy transfer from the source to the reaction molecules, uniform heating for homogeneous samples, and selective heating for heterogeneous samples. The unique capabilities of microwave treatment make it highly desirable for a wide range of research applications [Li & Yang 2008, Liu et al. 2018].

Two commonly used applicators are multi-mode and single-mode configurations. In multi-mode microwaves, the microwaves and electric field distribution is non-uniform, as shown in Figure 2.15. The cavity dimensions are precisely regulated, often with a mechanical mode stirrer to prevent the formation of standing wave patterns. This ensures that microwave – absorbing materials can be heated anywhere within the cavity [Cundy 1998].

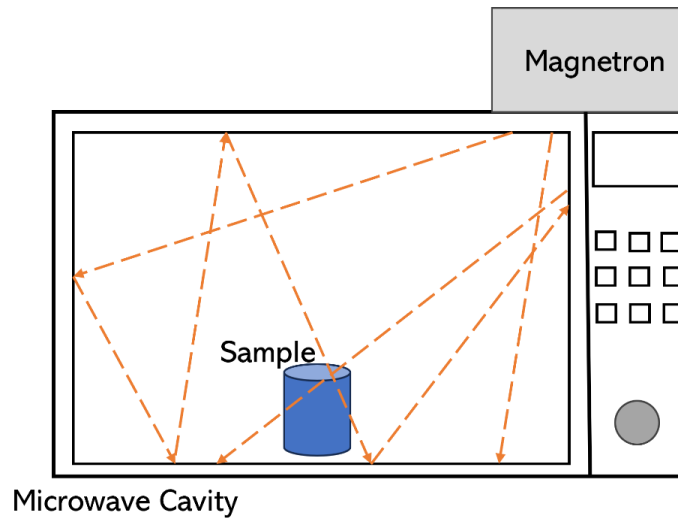


Figure 2.15: Schematic of multi-mode microwave adapted from [Cundy 1998]

In contrast, single-mode microwaves generate a single standing wave within the cavity, usually achieved through the use of waveguides. The cavity dimensions are precisely adjusted to correspond to the wavelength of the microwave at the specific frequency employed (for 2.45 GHz, a single full wave corresponds to a length of 12.24 cm) [Li & Wang 2008]. Single-mode cavities, which generate radiation with higher field strength, are well-suited for research purposes despite having a relatively smaller area of irradiation. Careful positioning of materials, as shown in Figure 2.16, is essential to avoid standing wave nodes where no heating occurs and to prevent the material being treated from disrupting the standing wave. This configuration necessitates the irradiation of only one material at a time in a single-mode setup [Cundy 1998].

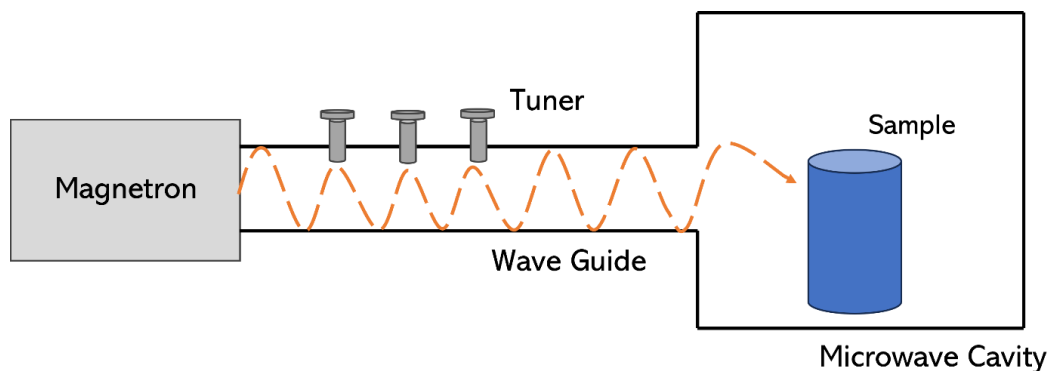


Figure 2.16: Schematic of single-mode microwave adapted from [Cundy 1998]

In a study conducted by Zhao et al., it was demonstrated that microwave heating offers several distinct advantages. Unlike traditional heating methods, microwave heating operates without the need for heat conduction processes, effectively heating both the interior and exterior of materials simultaneously. This results in rapid and uniform heating, significantly reducing energy consumption compared to conventional heating methods while achieving the desired heating outcomes. Furthermore, microwave heating has the added benefit of reducing production time and costs. In the context of carbonization, microwave-assisted carbonization stands out as it allows for the production of carbon fibres with higher initial modulus even at lower carbonization temperatures [Zhao et al. 2022].

The utilization of microwave-assisted heating, as highlighted in the study by Singh et al. presents several notable advantages over traditional heating methods. This approach offers rapid, uniform, and selective heating, along with precise control over particle sizes, making it a favored choice in both academic research and industrial applications over the past few decades [Singh et al. 2019]. Microwave heating facilitates shorter crystallization times and promotes more homogeneous nucleation in comparison to conventional heating techniques. Maximum temperatures of 1170 °C can be achieved using microwave heating [Wang et al. 2015].

### *2.3.5 Microwave Plasma Carbonization*

Plasma is commonly recognized as the “fourth state of matter”. Similar to how an increase in energy can cause a solid to become a liquid or a liquid to become a gas, if the supplied energy reaches sufficient level, the collision processes become intense enough to dissociate gaseous atoms into their constituent sub-atomic particles carrying electrical charges [Riccardo et al. 2005; Fridman 2012]. Plasma, as an ionized gas, can exist in a partially or fully ionized state, comprising electrons, ions, and neutral atoms or molecules. Despite the presence of charged particles, plasmas are considered quasi-neutral, indicating that the concentration of positively and negatively charged ions is balanced and roughly equal [Plasma processing of materials 1991].

Plasma, with its abundance of free electric charges, possesses electrical conductivity, internal interactivity, and a strong responsiveness to electromagnetic fields. These characteristics allow plasma to efficiently conduct electricity and interact with its surroundings, making it highly sensitive to electromagnetic influences [Fridman 2012]. Plasma has a history dating back to the 18<sup>th</sup> century when G.C. Lichtenberg observed brush-like patterns resulting from discharges between pointed electrodes on insulating surfaces. Sir William Crookes successfully generated plasma and recognized its connection to electrically charged particles, while Werner Von Siemens potentially pioneered the application of plasma in chemical processes. However, it was not until Sir J.J. Thomson’s discovery of electrons in 1897 that a comprehensive understanding of plasma became possible. Thomson’s groundbreaking work shed light on the nature and behaviour of charged particles within plasma, enabling a deeper comprehension of this unique state of matter [Riccardo et al. 2005].

Plasma is believed to make up over 99% of the observable universe, encompassing various environments such as stellar interiors and intergalactic space [Langmuir 1928]. On Earth, natural

occurrences of plasma are limited, except for certain exceptions like lightning and the phenomenon of the aurora borealis [Riccardo et al. 2005]. Plasmas are also artificially created in laboratory and industrial settings by exposing a gas to an electric field, either constant or alternating in amplitude [Thirumdas et al. 2014]. Different energy sources, such as thermal, electric, and microwave frequencies, can be utilized to produce plasma, and the specific characteristics of the plasma formed are determined by the conditions employed during the generation process [Riccardo et al. 2005].

Microwave radiation is responsible for initiating and sustaining the energy in plasma. The majority of microwave energy directly couples with plasma, which consists of electrons, positive or negative ions, gaseous atoms and molecules in the ground or excited states, neutral free radicals, and photons. The collective flux of these species impacts the surface of the fibres, leading to enhanced carbonization due to their higher energies compared to conventional thermal fluxes. This type of plasma, known as low-pressure “cold” plasma, maintains an ambient gas temperature and includes electrons with sufficient kinetic energy to induce chemical bond cleavage, thereby promoting gas release [Thirumdas et al. 2014].

Microwave energy serves as the driving force for plasma and simultaneously transfers energy directly to the fibre. Carbon exhibits excellent microwave absorption properties, making it an ideal absorber of microwave energy. The coupling between the plasma and microwave energy enables uniform and homogeneous heating, facilitating the exchange of oxygen and evolved gases throughout the fibre. These released gases can serve as supplementary fuel for plasma and provide indications of carbonization completion or the need for adjusting the microwave energy level [Paulauskas 2000]. Microwave plasma carbonization shows promise as a next-generation method for carbon fibre production. In the study conducted by Kim et al., a meticulously designed



microwave plasma system for the carbonization process has been implemented, as shown in the Figure 2.17. This system contained of key components, including a magnetron, waveguide, dual quartz cylinder system, and two chambers. The magnetron emitted microwave energy at a frequency of 2.45 GHz which was channeled through a waveguide to initiate a plasma discharge within the dual quartz cylinder system.

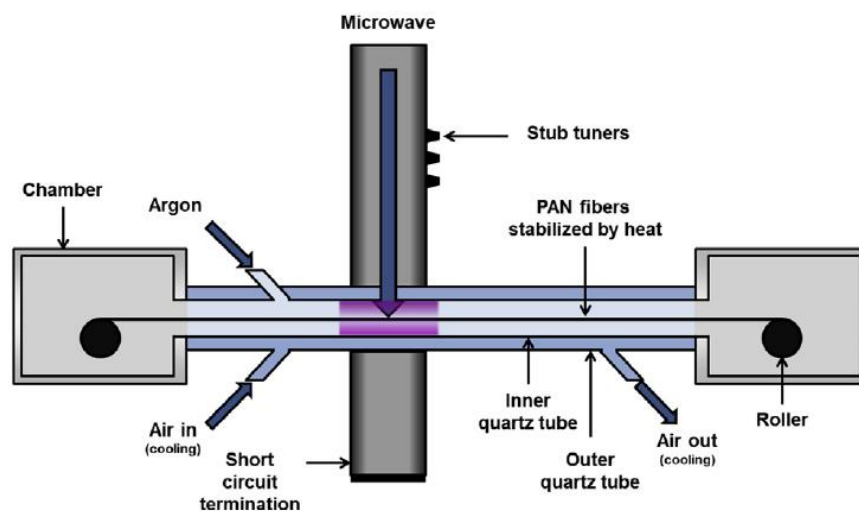


Figure 2.17: Microwave plasma system for the carbonization process [Kim et al. 2015]

The influence of various power levels on the properties of the resulting carbon fibres have been studied. It was observed that, while microwave plasma carbonization offered significant advantages, such as rapid heating, it also introduced a degree of surface damage to the carbon fibres due to the intense energy absorption. Consequently, some of the resulting filaments exhibited brittleness. This surface damage aspect became a focal point for further investigation and optimization within the study [Kim et al. 2015].

In a study conducted by [Kuptajit & Sano 2019], the focus was on exploring the utilization of microwave-induced plasma for the rapid production of activated carbon. Multi-mode conventional microwave oven was used to create microwave-induced plasma by irradiating

microwaves onto conductive porous materials, particularly carbonized powders. It also showcased the potentiality of paving the way for continuous systems in activated carbon manufacturing, offering improved efficiency and scalability. These findings underscore the potential of microwave-induced plasma as an innovative technology, with far reaching implications for industry and materials science.

## **2.4 Modelling of Microwave Plasma**

Due to the inherently rapid nature of microwave plasma, obtaining an absolute temperature measurement can be slightly challenging. Furthermore, the Microwave-Plasma process is influenced by various parameters, including power, pressure, and gas composition. To optimize the process or tailor experiments to specific requirements, it is essential to look into the modeling of microwave plasma. Baeva et al. conducted a two-dimensional model of microwave-induced plasma in argon at atmospheric pressure. This model includes the study of how microwave energy is coupled with the plasma and the pertinent reaction kinetics associated with atmospheric-pressure argon plasma. This includes the consideration of molecular ion species in relation to consistent gas flow and heat transfer. The model presented in this study yields valuable insights the distributions of gas and electron temperatures (Figure 2.18), as well as the number densities of electrons, ions, and excited states. The model provides information on how temperatures are distributed spatially and temporally within the plasma. This includes variations in temperature along different regions or axes, offering a comprehensive view of the thermal dynamics. The model reveals how the temperature of the argon gas varies spatially and temporally within the plasma. Variations in electron temperature across different regions or axes provide a nuanced understanding of the electron energy states. The plasma was found to be far from thermodynamic equilibrium, with a

maximum heavy particle temperature of about 2100 K, an electron temperature of about 1 eV, and an electron density slightly above  $4 \times 10^{21} \text{ m}^{-3}$ . To validate the findings of this study, a comparison with experimental data is included, illustrating a strong quantitative and qualitative agreement between the model's predictions and the actual experimental results [Baeva et al. 2012].

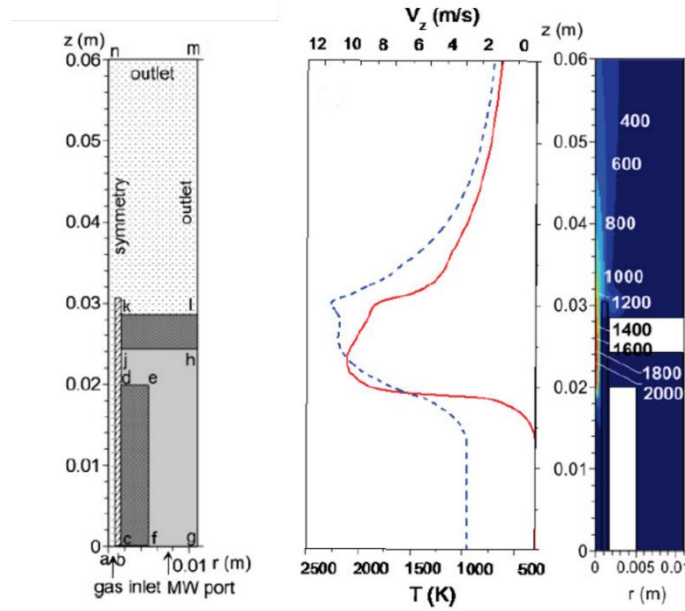


Figure 2.18: 2D plot of the gas temperature distribution in the computational domain [Baeva et al. 2012]

Shen et al. conducted a self-consistent three-dimensional plasma model coupled with Maxwell's equations. This study demonstrated the growth of electron density over the time (Figure 2.19b), the distribution of the microwave electric field module in the setup, distributions of conductivity, and gas temperature at various pressures and durations. A plasma model was constructed using Maxwell's equations, taking into account the presence of argon atoms in the metastable state and considering coupling with flow, heat transfer, and microwave multi-physical fields as shown in Figure 2.19a [Shen et al. 2020].

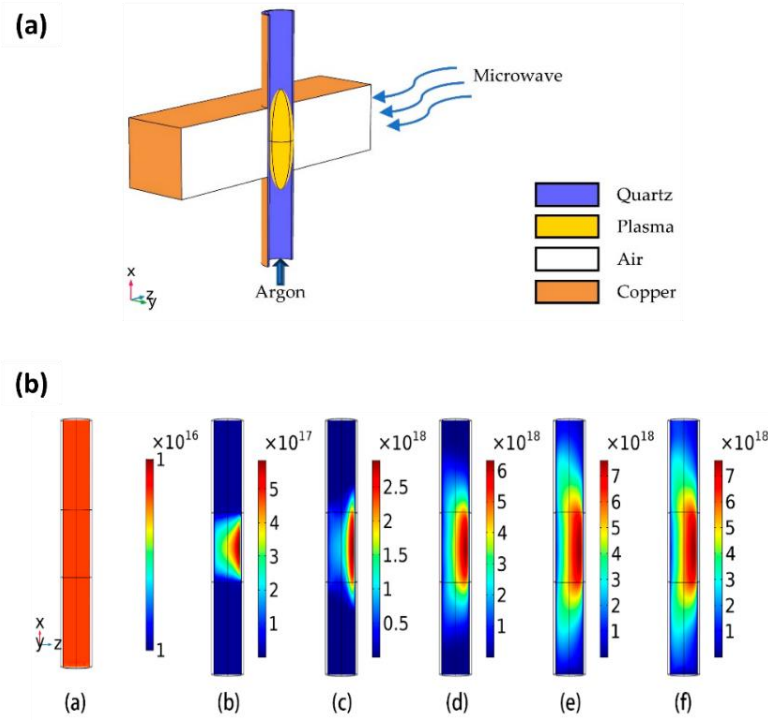


Figure 2.19: a) Cutaway view of the microwave plasma torch b) slice plots of the distribution of the electron density ( $\text{m}^{-3}$ ) inside the quartz tube [Shen et al. 2020]

## 2.5 Applications

Carbon fibres have gained significant utilization across commercial and civilian aircraft, industrial, recreational, and transportation sectors. These versatile materials are particularly well-suited for applications demanding exceptional strength, stiffness, low weight, and exceptional fatigue resistance, aligning with the critical requirements in various industries [Park 2018]. Carbon fibres find broad utility in various electrochemical applications, such as Lithium-ion, Lithium-sulfur, Sodium, Zinc-air, and Aluminum-Air batteries. Their distinctive advantages, including stable electrochemical performance, exceptional mechanical strength, high electrical conductivity,

efficient electron transmission, and minimal volume variation, are pertinent to this study [Yang et al. 2020].

Lightweight Carbon Fibre Reinforced Plastics (CFRP) composites serve multifunctional roles from manufacturing to structural state monitoring. Leveraging their electrical properties reduces weight and enables structural supercapacitors, meeting Industry 4.0 and autonomous vehicle demands [Forintos & Czigany 2019]. Carbon fibre's biocompatibility, corrosion resistance, and ability to promote bone tissue generation make it a versatile biomaterial. Its combination with other materials enhances their properties, holding promise for advanced medical applications like artificial joints, bone fracture treatments and dental implants [Saito et al. 2011]. Carbon Fibre reinforcement in cement materials greatly improves their strength, toughness, and electrical conductivity, enabling self-sensing and self-adjusting capabilities. This advancement is valuable for creating intelligent material structures that can monitor internal damage and control temperature, stress, and deformation [Hao et al. 2023].

The unique thermal properties exhibited by carbon materials derived from asphaltene render them exceptionally well-suited for a wide array of thermal processes. Asphaltene-derived carbon fibres have a distinctive advantage over commercially available PAN-based carbon fibres due to their lower cost. This affordability makes them a revolutionary option that can unlock numerous applications in different industries.

## **2.6 Summary**

Numerous precursor materials, such as PAN, mesophase pitch, and rayon, have been extensively examined in prior research. However, this study distinguishes itself by focusing on the utilization of asphaltenes derived from Alberta oilsands for carbon fibre production. Asphaltene

fibres were successfully manufactured using a twin-screw extruder equipped with a spinneret and godet system. These cost-effective asphaltene fibres hold the potential to serve various markets, including automotive interiors, construction fillers, and more.

In the pursuit of more sustainable methods for carbon fibre production, microwave plasma carbonization has emerged as a promising alternative. This innovative approach offers potential reductions in GHG emissions compared to traditional manufacturing processes outlined in previous literature. While prior studies on microwave plasma carbonization mainly focused on PAN-based carbon fibres, it is important to consider that these treatments often resulted in surface defects due to intense energy exposure. Therefore, this research aims to investigate the effects of microwave induced plasma, generated by multi-mode microwave oven, on asphaltene fibres. The study includes the investigation of the process parameters based on a comprehensive model of microwave plasma within the setup.

### **CHAPTER 3. MICROWAVE PLASMA MODELLING**

In order to understand the behaviour of plasma at different power levels, a thorough investigation into plasma electron temperatures and electric field in the cavity is necessary. It provides information about the temperatures within the plasma when exposed to microwaves of 1000 W. The accuracy of measuring microwave plasma heating is limited due to the rapid and unpredictable nature of plasma. This comprehensive study will allow for real-time optimization of processing durations and power settings. To model and simulate the microwave plasma process in our custom-designed conventional microwave setup, COMSOL™ Multiphysics software was employed.

COMSOL™ Multiphysics utilizes finite element analysis to solve partial differential equations that govern electromagnetic interactions with plasma. It provides valuable insights into various aspects of plasma behaviour, including temperature distributions in the chamber, and electric field distribution. This simulation results provide important data on energy dynamics and temperature profiles, which can be used to optimize process parameters. The objective of this study is to investigate microwave plasma conditions and contribute towards improvements in discharge system configurations, optimal operation durations, and effective operational management without compromising safety or efficiency. This modelling study is decisive for estimating the maximum temperatures that carbon fibres can be exposed to during the microwave plasma carbonization process.

### 3.1 Geometric description

The experimental setup for the microwave plasma is shown in Figure 3.1. This experimental configuration involves the utilization of a conventional microwave oven with a maximum power output of 1000 W, coupled with a custom-designed quartz tube and an argon cylinder. The choice of quartz material is deliberate, given its commendable thermal stability at high temperatures and efficient transmission of microwaves. Within the microwave oven, the quartz tube is strategically positioned to ensure that the emitted microwaves from the magnetron predominantly impact the longitudinal axis of the tube. The magnetron inside the oven emits electromagnetic waves at 2.45 GHz, which are distributed evenly throughout the cavity by a mechanical stirrer within the multi-modal cavity.

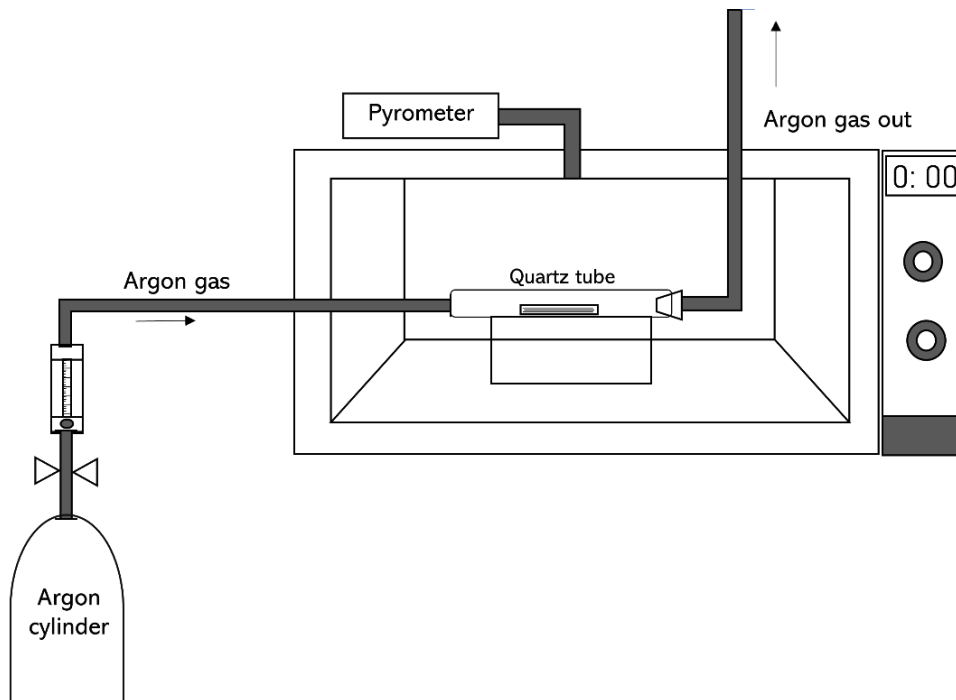


Figure 3.1: Schematic of microwave plasma experimental arrangement



The quartz tube was strategically positioned inside a microwave oven to ensure maximum exposures to microwave. The outer diameter of the tube is 60 mm, and the inner diameter is 56 mm. To minimize gas ingress and facilitate easy penetration through the oven walls, smaller diameters are present at both ends of the tube. Argon gas enters from the left side and exits from the top of the chamber. In order to conveniently introduce and remove samples, an opening-closing mechanism is implemented on the right side of the quartz tube.

For the purpose of efficient modeling, the configuration detailed in prior sections was simplified into a simpler version that incorporates an identical measurement quartz tube within a multi-modal microwave cavity. Figure 3.2 illustrates this adjusted setup as depicted within COMSOL™ Multiphysics environment. This representation was chosen to eliminate potential sources of interference and ensure a focused and accurate modeling approach.

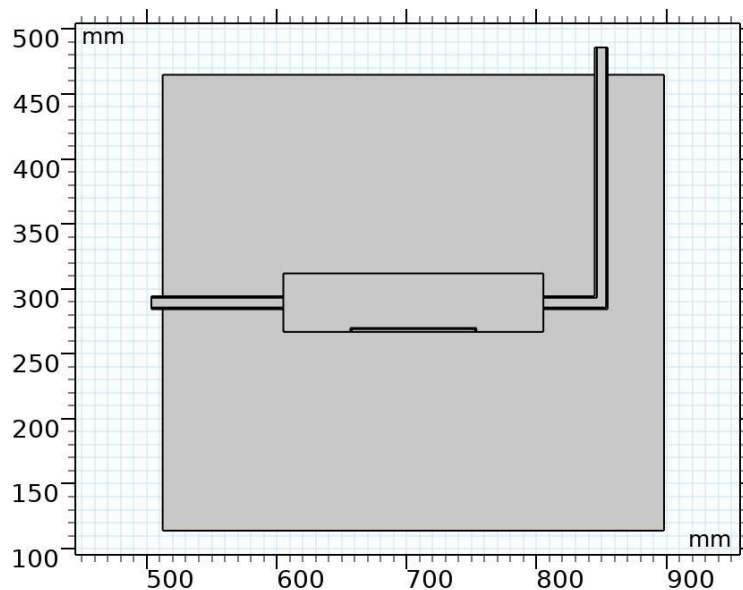


Figure 3.2: Simplified geometry of the experimental set up for modelling in COMSOL™

Multiphysics

A fine mesh was specifically defined within the quartz tube where plasma is generated, as shown in Figure 3.3. This fine mesh contributed to precision in simulations of temperature and electromagnetic characteristics and was also adept at capturing the intricate and rapidly evolving physical processes inherent to plasma, ultimately leading to more reliable and informative results. As previous studies have indicated, the rapid nature of plasma phenomena demands a finer mesh for improved precision in capturing relevant data.

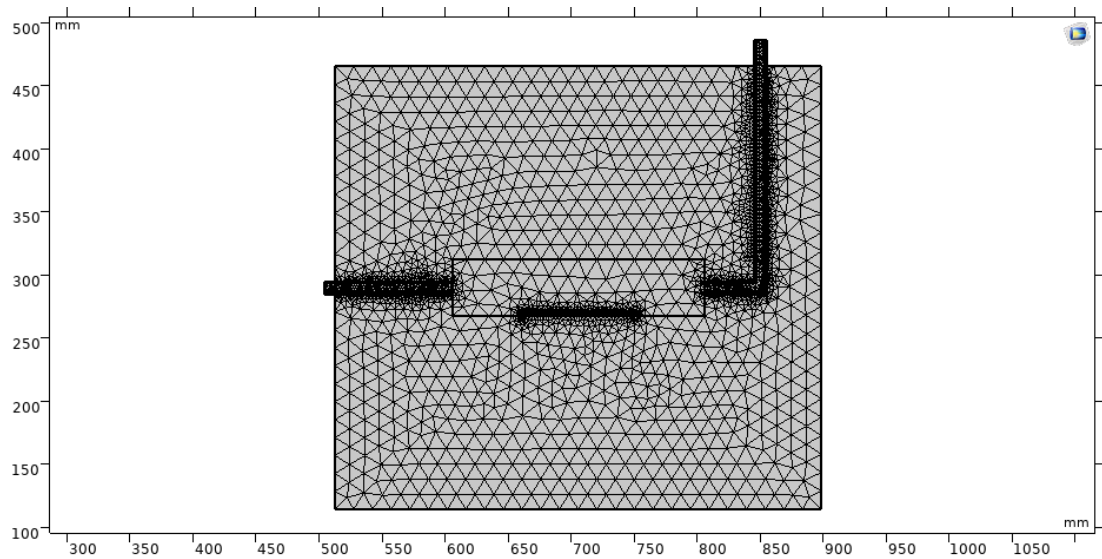


Figure 3.3: Fine mesh defined within the quartz tube

### 3.2 Theory of the model

In order to understand the interaction between electromagnetic waves and plasma, physical models are constructed and simulated. Maxwell's equations govern the behaviour of electromagnetic fields and waves, while the Boltzmann equations describes plasma physics [Salem 2021]. The integration of the two physics which are plasma physics and electromagnetic wave is used to predict the generation and motion of plasma within a defined quartz tube geometry. There

are three main approaches used to study plasmas: the kinetic approach, fluid approximation, and hybrid methods [Yang et al. 2014].

The fluid approximation method is utilized in this study to simulate our model due to its effectiveness in solving partial differential equations, defining complex plasma chemistries, and coupling electron dynamics with electromagnetic fields. This approach requires intricate modeling to consider gas discharge processes, boundary conditions, gas reactions, collision processes, plasma dynamics, and power conservation of electrons [Shen et al. 2020]. In this model, the excitation of the plasma is predominantly caused by electromagnetic wave energy. Therefore, it is vital to incorporate dynamic changes of the involved electromagnetic waves into the reaction process under microwave effects.

To analyze the influence of various plasma parameters on electromagnetic wave propagation, it is necessary to establish the formula for the electromagnetic wave in the plasma. A fluid equation was developed to study changes in electron density over time, while the Boltzmann equation was employed to examine the heating effect of strong electromagnetic pulses on electrons. The transfer of power from accelerated electrons to heavy particles via collisions was considered, and the rate of change of particle energy affected by the electromagnetic field was computed using the heat conduction formula. By combining all these equations, an iterative approach was applied to analyze plasma behaviour [Shen et al. 2020; Yang et al. 2014]. The equation formulation for each module is described in the following sections.

### *3.2.1 Electromagnetic Wave Equations*

For simulating microwaves in plasma, electromagnetic waves are employed. These waves play an important role in energizing the electrons within the chamber. The incident

electromagnetic wave on the plasma satisfies Maxwell equations [Shen et al. 2020] which are as follows:

$$\nabla \times H = i\omega\epsilon_0\epsilon_r E \quad 3.1$$

$$\nabla \times E = -i\omega\mu_0 H \quad 3.2$$

where  $E$  and  $H$  represent the electric and magnetic field strength vectors, respectively. In addition,  $i$  is the imaginary unit,  $\omega$  signifies the angular wave frequency,  $\epsilon_0$  represents permittivity of vacuum,  $\epsilon_r$  denotes relative electric permittivity of vacuum,  $\mu_0$  represents permeability of vacuum. By combining equations 3.1 and 3.2 and substituting the following values: wave number in a vacuum given by  $k = \omega/c$ , where  $c = \epsilon_0/\mu_0$ , we obtain a modified equation denoted as (3.3).

$$\nabla \times \nabla \times E = k^2 \epsilon_r E \quad 3.3$$

the relative permittivity of the plasma,  $\epsilon_r$  is given by equation 3.4.

$$\epsilon_r = 1 - \frac{\omega_p^2}{\omega(\omega - i\nu)} \quad 3.4$$

Here, the electron elastic collision frequency is denoted by  $\nu$ . The electronic conductivity,  $\sigma$  can be calculated using equation 3.5.

$$\sigma = \frac{n_e e^2}{m_e(\nu + i\omega)} \quad 3.5$$

The terms  $n_e$ ,  $m_e$  and  $e$  represent the electron density, electron mass, and fundamental charge respectively. Equation 3.3 can now be expressed as follows:

$$\nabla \times \nabla \times E = k^2 \epsilon_r \left( 1 - i \frac{\sigma}{\omega \epsilon_0} \right) E \quad 3.6$$

Equation 3.6 describes the behaviour of electromagnetic wave propagation in complex media. According to equation 3.4, when the microwave directly encounters the plasma, the real part of  $\epsilon_r$  becomes negative for the plasma, indicating collision free behaviour. When a medium is present between the plasma and incident electromagnetic wave, the plasma frequency ( $\omega_p$ ) can be expressed by equation 3.7 [Kaw et al. 1970; Shen et al. 2020]:

$$\omega_p^2 = (1 + \epsilon_d) \omega^2 \quad 3.7$$

In this setup, which is implemented, the effective permittivity of the quartz tube is 4.0,  $\epsilon_d$  is dielectric constant of the medium and the incident electromagnetic wave is operating at the frequency of 2.45 GHz.

### 3.2.2 Plasma Equations

The governing equations for plasma generation are given by the Boltzmann transport equations and drift-diffusion formulae. The electron governing equations describe a system that calculates the time changes for electrons inside the quartz tube, which depend on the outgoing and incoming electron flux passing through the quartz tube and inner generation. The electric field vector, electron diffusion coefficient, and electron mobility affect both the electron density and energy of electrons. Equations 3.8 and 3.9 depict the changes in electron density with time and spatial distribution according to Boltzmann equations. Equations 3.10 and 3.11 further illustrate

the modifications in electron density energy over time as well as spatial distribution using drift-diffusion formula.

$$\frac{\partial n_e}{\partial t} + (u \cdot \nabla) n_e + \nabla \cdot \Gamma_e = R_e \quad 3.8$$

$$\Gamma_e = -(\mu_e \cdot E) n_e - D_e \cdot \nabla n_e \quad 3.9$$

$$\frac{\partial n_\varepsilon}{\partial t} + \nabla \cdot \Gamma_\varepsilon + E \cdot \Gamma_\varepsilon = R_\varepsilon - (u \cdot \nabla) n_\varepsilon \quad 3.10$$

$$\Gamma_\varepsilon = -(\mu_\varepsilon \cdot E) n_\varepsilon - D_\varepsilon \cdot \nabla n_\varepsilon \quad 3.11$$

$\Gamma_\varepsilon$  represents the electron flux and  $\Gamma_e$  denotes the electron energy flux.  $n_e$ ,  $\mu_e$ ,  $n_\varepsilon$ ,  $\mu_\varepsilon$ , and  $u$  denote represent the electron density, electron mobility, electron energy density, electron energy mobility, and vector velocity of the fluid respectively.  $D_e$  signifies the electron diffusion coefficient,  $D_\varepsilon$  while  $D_\varepsilon$  signifies their energy diffusivity. Additionally,  $R_e$  expresses the rate of change in electron density and  $R_\varepsilon$  represents energy gain or loss due to inelastic collisions [Shen et al. 2020]. The gas flow in the quartz tube can be described using equations 3.10 and 3.11, which involve mass continuity and Navier-Stokes equations.

$$\frac{\partial \rho}{\partial t} + \nabla \cdot (\rho u) = 0 \quad 3.10$$

$$\rho \frac{\partial u}{\partial t} + \rho (u \cdot \nabla) u = -\nabla p + \nabla \cdot \left( \mu (\nabla u + (\nabla u)^T) - \frac{2}{3} \mu (\nabla \cdot u) I \right) + F \quad 3.11$$

The pressure, mass density, dynamic viscosity, and unit tensor are represented as  $p$ ,  $\rho$ ,  $\mu$ , and  $I$  respectively. The Lorentz force, which describes the combined effect of electric and magnetic

forces on a charged particles moving through electromagnetic field is denoted by  $F$  [Bouherine et al. 2016]. The heat transfer in this model was primarily governed by equation 3.12, where the temperature ( $T$ ) was determined by the dominant species such as ions and neutral atoms. Equation 3.12 describes the rate of change of energy for these heavy particles.

$$\rho C_P \frac{\partial T}{\partial t} + \rho C_P u \cdot \nabla T = \nabla \cdot (\sigma_k \nabla T) + Q_{el} - Q_w \quad 3.12$$

$C_P$ ,  $\sigma_k$ ,  $Q_{el}$ ,  $Q_w$  represent the specific heat capacity, thermal conductivity, the gain of energy balance due to elastic collisions between heavy particles and electrons, and heat release because of non-elastic collisions, respectively [Baeva et al. 2012].

### 3.2.3 Plasma Chemistry

The interaction between an electromagnetic wave and a plasma medium gives rise to various types of reactions among its constituent particles. These reactions can be broadly classified as elastic and inelastic collisions, excitation and ionization processes, charge transfer, and charge recombination [Shen et al. 2020]. Elastic collisions involve only the exchange of kinetic energy between colliding particles without altering their internal energy. On the other hand, inelastic collisions result in changes to the internal energy of particles. Excitation and ionization reactions play a role in modifying the energy levels of atoms within the plasma and are influenced by interaction probabilities that determine their likelihood of occurrence. Charge transfer reactions involve the exchange of charge between particles and are commonly observed during collisions between ions and neutral particles. Charge recombination can occur in two distinct forms: diffusion and recombination. Diffusion refers to the migration of charged particles towards walls or electrodes, eventually leading to their disappearance. Recombination involves

positive ions capturing free electrons and merging with electrons or negative ions to form new neutral atoms [Baeva et al. 2012].

As argon is used as the carrier gas in this study, an overview of the reactions taking place in the plasma process can be found in Table 3.1.

Table 3.1: Primary chemical reactions and collision mechanisms during argon discharge [Shen et al. 2020; Yadav et al. 2021]

S. No	Process	Reactions	Rate coefficient (m <sup>2</sup> /s)	ΔE
1	Elastic scattering	$Ar + e \rightarrow Ar + e$	$K_{es}$	-
2	Ground state excitation	$Ar + e \rightarrow Ar^* + e$	$K_{ex}$	11.56
3	Ground state ionization	$Ar + e \rightarrow Ar^+ + 2e$	$K_i$	15.8
4	Stepwise ionization	$Ar^* + e \rightarrow Ar^+ + 2e$	$K_{si}$	4.24
5	Super elastic collision	$Ar^* + e \rightarrow Ar + e$	$K_{sc}$	- 11.56
6	Metastable pooling	$Ar^* + Ar^* \rightarrow Ar^+ + Ar + e$	$1.625 \times 10^{-16} T^{0.5}$	
7	Two-body quenching	$Ar^* + Ar \rightarrow 2Ar$	$3 \times 10^{-21}$	
8	Three-body recombination	$Ar^+ + e \rightarrow e + Ar$	$8.75 \times 10^{-39} T^{-4.5} \text{ m}^6/\text{s}$	- 15.76
9	Dissociative recombination	$Ar_2^+ + e \rightarrow Ar^* + Ar$	$1.03 \times 10^{-12} \left( \frac{0.026}{T} \right)^{0.67} \times \frac{1 - \exp(-\frac{418}{T})}{1 - 0.31 \exp(-\frac{418}{T})}$	



10	Electron impact	$Ar_2^+ + e \rightarrow e + Ar^* + Ar$	$1.11 * 10^{-12} \exp(-2.94 + 3(\frac{T}{11600} - \frac{0.026}{Te}))$	
11	Atomic ions conversion	$Ar^+ + 2Ar \rightarrow e + Ar + Ar_2^+$	$7.5 * 10^{-41} T^{-1} m^6/s$	
12	Molecular ions dissociation impact	$Ar_2^+ + Ar \rightarrow 2Ar + Ar^+$	$6.06 * 10^{-12} \exp[-\frac{12580}{T}]$	
13	Diffusion	$m \rightarrow wall(Ar, Ar^+, e, Ar^*, Ar_2^+)$		

### 3.2.4 Modelling Parameters

The model is designed for Multiphysics finite element modeling, and the important variable parameters that influence plasma dynamics are presented in Table 3.2. This data is derived from the experiments and variety of literature references [Zaitsev et al. 2021; Shen et al. 2020].

Table 3.2: Variable parameters implemented in the model

Parameters	Value
Temperature of carrier gas (Argon)	298.15 K
Flow rate of the carrier gas	200 mL/min
Microwave Power	1000 W
Frequency	2.45 GHz
Pressure in the system	1 bar

### 3.3 Simulations

Model calculations were conducted under atmospheric pressure, considering specific gas flow rates and initial gas room temperatures at the tube inlet, as well as microwave power of 1000 W input as given in the Table 3.2. Figure 3.4 illustrates the dynamic variations in calculated plasma temperature within the quartz tube.

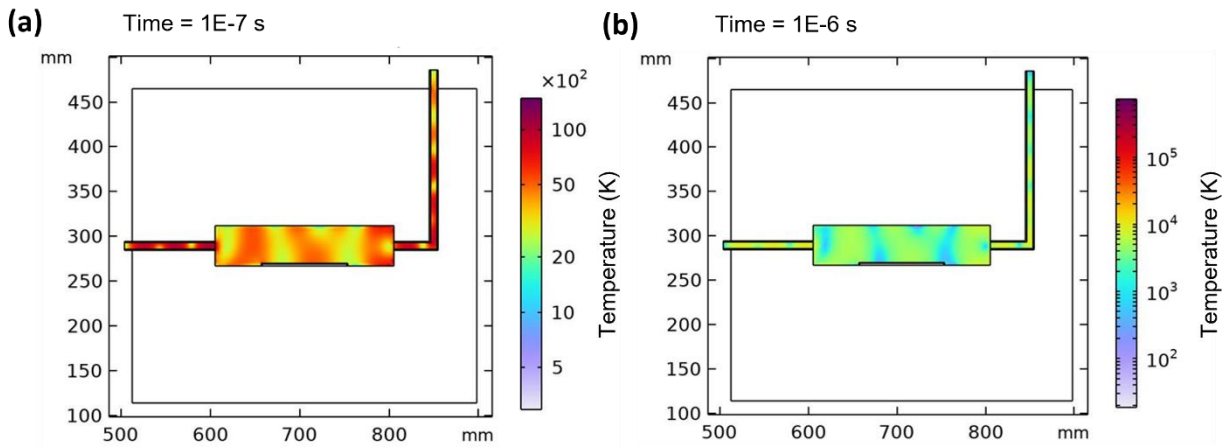


Figure 3.4: Contour temperature plots of plasma temperatures in quartz tube at a) 1E-7 seconds  
b) 1E-6 seconds

The presence of plasma throughout the quartz tube, generated by microwaves with a power of 1000 W, can be observed. Inside the quartz tube, temperatures reaching up to 1595 – 1667 K (1322 – 1394 °C) are evident in Figure 3.4b. However, these temperatures show inconsistency within the quartz tube due to factors such as random particle collisions, variations in plasma density, and different resonant wave modes interacting with the gas that generates the plasma [Shen et al. 2020]. It is important to note that this plasma is significantly influenced by electron potential, microwave power, gas flow rate and pressure within the system.

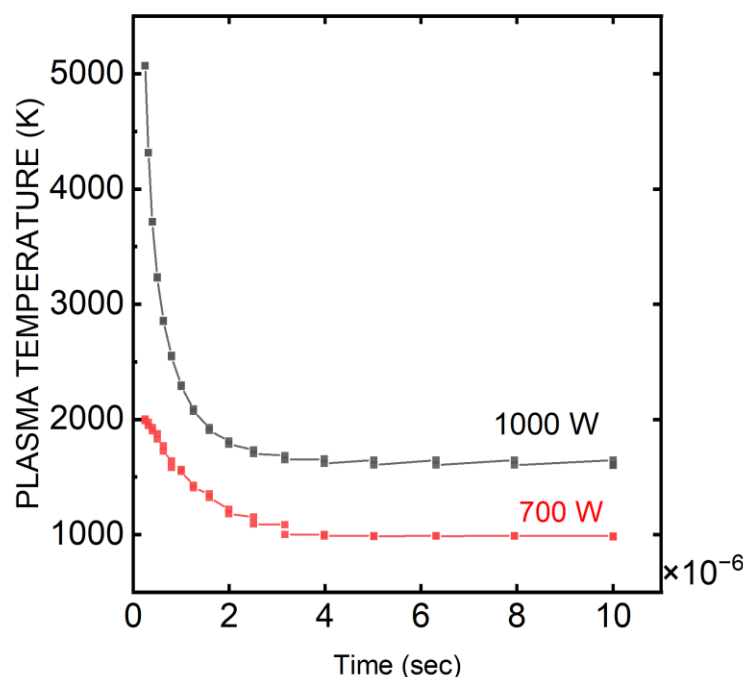


Figure 3.5: Temperature in quartz tube progressing over the time (1000 W, 700 W)

Figure 3.5 illustrates the axial temperature changes observed within the plasma in the quartz tube during the microwave plasma process. The higher (1000 W) input of microwave power effectively excites the argon gas, leading to rapid ionization and collision reactions. This initial burst of energy causes an immediate spike in temperature, reaching approximately 5,000 K (4726 °C) for 1000 W and 2000 K (1726 °C) for 700 W. However, this intense reaction quickly stabilizes within a very short time frame as seen in Figure 3.5. As shown in Figure 3.5, the temperature stabilizes at around 1600 K (1327 °C) for 1000 W and 980 K (706 °C) for 700 W. At a gas flow rate of 250 mL/min, most of the heat transferred to the gas through elastic collisions with electrons is dissipated through thermal conduction to both fibres and tube walls. The increased temperatures observed at specific spots along the quartz tube are attributed to localized electron potential present in those areas [Baeva et al. 2012]. Based on this simulation, it can be inferred that the carbon fibres

in the crucible experience temperatures approximately in the range of 1322 - 1394 °C at microwave power of 1000 W.

Figure 3.6 depicts the electric field distribution within the microwave cavity, as calculated. The maximum magnitude of the electric field norm in the cavity is reached at 1E-7 seconds and quickly stabilizes. When the electric field magnitude is unstable, it indicates that plasma has not been initiated in the chamber. Once the electric field stabilizes and becomes continuous, surface waves propagate and excite the carrier gas to generate plasma. This phenomenon can be attributed to both generation and propagation of surface waves which carry microwave energy, leading to excitation of previously unexcited plasma.

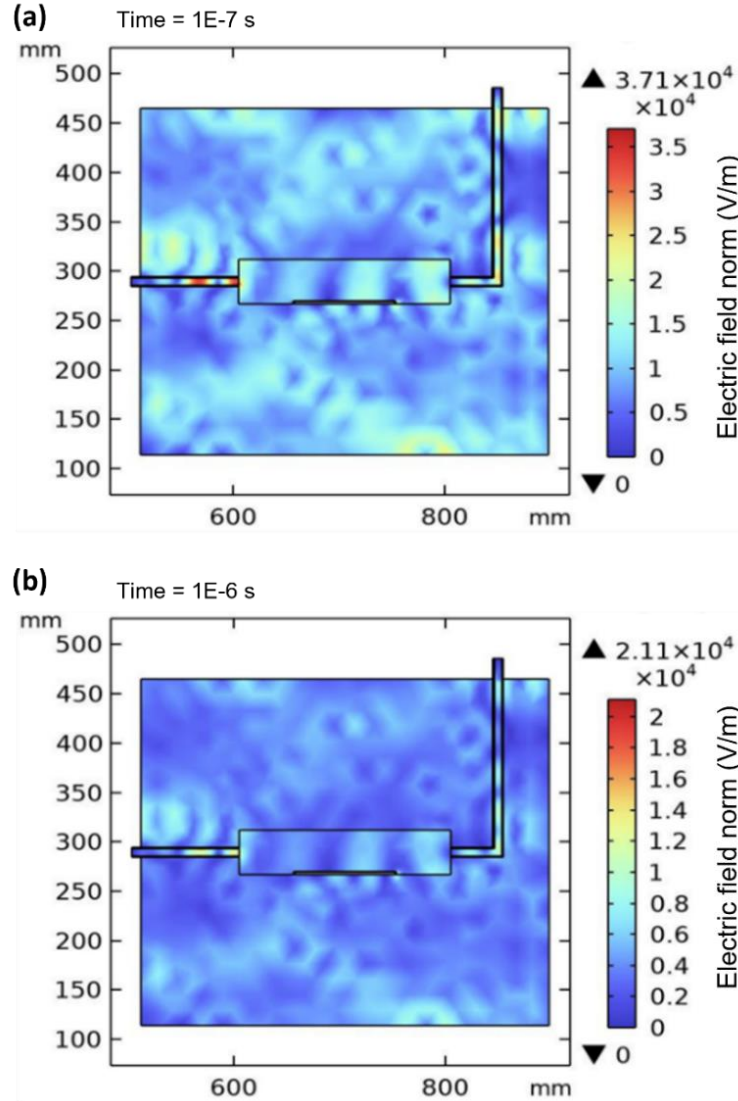


Figure 3.6: Electric field norm dynamics at a) 1E-7 seconds b) 1E-6 seconds

In the current model, the behaviour of electron potential can be explained through a series of distinct phases. Firstly, there is a potential barrier within the plasma that prevents interference from external factors and promotes internal equilibrium. The applied electromagnetic field cannot significantly alter the particle balance within the plasma under these conditions when insufficient power is supplied over a short time span for collisional reactions [Yadav et al. 2021]. Secondly, once a sufficient energy threshold is reached and capable of disrupting the internal balance of the

plasma, stronger collisions occur resulting in a rapid increase in electron potential reaching values on par with 5000 K (4726 °C) as seen in Figure 3.5 within a relatively short duration. Finally, dynamic equilibrium occurs when there is an approximate equivalence between charged particles lost due to diffusion to exterior walls and those gained within the plasma itself [Baeva et al. 2012]. Figure 3.7 depicts the electron potential in the quartz tube during microwave plasma processing.

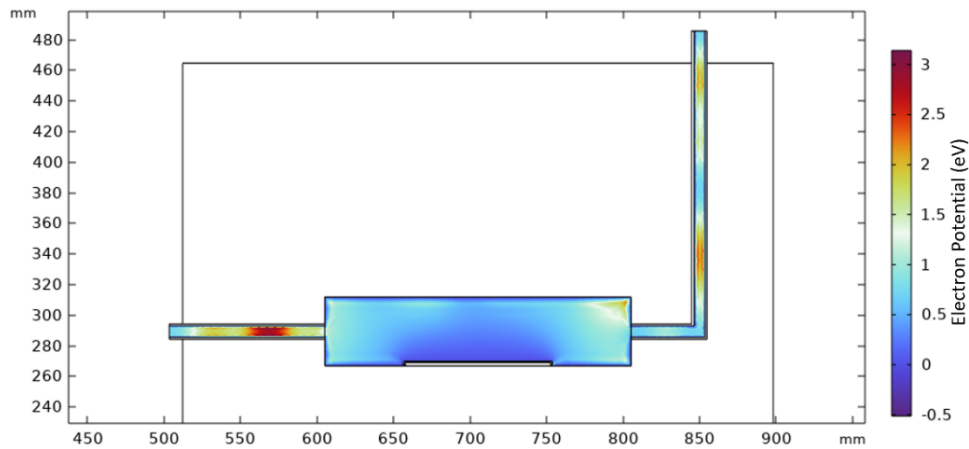


Figure 3.7: Electron potential distribution in the quartz tube

### 3.4 Validation

To validate the accuracy of our current plasma simulation model, two distinct methods were employed for comparison. Firstly, temperature measurements were obtained using a pyrometer operating on a two-color model, which relies on the comparison of measurements acquired from two different wavelengths. This approach is particularly suitable for measuring fine spots accurately. The pyrometer was strategically positioned to focus on the surface of the carbon fibres and was able to transmit measurements through the quartz tube continuously during plasma generation, as depicted in the Figure 3.8. The obtained data from this method indicated an average

temperature of approximately 1300 °C within our custom-designed setup while the plasma was being generated as shown in the Figure 3.8.

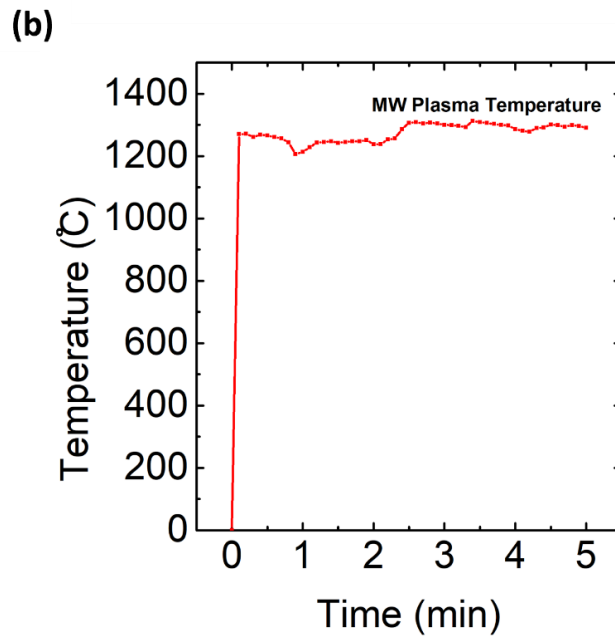
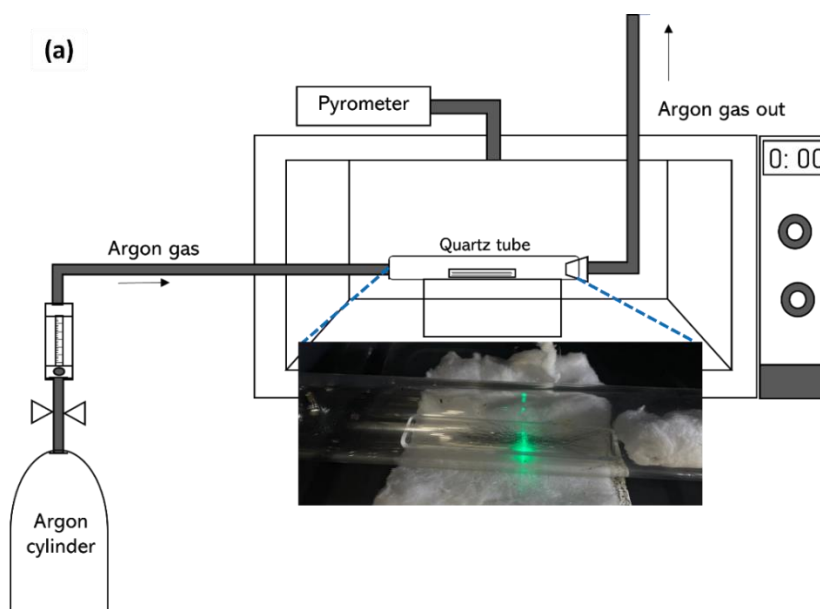


Figure 3.8: a) Arrangement of pyrometer in the setup b) Temperature – plot measurement

This simulated model closely mirrored these experimental conditions, yielding temperatures in the range of 1322 - 1394 °C. This comparison highlights the reliability and precision of our simulation model in accurately reproducing the actual experimental setup. It is important to note that slight discrepancies may arise due to factors such as reflection and refraction as the pyrometer's laser passes through the quartz tube, as well as the inherent rapidity of plasma, which may not be entirely present within the tube.

The second approach involves comparing the simulation results to existing studies. Although it is challenging to directly validate the custom-designed microwave setup using the same existing study, various distinctive microwave plasma setups have been utilized in previous research. Zaitsev et al. conducted plasma treatments on cellulose fibres and determined a plasma temperature of approximately 1300 °C, which aligns with the required temperature for thermal carbonization [Zaitsev et al. 2021]. However, the one key difference between their study and ours lies in the geometry of the setup and the specific material being treated. The geometry of the setup plays a significant role in determining how microwaves interact with the plasma, which in turn influences the temperature.

Table 3.3: Comparison of simulation temperature with existing literature

	<b>Carrier gas</b>	<b>Microwave Power (W)</b>	<b>Plasma Temperature (°C)</b>
Simulation study	Argon	1000	1322 - 1394
Experimental value from Literature [Zaitsev et al. 2021]	Argon	1000	1300



### 3.5 Summary

The microwave plasma simulation was carried out using COMSOL™ Multiphysics software. The simulation was conducted on a computer with an i7-7500U CPU and 16 GB RAM, completing the task in approximately 913 seconds. The model utilized integration of electromagnetic wave with the plasma physics to simulate the model. This study provided information about the temperatures within the plasma when exposed to microwaves of 1000 W, as well as insights into electron potential and overall plasma behaviour. From simulation, it was evident that temperatures of around 1322 – 1394 °C were generated in the quartz tube with the help of plasma. It allowed for optimization of the process and power based on these findings. The main objective of this simulation was to gain a thorough understanding of plasma behaviour while accurately determining its temperature within the experimental setup, which was successfully achieved.

## CHAPTER 4. EXPERIMENTS

The discussion of material properties of precursors, pre-processing of asphaltene feedstocks, fibre manufacturing steps including melt-spinning, post-treatment of fibres are discussed in this section. It also describes the post-treatment processes, including furnace stabilization and microwave plasma thermal treatment, along with a detailed experimental setup.

### 4.1 Materials

Asphaltene samples, designated as S-1 and S-2, were sourced from Alberta Innovates, potentially originating from distinct locations in the northern region of Alberta. These samples, obtained in powdered form, had previously undergone industrial-level deasphalting processes. Although the specific composition of asphaltenes from Alberta Oilsands can vary based on the isolating solvent, they share substantial similarities. Table 4.1 presents the chemical compositions for asphaltenes precipitated using n-pentane and n-heptane. This study primarily emphasizes the utilization of the S-1 sample, due to its favorable melting point, rendering it suitable for melt-spinning, a characteristic not shared by S-2, which exhibits higher melting points.

Table 4.1: Sample data obtained from Asphaltene sample Bank [Alberta innovates 2018]

	Sample S-1 (wt.%)	Sample S-2 (wt.%)
<b>Pentane insoluble content</b>	74	89.7
<b>Heptane insoluble content</b>	66	37.9

## 4.2 Processing of Asphaltene Fibres

To transform Alberta oilsands Asphaltenes (AOA) feedstocks into carbon fibres, several essential steps are employed. These steps include pre-treatment to separate asphaltenes from coke and resins, melt-spinning to transform the precursors into fibrous structures, and post-treatment in order to convert them into carbon fibres. The following sections will provide a detailed account of each of these processes.

### 4.2.1 Pre-treatment

The pre-treatment of asphaltenes is essential before their utilization in spinning processes due to the presence of coke and resins, which can significantly impact the final properties of carbon fibres. Asphaltenes are characterized by their solubility; they are insoluble in n-pentane or n-heptane but soluble in toluene. Following the ASTM standards [D6560-17], the pre-treatment process is designed as a three-step procedure, as shown in Figure 4.1.

In the first step, AOA sample filled in a cellulose thimble is placed within a Soxhlet setup containing pentane at a temperature of 80 °C on a hotplate. This sample is subjected to treatment in pentane for 24-48 hours until the color of pentane in the siphon tube turns pale yellow. Later in the second step, the sample is extracted from the cellulose thimble, thoroughly dried, and subsequently mixed with toluene. The ratio of AOA to toluene is maintained at 1:10, and this mixture is heated and stirred at 90 °C for 1 hour duration. Following this, the mixture undergoes centrifugation at 5000 rpm for 15 minutes. The supernatant portion in the centrifuge tubes gets separated from the coke and later filtered using Whatman grade 4 filter papers.

The filtered solution is placed in a rotary evaporator for overnight processing, aimed at removing and recycling the toluene. At the end, the pretreated asphaltene is collected from the

rotary evaporator and placed in a vacuum oven at 100 °C overnight to further evaporate the solvent.

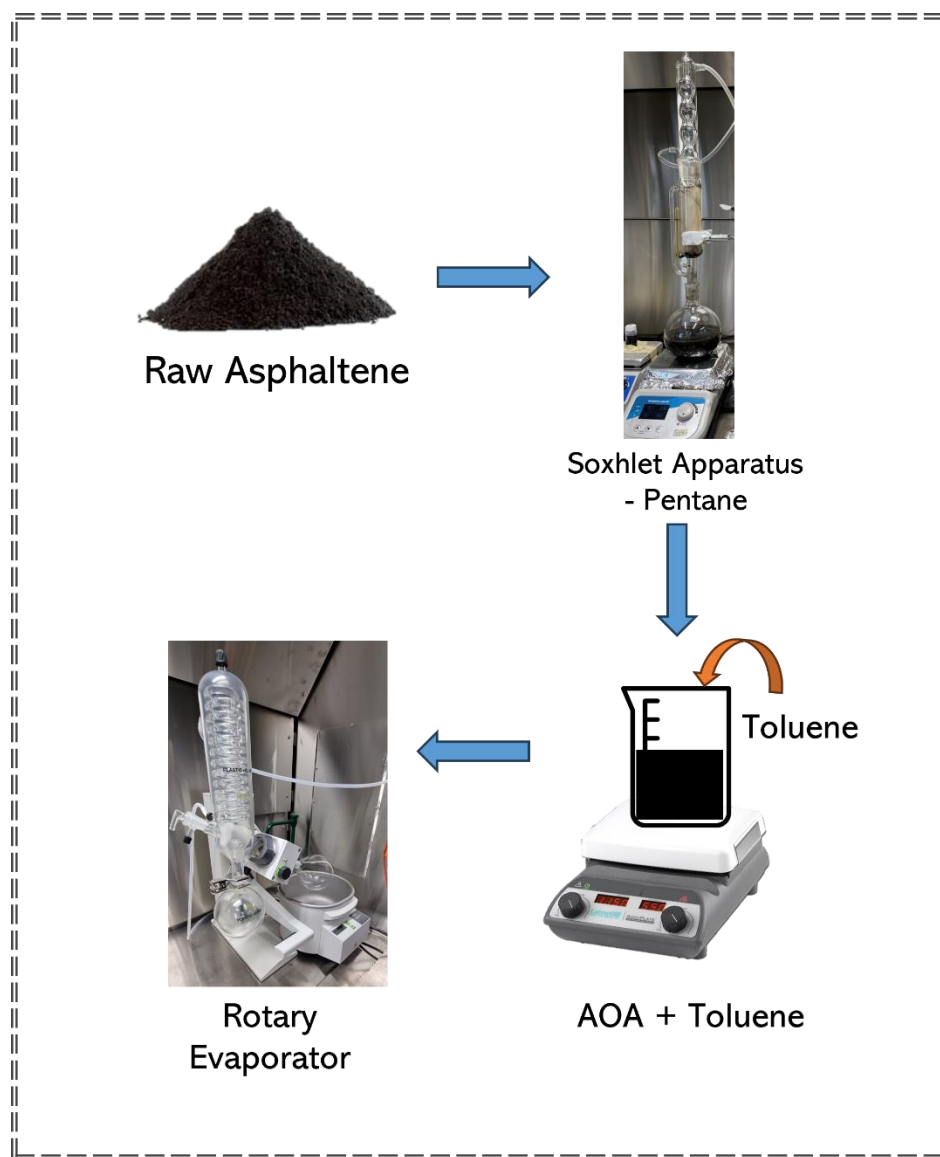


Figure 4.1: Pre-treatment process of Alberta Oilsands Asphaltenes (AOA)

#### 4.2.2 Melt-spinning

Considering the physical and chemical properties of AOA, melt spinning emerges as a well-suited method for fibre production, offering several advantages, including non-solvent use, a straightforward setup, large-scale operations, and significant time and cost savings.

In this study, a twin-screw extruder (EASTMAC) is utilized along with a melt pump (TrusTech) and a spinneret featuring a 0.5 mm nozzle to fabricate fibres. The feed sample is introduced into the twin-screw extruder through a hopper. Within the extruder, three heating zones facilitate the complete melting of the sample, and the screws convey the molten material to the melt pump section. Each of the zones is heated to 90 °C, 140 °C, and 240 °C, respectively. The melt pump's function is to regulate the flow rate of the molten sample to the spinneret, and it is set to 15 rpm, which corresponds to a pumping capacity of 15 cc of sample. The spinneret featuring a nozzle of 0.5 mm is employed for fibre extrusion. The melt-pump and spinneret sections are equipped with heaters and heated up to 240 °C to ensure the molten sample flows smoothly through these different sections. After exiting the spinneret, the fibres are passed through a heat chamber, where they are stretched and collected on a godet rotating at a speed of 200-300 rpm. This process is crucial for achieving fibres with thin diameters. The entire setup is shown in Figure 4.2

Precise control over the temperatures of the three heat zones in the extruder, melt pump, and spinneret sections, along with the rotational speed of the extruder, melt pump, and godet is maintained to achieve the desired thin fibre output.

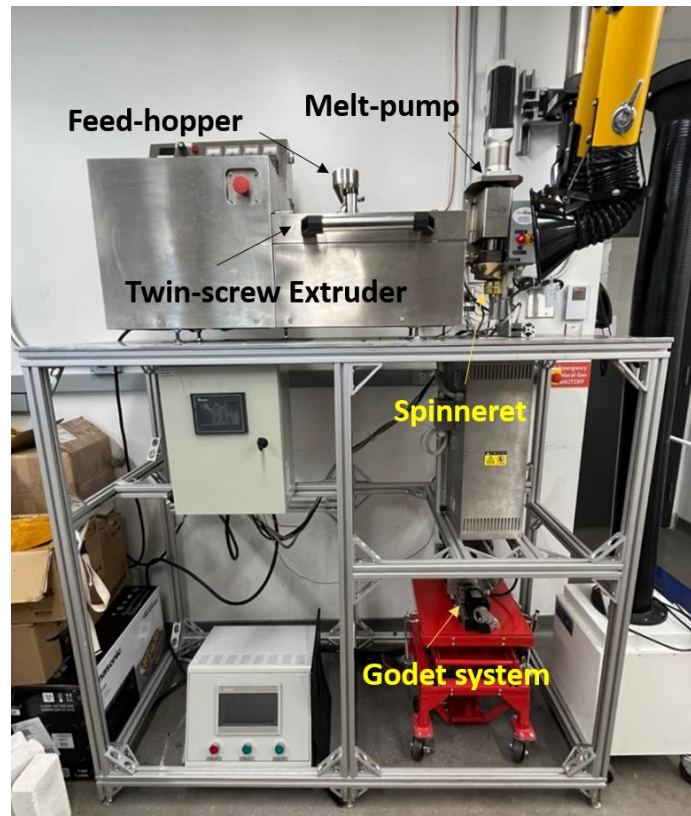


Figure 4.2. Twin-screw extruder setup with godet system

#### 4.2.3 Conventional Stabilization

The fibres obtained from the spinning process, referred to as "as-spun fibres," undergo a post-treatment involving a tube furnace. One of the crucial steps in this post-treatment is known as stabilization, which plays a pivotal role in eliminating volatile gases, converting the fibres into thermoset materials, and enabling cyclization and crosslinking. During this process, the spun fibres are affixed to a ceramic plate using Kapton tape (as shown in Figure 4.3). This setup imparts tension to the fibres, preventing shrinkage and deformation. The stabilization procedure is conducted across a range of temperatures, with optimization aimed at achieving improved results. The fibres are initially subjected to a temperature of 220 °C, with a gradual heating rate of 1 °C per minute and maintained at this temperature for 4 hours. Following, the temperature is raised to 280

°C at the same heating rate of 1 °C per minute and held at this temperature for another 4 hours. Throughout this process, an air atmosphere is maintained, with a flow rate of approximately 400 mL/min. Following the completion of the stabilization process, the samples are removed once the furnace has sufficiently cooled down and are processed for the following steps.

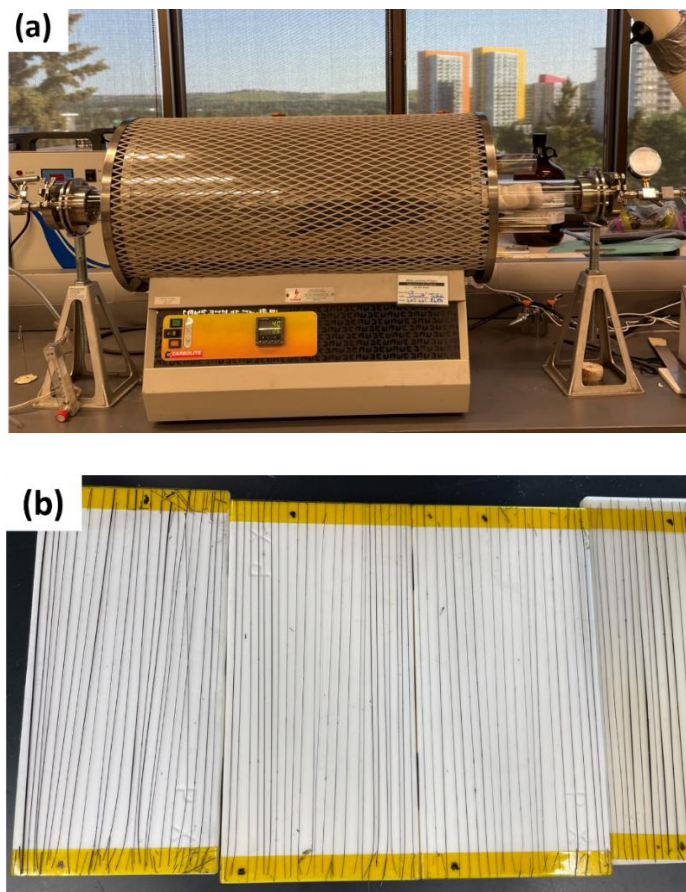


Figure 4.3. a) Tube furnace setup used for stabilization process, b) Sample prepared on ceramic plate for stabilization process

### 4.3 Microwave Plasma Carbonization

The evaluation of the microwave plasma treatment method on asphaltene-derived carbon fibres represents a pivotal aspect of this research, as it encompasses a comprehensive analysis of

various crucial properties. The experimental setup involves a conventional microwave oven, a custom-designed quartz tube, and an argon cylinder. The chosen quartz material ensures thermal stability at elevated temperatures and efficient microwave transmission. The setup incorporates a quartz crucible for sample placement within the quartz tube, where argon gas is introduced to establish a controlled environment. The microwave oven operates at different power settings, inducing plasma generation within the quartz tube.

This experimental configuration involves the utilization of a conventional microwave oven with a maximum power output of 1000 W, coupled with a custom-designed quartz tube and an argon cylinder. To prevent microwave leakage in the conventional microwave oven, two appropriately sized holes, each slightly larger in diameter than the quartz tube, are drilled, and aluminum tape is meticulously applied. The choice of quartz material is deliberate, given its commendable thermal stability at high temperatures and efficient transmission of microwaves. Within the microwave oven, the quartz tube is strategically positioned to ensure that the emitted microwaves from the magnetron predominantly impact the longitudinal axis of the tube.

The sample is placed within a quartz crucible, which is then positioned in the center of the larger quartz tube. Argon gas is introduced from the left side of the setup, as shown in Figure 4.4a, at a flow rate of 300 mL/min. Silica bricks provide support for the setup. The microwave oven is operated at different power settings, leading to the generation of plasma within the quartz tube, as shown in Figure 4.4(b).



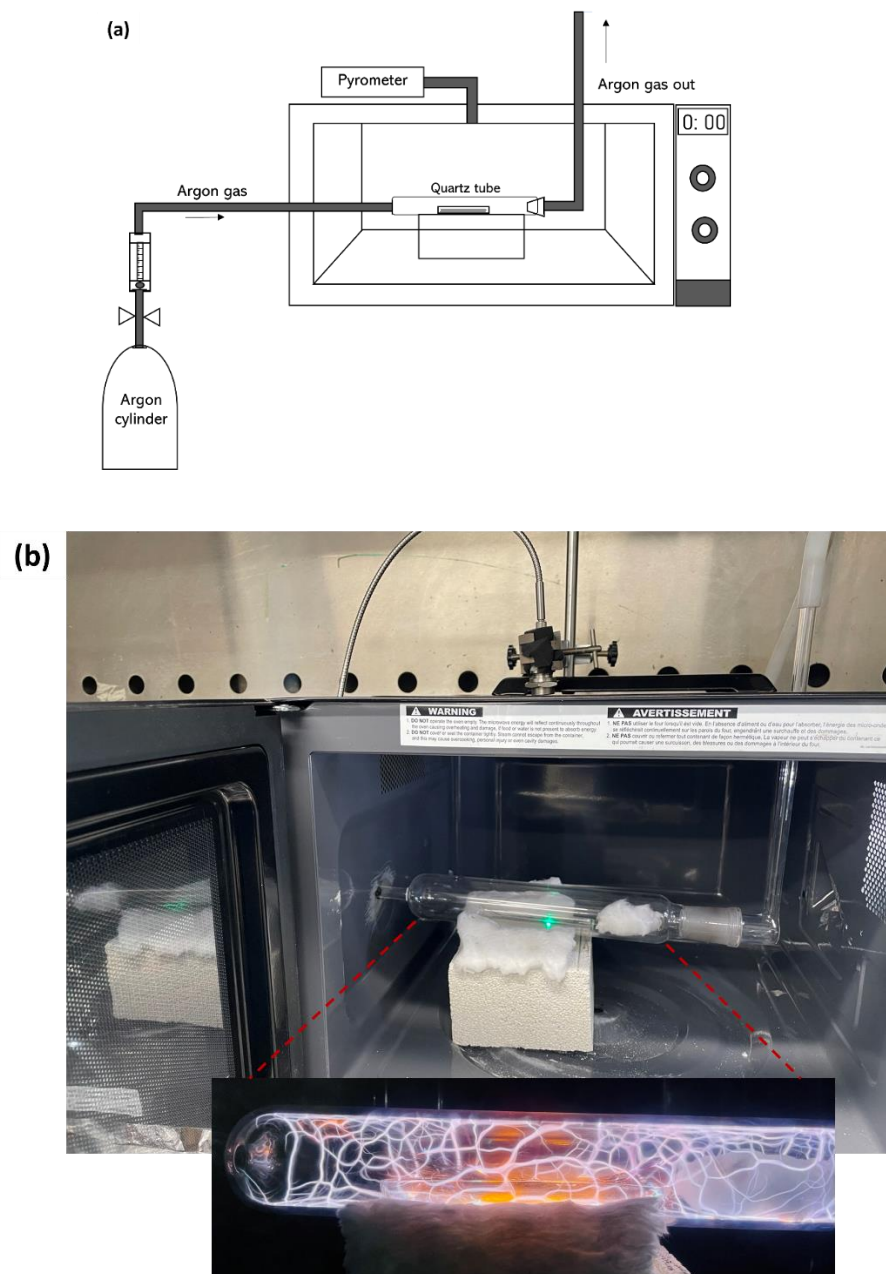


Figure 4.4: (a) Schematic diagram of microwave plasma setup, (b) Quartz tube setup housed in conventional microwave oven

The quartz tube undergoes thorough purging for a minimum of 10 minutes to establish a complete argon environment, ensuring the absence of any other gases. At the top of the microwave

oven, a fibre optics pyrometer (2MH1CFV model) is installed for temperature measurement. This pyrometer employs a 2-color model, comparing measurements from two different wavelengths, which ensures independence from variations in emissivity and remains unaffected by dust or other contaminants. The 2C mode employed enables accurate temperature measurements for objects, such as fibre, that are smaller than the measurement spot. The pyrometer boasts a temperature sensing range of 500 °C to 3000 °C, with a spectral range of 1.45 to 1.75  $\mu\text{m}$ . Careful adjustments are made to focus the pyrometer, ensuring that the fibre sample falls within the range of 15 cm to 35 cm. The pyrometer exhibits a rapid response time, measured in milliseconds.

The careful adjustments made to focus the pyrometer within a specified range ensure that temperature measurements accurately reflect the conditions experienced by the fibre sample. Overall, this detailed experimental setup, combined with the sophisticated temperature measurement capabilities of the pyrometer, provides a robust foundation for the subsequent analysis of chemical, morphological, crystallographic, and mechanical properties of asphaltene-derived carbon fibres subjected to microwave plasma treatment.

## **4.4 Testing Conditions**

### *4.4.1 Element Analysis and SEM*

Elemental analysis plays a crucial role in quantifying the degree of carbonization and evaluating the elemental composition of microwave plasma-treated asphaltene fibres. Before undergoing elemental analysis, asphaltene-derived carbon fibre samples were finely ground. The analysis was conducted using an Elementer Unicube CHNS analyzer, and four sets of samples were tested. To facilitate SEM imaging, the fibres were chopped. Scanning Electron Microscopy (SEM) was performed using a Phenom XPro Scanning Electron Microscope to examine samples

exposed to various treatment durations, including conventionally carbonized asphaltene fibres and microwave plasma-treated carbon fibres.

#### 4.4.2 Spectroscopic and Crystallographic Properties

X-ray diffraction analysis was conducted using the Bruker D8 Advance to study the structural characteristics of carbon materials within microwave plasma treated asphaltene-derived carbon fibres, yielding insights into lattice constants and diffraction planes. A Cu K $\alpha$  laser source ( $\lambda = 0.15418$  nm) was used at 40 kV and 25 mA, over the scanning range of 10° - 80° to observe the structural change of asphaltene-derived carbon fibres after the microwave-plasma treatment process. To quantify these structural changes, important parameters including crystalline thickness ( $L_c$ ), layer-plane length parallel to the fibre axis ( $L_a$ ) and the average interlayer spacing ( $d$ ) were calculated using Bragg's and Scherrer's formulae [Alarifi et al. 2015] as shown below.

$$d = \frac{\lambda}{2 \sin \theta} \quad (5.1)$$

$$L = \frac{K\lambda}{\beta \cos \theta} \quad (5.2)$$

where  $\theta$  is the Bragg's angle in degrees,  $\lambda$  denotes the wavelength of the X-ray used, which is 0.15418 and  $\beta$  is the full-width half maximum of a given peak in radians. In the case of  $L_c$  and  $L_a$ , the shape factor  $K$  is set to 0.89 and 1.84, respectively. Scherrer's equation was applied to calculate the values of  $L_c$ , representing the stacking height of layer planes from the width of the (002) reflection. The crystalline and molecular structures of asphaltene-derived carbon fibres were characterized using a Teledyne Princeton Instruments IsoPlane 81 Raman Spectrometer with a PSU-H-LED 532 nm laser source. An objective lens with a resolution of 100x was employed to focus the laser beam onto the sample and capture the resulting backscattered Raman radiation

signal. The laser beam was directed perpendicularly onto the sample, generating a spot diameter of approximately 1  $\mu\text{m}$ . The incident spot diameter was larger than the size of the carbon microcrystalline structures present within the carbon fibres. To ensure the credibility of the obtained results and to derive a mean crystallization degree, Raman measurements were conducted at various positions across the sample surface. These positions included the central region, edge areas, and corners of the sample, ensuring comprehensive coverage and representing the overall heterogeneity of the material. By systematically capturing data from multiple positions, the aim was to provide a robust and representative assessment of the crystallization degree, minimizing the impact of potential localized variations within the sample. Key Raman parameters, such as band position, peak areas, and intensity were obtained using Lorentzian curve-fitting procedure. The band area ratio of D band to that of G band was used to represent the carbon microstructure and the degree of carbonization.

#### *4.4.3 Mechanical Properties*

To evaluate the effects of microwave plasma treatments, this study examines the mechanical properties of conventionally carbonized and microwave-plasma treated asphaltene-derived carbon fibres. The assessment includes testing for tensile strength and Young's modulus using a tensile tester (Mark-10 ESM Motorized Force Tester equipped with an M5-05 force gauge) following ASTM D3822/D3822M-14 standards. In this standard tensile testing method, a single fibre is securely fixed to paper tabs using epoxy at both ends to prevent any slippage during testing, as shown in Figure 4.5. The length of the single fibre segment between the tabs remains consistently maintained at 20 mm. To conduct the test, the fibres are mounted within frames on to the grips of the testing apparatus. Subsequently, both sides of the paper tabs are centrally cut, and tension is applied to the fibre at a rate of 2 mm/min. After completion of the test, a Zeta 20 Optical

Profiling Microscope is used to determine and measure the fibre diameter which is then utilized in calculating cross-sectional area for determining tensile strength. The tensile strength and Young's modulus were calculated by plotting the stress-strain curve using data from the Mark-10 testing equipment. After subjecting numerous fibres with diameters ranging from 55-80  $\mu\text{m}$  to conventional carbonization and microwave plasma carbonization, tensile testing was conducted.

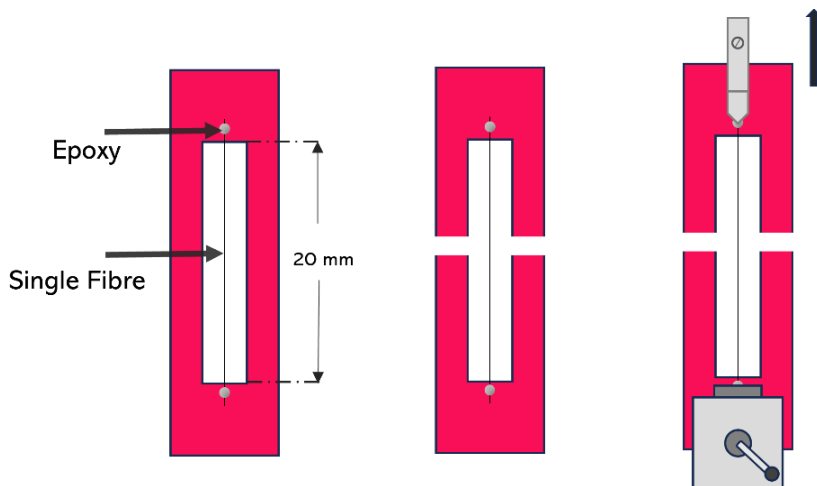


Figure 4.5: Schematic diagram of fibre prepared for tensile testing

#### 4.5 Summary

The experimental procedures closely followed the general manufacturing steps for carbon fibres, involving the pre-treatment of asphaltene samples, fibre spinning, and furnace stabilization. A custom-designed setup featuring a quartz tube was employed for the carbonization process. The pyrometer was precisely positioned to ensure that the measurement spot was accurately focused on the fibres. Microwave plasma thermal treatments are conducted over varying durations of treatment time. Subsequently, all the samples were prepared for further characterizations to assess their respective effects.

## **CHAPTER 5. RESULTS AND DISCUSSIONS**

This comprehensive study focuses on investigating the production of carbon fibres using asphaltene precursors, employing melt-spinning and subsequent microwave plasma thermal treatments. Different analytical techniques were selected to evaluate the transformative impact of microwave plasma treatment on asphaltene-derived carbon fibres. The elemental composition was analyzed using Element analysis to reveal detailed alterations in carbon, hydrogen, nitrogen, and oxygen content during diverse thermal treatments. The morphological evolution of the fibres was meticulously examined through scanning electron microscopy (SEM), providing a visual representation of surface changes induced by varying microwave plasma durations. In parallel, crystallographic shifts were observed through X-ray diffraction (XRD), offering insights into the layered graphite-type structures developed during both conventional carbonization and microwave plasma treatments. Raman spectroscopy further explored the structural changes, revealing the conversion of carbon hybridization states and the emergence of ordered graphitic structures under the influence of microwave plasma. The mechanical properties were assessed through tensile testing, scrutinizing the tensile strength and elastic modulus of fibres subjected to various treatment durations. Finally, a comprehensive exploration into the mechanism of microwave and microwave plasma elucidated the intricacies of heat transfer and plasma-induced effects on fibre structure.

### **5.1 Element Analysis**

Element analysis is vital in quantifying the degree of carbonization and assessing the elemental composition within microwave plasma treated asphaltene fibres. The results yielded information on concentrations of carbon (C), hydrogen (H), nitrogen (N), and sulfur (S). The

oxygen content was calculated by deducting the sum of these elements from 100. The carbonization process involves the partial removal of non-carbon elements at elevated temperatures which enhances the strength of the fibres [Park 2018]. Samples consisting of conventionally carbonized asphaltene fibres and microwave plasma treated carbon fibres, exposed to different treatment durations were examined. The resulting findings are presented in Table 5.1.

Table 5.1: Comparison of Element analysis of samples

Sample	%C	%H	%N	%S	%O
Conventionally stabilized fibres	76.80 ± 0.40	4.03 ± 0.18	1.06 ± 0.10	6.93 ± 0.16	11.17 ± 0.50
Conventionally carbonized fibres	87.8 ± 0.18	0.50 ± 0.02	0.60 ± 0.01	5.44 ± 0.09	6.15 ± 0.19
Microwave-plasma (5 min)	82.60 ± 0.09	1.78 ± 0.03	0.73 ± 0.01	6.33 ± 0.10	8.53 ± 0.09
Microwave-plasma (7 min)	83.50 ± 0.07	1.56 ± 0.01	0.77 ± 0.08	6.57 ± 0.02	7.51 ± 0.10
Microwave-plasma (9 min)	87.33 ± 0.22	0.41 ± 0.02	0.66 ± 0.01	5.50 ± 0.08	6.09 ± 0.24

In the traditional carbonization process conducted in a tube furnace at high temperatures of 1150 °C, the carbon content is raised from 76.80% to 87.33%, indicating partial removal of non-carbon elements. However, during microwave plasma treatments, the carbon content gradually

increases with longer treatment duration, emphasizing the significance of treatment time. The reduction of heteroatoms such as hydrogen, nitrogen, and oxygen can be observed in the form of gaseous compounds like carbon dioxide and water. Microwave plasma treatments of 9 minutes result in comparable outcomes to conventionally carbonized fibres, affirming heteroatom removal and effective fibre carbonization.

Based on the results, it becomes evident that there is a clear upward trend in carbon content as the duration of microwave plasma treatment increases. In parallel, the H/C ratio demonstrates a consistent decrease. These parameters play an important role in confirming the extent of carbonization, indicating the conversion of precursor materials into a high-carbon fibre structure, which is important for achieving improved mechanical properties. Additionally, it is important to monitor and manage the elemental composition of the fibres as other elements like sulfur have a significant impact on their mechanical properties [Raskovic & Marinkovic 1978]. Through microwave plasma treatments, there is observed a decrease in sulfur content (6.93% to 5.55%).

## **5.2 Morphological Properties**

Figure 5.1 depicts the surface morphology of conventionally stabilized spun fibres, which are subjected to a furnace at temperatures ranging from 280-350 °C with a slower heating rate of 1-2 °C/min in an air environment. Notably, the outer layer of the fibres shows minimal signs of surface damages or dents. Additionally, it can be stated that there might be a slight increase in diameter corresponding to the presence of oxygen within the fibres following the stabilization process.



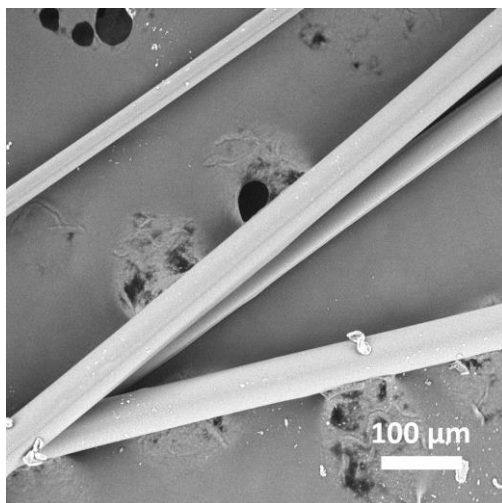


Figure 5.1: SEM image of furnace stabilized asphaltene fibres

During conventional carbonization, the stabilized asphaltene-derived fibres are heated at temperatures around 1150 °C with a heating rate of 5 °C/min in an inert atmosphere. Figure 5.2 shows that little to no surface defects are observed in the stabilized asphaltene-derived fibres. These defects can be attributed to the different reaction mechanisms that occur at higher temperatures in order to remove hetero atoms from the fibres. Carbonization typically leads to changes in microstructure, such as the formation of voids, pores, and minor defects within the fibres. The internal structure of this fibre (as shown in Figure 5.2) does not exhibit an uneven or shell-core nature like mesophase pitch fibres [Edie 1998], indicating complete carbonization throughout its core.

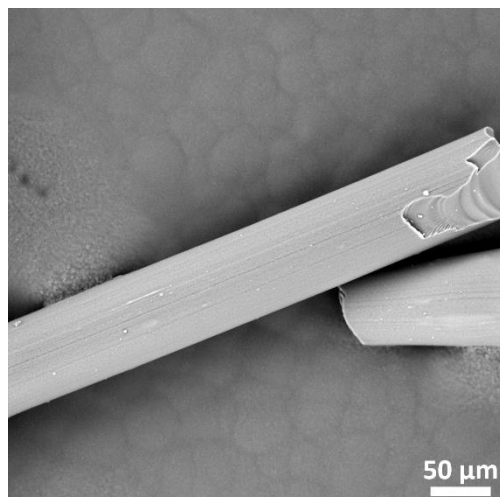


Figure 5.2: SEM image of conventionally carbonized asphaltene fibres

The furnace stabilized asphaltene-derived fibres were subjected to microwave plasma treatments for different durations. The surface morphology of the fibres is evaluated and presented in Figure 5.3. Argon gas is used as the plasma-generating gas to prevent oxidation of the fibres at high temperatures. Asphaltene-derived fibres treated for 5 minutes exhibit dents and pores on their surface, as shown in Figure 5.3 a-b. With longer treatment durations, the level of surface damage increases significantly with various striations and pores, resulting in a decrease in fibre quality.

Argon has lower reactivity compared to other plasma-generating gases such as nitrogen [Farrow & Jones 1994] and oxygen [Yuan et al. 1992]. However, the fibres were still subjected to bombardment by excited argon ions generated by the plasma, resulting in surface damage. When the treatment time was extended to 9 minutes, large-area pits and perforations could be observed on the fibre's surface (Figure 5.3 e-f). The observed surface damage can be attributed to an increase in ion density and electron temperatures within the plasma environment [Kim et al. 2015].

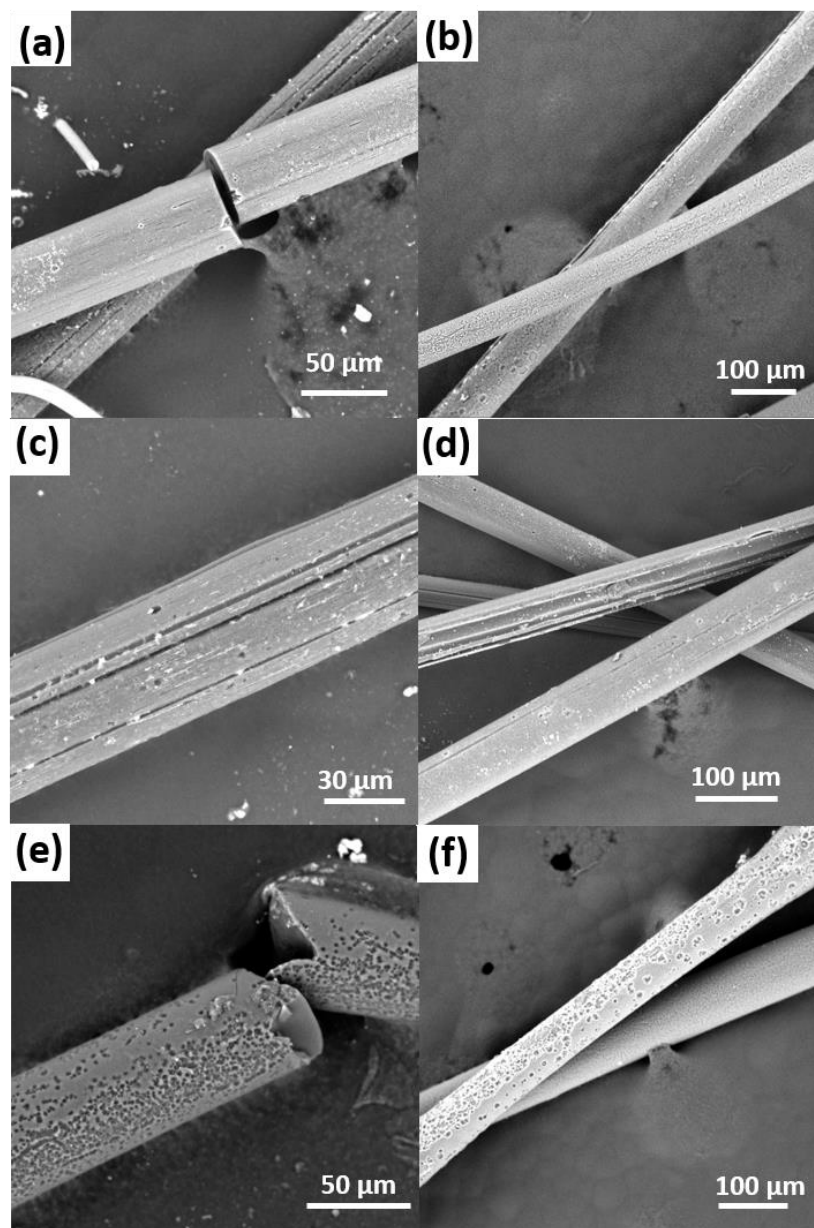


Figure 5.3: SEM images of microwave-plasma treated asphaltene fibres at 1000 W. (a-b) 5 min, (c-d) 7 min, (e-f) 9 min

The SEM images of conventionally carbonized asphaltene-derived fibres (Figure 5.2) exhibit a relatively smooth surface. However, microwave plasma treatments, although effective in treating the fibres at high temperatures, can introduce defects onto the fibre surface due to their

inherent rapidity. The SEM images (Figure 5.3) demonstrate how prolonged exposure to microwave-plasma greatly impacts the quality of the fibres.

### **5.3 Spectroscopic and Crystallographic Properties**

#### *5.3.1 XRD Analysis*

In Figure 5.4, the X-ray diffraction (XRD) patterns provide a comparative analysis between the conventional carbonization of asphaltene-derived carbon fibres and the carbonization process with microwave plasma treatment carried out for different durations. The XRD pattern of carbonized asphaltene fibres shows the diffraction peak at  $2\theta = 23.5^\circ$ , corresponding to the (002) crystallographic plane of graphite crystallites [Havigh & Chenari 2022]. This presence of the (002) peak suggests the development of a layered graphite-like structure during the conventional carbonization of asphaltene fibres.

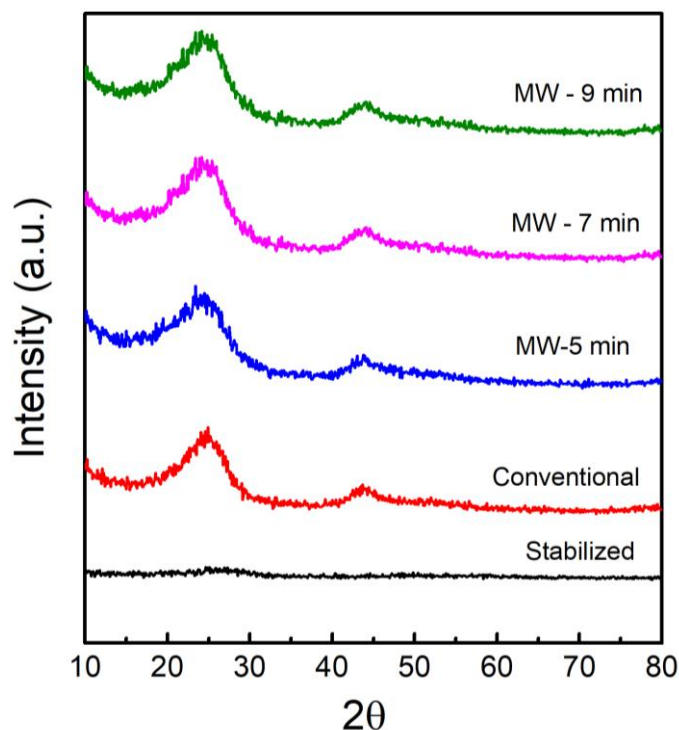


Figure 5.4: Comparative XRD analysis of conventionally carbonized fibres and microwave plasma treated fibres at 1000 W at various durations (5 min, 7 min, 9 min)

Similarly, the XRD patterns of microwave-plasma treated fibres subjected to various treatment durations exhibits the (002) diffraction peaks which serve as a clear indication of the formation of a layered graphite-type structure in these fibres as well. In addition, these patterns provide valuable insights into the structural transformations that occur during the microwave plasma treatment of asphaltene-derived carbon fibres. The observed sharpening of the (002) diffraction peaks with increasing treatment time signifies a progressive enhancement in the degree of crystallinity within the fibres. This suggests that prolonged microwave plasma treatment supports the development of a more ordered and well-defined layered graphite-type structure. The intensity and sharpness of the (002) peak can be correlated with the quality of the carbonization process, indicating that extended treatment durations contribute to a higher degree of structural

organization. Furthermore, the consistency of the (002) diffraction peaks in both conventionally carbonized and microwave-plasma treated fibres underscores the comparable development of this layered graphite-like structure in both processes. Overall, the XRD patterns offer clear insights into the evolving crystalline structure of the carbonized fibres, highlighting the impact of microwave plasma treatment on achieving a desired structural outcome.

The emergence of the (100) peak signifies the development of a highly ordered and graphitic carbon structure, indicative of the regular and repetitive arrangement of carbon atoms [Ryu et al. 2002]. Throughout this process, a transformation occurs wherein some of the  $sp^3$  hybridized carbon atoms, characteristic of graphite-like structures, convert into  $sp^2$  hybridized carbon atoms. This conversion process contributes to the creation of a more organized and crystalline carbon structure [Park 2018]. This structural modification reflects the distinct influence of microwave plasma treatment on asphaltene-derived carbon fibres, setting it apart from conventional carbonization methods. The conversion of carbon hybridization states is a crucial aspect of this structural evolution, underlining the unique impact of microwave plasma treatment on enhancing the ordered nature of the carbon matrix within the fibres.

Table 5.2 presents the estimated microstructural parameters of the asphaltene-derived carbon fibres, including the interplanar spacing ( $d_c$ ), the crystallite thickness ( $L_c$ ), and layer plane length ( $L_a$ ) from the XRD patterns. The results of the study show that with increasing treatment durations, there was a decrease in the  $d_c$  value and an increase in both the  $L_c$  and  $L_a$  values. The microwave plasma treated samples at 9 minutes showed similar values to those treated conventionally through carbonization. The growth of lateral size,  $L_a$ , with longer microwave-plasma treatment durations may be attributed to the removal of hetero atoms [Torres et al. 2017].

As a result, the microwave-plasma treatment promoted structural rearrangements in graphite crystallites leading to their enlargement and enhanced order.

Table 5.2: The average interplanar spacing ( $d_c$ ), the crystallite thickness ( $L_c$ ), and layer plane length ( $L_a$ ) of conventionally carbonized fibres and microwave-plasma treated fibres (1000 W)

Sample	$d_c$ (nm)	$L_c$ (nm)	$L_a$ (nm)
Conventional carbonization	0.188	0.74	1.91
MW-plasma (5 min)	0.197	0.51	1.59
MW-plasma (7 min)	0.193	0.59	1.62
MW-plasma (9 min)	0.191	0.65	1.79

### 5.3.2 Raman Spectroscopy

Figure 5.5 shows the comparative analysis of Raman spectra results of asphaltene-derived carbon fibres at different microwave-plasma treatment times. All samples exhibited two obvious peaks in the first order spectrum ( $1100 - 2000 \text{ cm}^{-1}$ ) at approximately ( $1340\text{-}1380 \text{ cm}^{-1}$ ) and ( $1600\text{-}1630 \text{ cm}^{-1}$ ), which were assigned to peaks D and G, respectively. Peak G is associated with  $E_{2g}$  symmetry stretching vibration mode of  $sp^2$  hybridized carbon atoms in the aromatic layers of the graphite crystalline, which stands for the ordered structure of the carbon fibre [Jawhari et al. 1995].

Peak D indicates the presence of some of disordered structure in the carbon fibre, which is induced by the imperfections of graphite-like sheets and nano-pores in the microcrystalline [Wei et al. 2022]. The intensity of peak G specifically is observed to be increasing with the longer microwave-plasma treatment durations, indicating a formation of higher graphitic structure. This formation typically occurs at temperatures ranging from 900-1200 °C [Banerjee et al. 2021], indicating that the microwave plasma is reaching elevated temperatures and confirming the carbonization process.

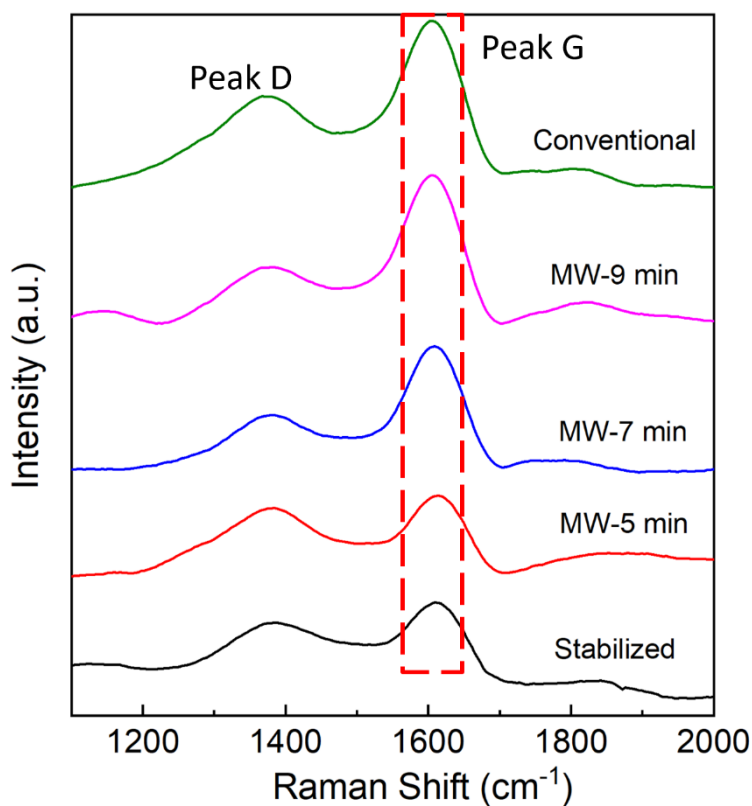


Figure 5.5: Raman spectra of asphaltene carbon fibres after microwave plasma treatment (1000 W) at various durations (5 min, 7 min, 9 min)

In Table 5.3, Raman parameters such as peak positions, peak area, and Intensity ratio has been estimated from Raman peaks and presented. Intensity ratio ( $I_D/I_G$ ) is a crucial parameter that indicates the relative amount of disordered and defective carbon (Peak D) compared to graphitic



carbon (Peak G). The  $I_D/I_G$  ratio decreases as the duration of microwave-plasma treatments increases, which can be attributed to changes in crystallite size and carbon structure [Rahaman et al. 2007].

Table 5.3:  $I_D/I_G$  calculated from obtained Raman peaks of conventionally carbonized and microwave plasma (1000 W) treated fibres

Sampl e	Conventional carbonization (30 mins)	MW-plasma (5 min)	MW-plasma (7 min)	MW-plasma (9 min)
$I_D/I_G$	0.82	0.86	0.85	0.83

The  $I_D/I_G$  ratio of the conventionally carbonized fibres is comparable to that of the fibres treated for 9 minutes in microwave-plasma. However, an increase in surface damage sites was observed with longer exposure times to plasma on the microwave plasma-treated fibres, indicating differences in crystallite size or carbon structures formed between these two methods. A lower  $I_D/I_G$  ratio typically denotes a higher proportion of ordered, graphitic carbon demonstrating  $sp^2$  hybridization, while a higher  $I_D/I_G$  ratio signifies an increased amounts of disordered, amorphous carbon representative of  $sp^3$  hybridization in the fibre [Wang et al. 1990]. In conventional carbonization process, the fibres are gradually heated at a rate of 5 °C/min up to temperatures around 1150 °C. This gradual increase in temperature allows for the orderly transformation of precursor into more graphitic structures while minimizing the structural defects or disordered regions within the fibre, consequently achieving uniform heating throughout the fibre [Zaitsev et

al. 2021]. In microwave plasma treatments, the rapid heating rate and thermal stress have resulted in higher  $I_D/I_G$  ratios signifying the presence of disordered amorphous carbon.

#### 5.4 Thermal Analysis

The power attributed to microwave plasma in the carbonization process can have a significant impact on temperature. However, the use of a multi-modal cavity limits direct contact between microwaves and the quartz tube, resulting in relatively low plasma generation compared to single-mode microwave cavities. During interaction with the quartz tube, some microwaves are lost while most come into contact with argon gas, leading to plasma discharge within the tube. Pressure plays a crucial role in sustaining continuous plasma generation as well as influencing its temperature. In current experiments, pressure inside the tube remains constant at atmospheric level.

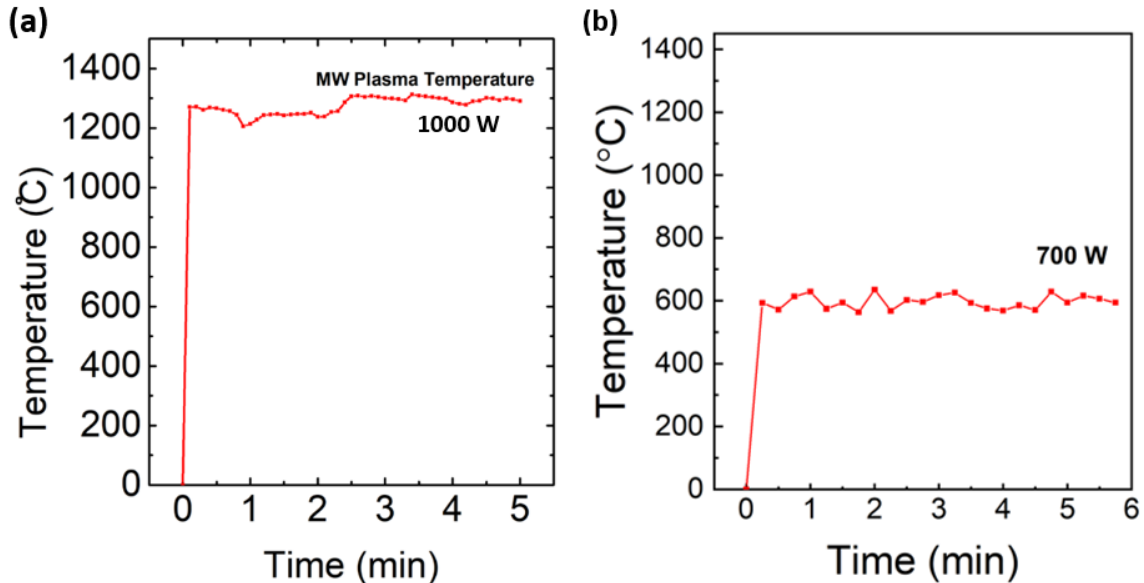


Figure 5.6: Temperature measurement at different power levels from the Pyrometer: a) 1000 W

b) 700 W

A fibre optic pyrometer (Model: 2MH1CFV) have been employed to measure temperatures of plasma generated in the quartz tube. The temperature displayed in Figure 5.6 is derived from experimental data obtained using pyrometer software at different powers. The plasma generated at 1000 W resulted in temperature range of 1210 - 1302 °C, which effectively carried out the carbonization process as observed from the results mentioned above. On the other hand, at 700 W, the plasma was yielding a temperature range of 570 - 635 °C which does not reach the target temperature as shown in Figure 5.6. The carbonization process typically takes place at temperatures between 900-1200 °C. During this process, hetero atoms are eliminated, which promotes the formation of a higher order crystalline structure [Banerjee et al. 2021].

The microwave heating generally operates through direct heat transfer [Menendez et al. 2010]. To support successful plasma generation, it is important to have sufficient microwave power to excite the argon ion composition within the setup. The electron temperature and ion density, which are critical for the plasma generation mechanism, are significantly influenced by the microwave power. It is important to study the behaviour of plasmas at different microwave powers in order to gain a deeper understanding. To achieve this, COMSOL™ Multiphysics software was employed to develop a model and simulate microwave plasma temperatures under varying microwave powers at 2.45 GHz frequency, atmospheric pressure, and an argon environment.

This parametric study provided valuable insights into the relation between microwave power and plasma temperatures and ion densities in the current setup. This study was instrumental in optimizing the process parameters to consistently achieve higher temperatures. The simulated data was compared with the experimental data, as discussed in chapter three. Furthermore, it is

important to validate both simulated results and experimental results by referencing relevant literature.

Zaitsev et al. conducted surface treatments on cellulose fibres using a plasma reactor in an argon and nitrogen environment. In their study, the plasma temperature was determined to be around 1300 °C, which is similar to the temperature required for thermal carbonization. Another study modeled and designed a microwave plasma reactor for gas-phase decomposition at atmospheric pressure conditions. Simulated temperatures of microwave plasma at 700 W resulted in temperatures of approximately 670 °C [Mohsenian et al. 2018].

Table 5.4: Temperature comparison between experiment, simulation, and literature

	<b>Microwave Power (W)</b> <b>(2.45 GHz)</b>	<b>Temperature (°C)</b>
Experimental	1000	1210 – 1302
	700	570 – 635
Simulated	1000	1322 – 1394
	700	692 – 710
Literature value	1000	1300 [ Zaitsev et al. 2021]
	700	670 [ Mohsenian et al. 2018]

There may be several factors that contribute to the discrepancy between the measured value by the pyrometer and the simulated value in this experiment. One potential factor is noise present between the pyrometer and setup. Another consideration is the presence of a quartz tube, which could affect laser pointer measurements of pyrometer due to effects like reflection or scattering on its curved surface. This interference has the potential to hinder or alter temperature measurements. Additionally, there seems to be a difference in values between simulation and literature, possibly because of the type of the microwave generators used and geometric differences in the setup. Some studies have utilized single-mode microwave setups, where the microwaves directly transmit to the gas used for plasma generation without any reflections. Conversely, other studies have designed their setup so that the microwaves are incident on a smaller area of the setup where the sample is located.

## **5.5 Mechanical Properties**

The results, displayed in Figure 5.8, present the average tensile strength and Young's modulus of the furnace stabilized, conventionally carbonized and microwave-plasma carbonized fibres at different durations (5 min, 7 min, and 9 min). The stabilized fibres exhibited a lower tensile strength of 20 MPa, attributed to disordered structure within the fibres. The conventionally carbonized asphaltene-derived carbon fibres exhibited an average tensile strength of approximately 590 MPa. This is supported by the smoother surfaces of the fibres observed in SEM images as well as highly ordered crystalline structures detected through XRD and Raman patterns.

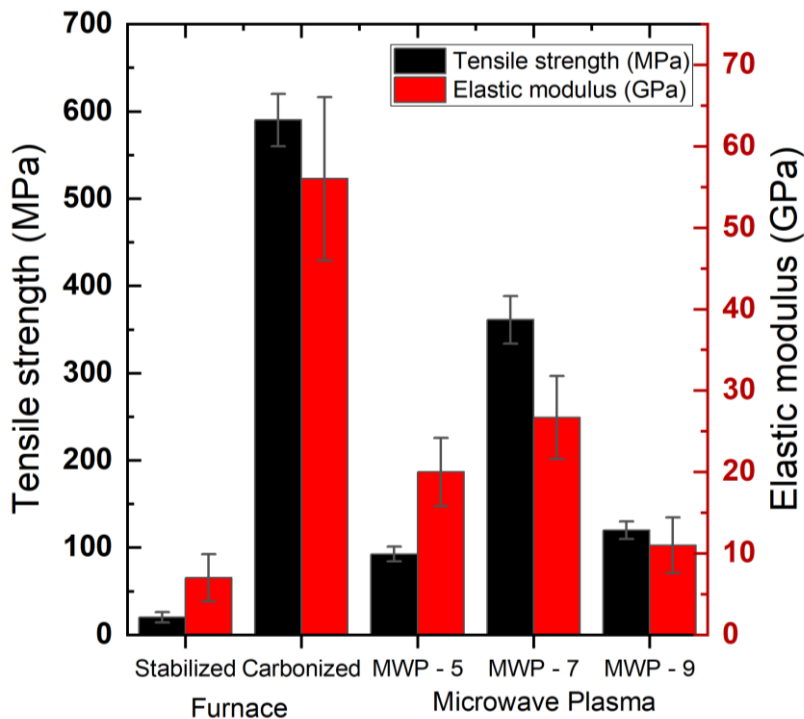


Figure 5.7: Comparison of average tensile strength and elastic modulus in stabilized, conventionally carbonized and microwave plasma treated fibres

The mechanical properties of microwave-plasma carbonized fibres were found to be lower than conventionally carbonized fibres. Fibres treated for 5 minutes exhibited an average tensile strength of 92.5 MPa, while those treated for 7 and 9 minutes had tensile strengths of 361.03 MPa and 120 MPa respectively. As the treatment time increased, the elastic modulus also exhibited a similar trend to that of tensile strength. The tensile strength of the fibres treated for 5 minutes was found to be low, possibly due to incomplete formation of the graphitic structure as indicated by XRD and Raman patterns. However, with an increased treatment time of 9 minutes, both the tensile strength and Young's modulus decreased significantly, likely attributable to the presence of defects, pores, and surface damage caused by the plasma treatment.

Defects in the morphological structure have a significant impact on the overall mechanical properties of the fibres and SEM images of these fibres (Figure 5.3) can provide supporting evidence for these results. Although longer microwave-plasma treatments have resulted in crystalline structure development, the formation of pores and striations on the surface has reduced both strength and fibre quality. This damage is attributed to the rapid nature of plasma processing and longer interaction of fibres with excited argon molecules. The presence of voids in fibre morphology is undesirable as it renders these fibres unsuitable for structural applications [Kim et al. 2015]. The impurities and sulfur content present in the fibres (Table 5.1) can highly impact the spinnability and mechanical properties [Bisheh & Abdin 2023].

The mechanical strengths of carbon fibres produced from different precursors, processed at varying powers and durations under microwave plasma treatment, differ considerably as presented in Table 5.5. Carbon fibres made from cellulose fibres and those made from PAN that have undergone traditional high-temperature carbonization reflect higher tensile strength when compared to fibres treated with microwave plasma. This could be due to the slow and controlled heat in traditional carbonization that allows the precursor to gradually transform without temperature stress [Zaitsev et al. 2021]. In contrast, microwave plasma treatment can cause inconsistent heating and result in thermal tension within large diameter fibres, increasing potential for defects or damaging structural damages. The observed trend in mechanical properties concerning the precursor and fibre diameter can serve as a supporting reason for understanding the mechanical properties of asphaltene-derived carbon fibres as shown in Figure 5.8. Microwave plasma enables efficient carbonization within a span of 6 – 26 minutes due to its rapid heating capabilities.

Table 5.5: Comparative analysis of mechanical properties of different microwave plasma treated carbon fibres

Precursor	Diameter ( $\mu\text{m}$ )	Gas	Microwave Power	Duration	Mechanical Properties	References
PAN – oxidised fibres	12-15	Argon	1000 W	6 minutes	1700 MPa, 110 GPa	Kim et al. 2015
PAN – oxidised fibres	12-15	Argon	1000 W	5 minutes	1450 MPa, 120 GPa	Kim et al. 2015
Cellulose + 0.3% CNT – oxidised fibres	17-23	Argon	320 W	5 minutes	240 MPa, 12 GPa	Zaitsev et al. 2021
PAN- oxidized fibres	14-18	Nitroge n	1000 W	26 minutes	1400 MPa, 112 GPa	Paulauskas et al. 2000

The mechanical properties of asphaltene-derived carbon fibres manufactured using conventional heat treatments are presented in Table 5.6. The influence of fibre diameter on tensile strength is found to be more significant compared to other processing conditions such as



temperature and pre-treatment. Fibres with smaller diameter and appropriate pre-treatment conditions exhibit superior tensile properties, reaching up to 1100 MPa, while larger diameter fibres show a lower tensile strength of 400 MPa. This can be attributed to the diffusion barrier that occurs during oxidative stabilization [Sieira et al. 2021]. The process of stabilization relies on the diffusion of oxygen from the outer layer of the fibre to core of the material. For fibres with larger diameters, cyclization reactions predominantly occur at the outer layer resulting in a denser cortical structure and reduced oxygen diffusion rate towards the core area, as shown in the Figure 5.9 [Liu et al. 2018].

When partially stabilized fibres undergo exposure to elevated temperatures, a notable escalation in imperfections occurs, attributed to restricted oxygen diffusion, diminished thermal stability, and the liberation of volatile substances. This phenomenon holds significant technical importance as it underscores the intricate interplay of factors influencing the structural integrity and thermal behaviour of the fibres during the high-temperature treatment process. These defects significantly decrease the tensile strength of the fibres [Sieira et al. 2021]. The tensile strength of asphaltene-derived fibres with larger diameters presents similar issues and exhibits relatively low tensile strength.

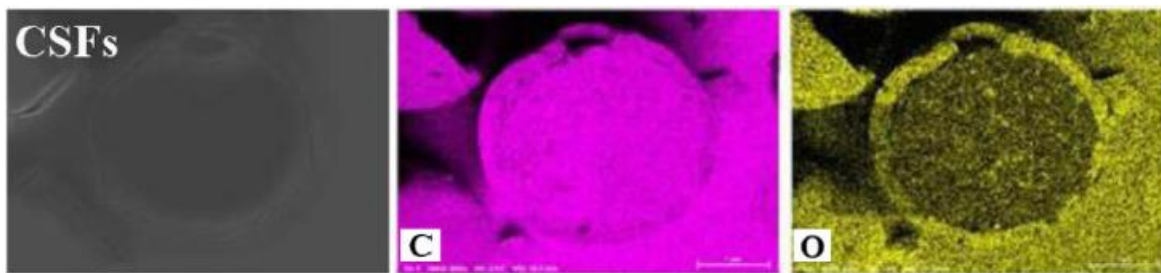


Figure 5.8: Elemental mapping of the Conventional Stabilized Fibres [Liu et al. 2018]

Table 5.6: Comparative analysis of mechanical properties of asphaltene-derived carbon fibres using conventional heating techniques

<b>Fibre Diameter (<math>\mu\text{m}</math>)</b>	<b>Pre-treatment Conditions</b>	<b>Stabilization Conditions</b>	<b>Carbonization Conditions</b>	<b>Mechanical Properties</b>	<b>Referenc e</b>
$\sim 9.5 \pm 1.0$	n-pentane, Debromination	300 °C – 60 min, $\text{HNO}_3$ (acid stabilization)	1500 °C – 120 min	$400 \pm 200$ MPa, $35 \pm$ 15 GPa	Kim et al. 2021
$\sim 9.9 \pm$ 1.0	n-pentane, Heat treatment: 300 °C	300 °C – 60 min, $\text{HNO}_3$ (acid stabilization)	1500 °C – 120 min	$1100 \pm 200$ MPa, $68 \pm$ 12 GPa	Zuo et al. 2021
$\sim 12.2 \pm$ 0.6	n-pentane, Heat treatment: 300 °C	300 °C – 180 min	1500 °C – 120 min	$400 \pm 200$ MPa, $25 \pm 8$ GPa	Zuo et al. 2021
$\sim 20 - 50$	-	260 °C – 240 min, 350 °C – 120 min	500 °C – 30 min, 800 °C – 30 min	400 MPa, 70 GPa	Saad et al. 2021
$\sim 30 \pm 20$	n-pentane	280 °C – 480 min	600 °C – 30 min, 1150 °C – 30 min	$590 \pm 30$ MPa, $56 \pm$ 10 GPa	Current study

## 5.6 Mechanism of Microwave and Microwave Plasma

Microwave heating is a widely used method for processing various materials, including polymers, ceramics, and chemicals. It utilizes microwaves from the electromagnetic spectrum with wavelengths ranging from 1 mm to 1 m and frequencies between 300 MHz and 300 GHz [Zhang et al. 2018]. Microwave furnaces can achieve temperatures up to 1285 °C but noted that higher temperatures present complexities due to temperature-dependent dielectric properties of carbon fibres and chamber materials resulting in non-uniform heating capabilities [Jin et al. 2017].

During the microwave heating process, oxidation reactions initially occur at the fibre core. The occurrence of volumetric heating allows for direct delivery of microwave energy to the materials through molecular interactions, bypassing the skin-core structure as illustrated in Figure 5.10 [Liu et al. 2018]. Dielectric constants of the material play a crucial role in the heating mechanism during microwave heating. Materials with high dielectric constants are effective electromagnetic absorbers and can efficiently convert electromagnetic energy into heat [Kappe et al. 2013].

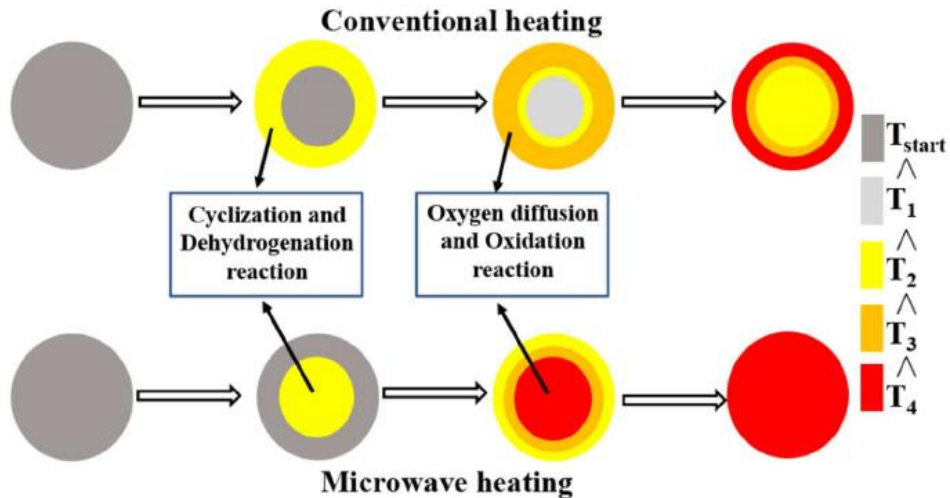


Figure 5.9: Schematic diagram of PAN fibres stabilized by conventional and microwave heating [Liu et al. 2018]

Table 5.7: Dielectric constants of materials at 20 °C

Material	Dielectric constant	Reference
Asphaltene	3.3 – 5.0	[Punase & Hascakir 2016]
Carbon fibre	6.5	[Chao et al. 2021]
Glass	3.7 – 10	[Clipper control Inc. 2023]
Graphite	12 – 15	
Quartz	4.2	

The dielectric constant of asphaltene material is relatively less which is around 3.30-5.00 which might pose a problem of inefficient electromagnetic heating. For utilizing electromagnetic energy to reach high temperatures, an electromagnetic absorbing medium is necessary. In this study, microwaves with a frequency of 2.45 GHz and power of 1000 W were utilized to create plasma by ionizing carrier gas such as argon, as shown in Figure 5.9. The excited ions in the plasma generated high temperatures reaching the range of 1210 – 1302 °C, effectively heating the material within a shorter time period (Figure 5.6). The generated plasma can aid in the development of a more ordered carbon structure, transitioning from a turbostratic structure to more graphitic [Wei et al. 2022].

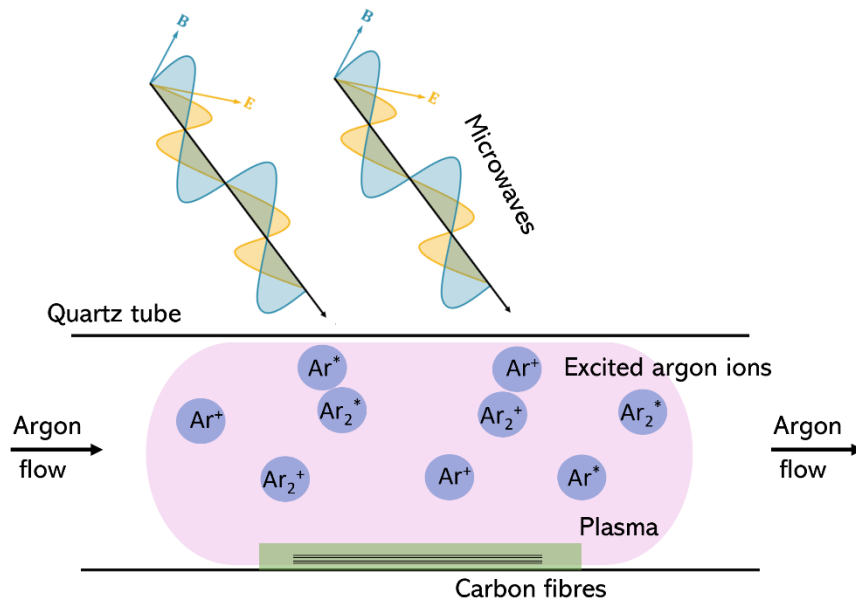


Figure 5.10: Schematic diagram of generation of microwave plasma

The presence of excited argon ions in the plasma and inherent instability of plasma under atmospheric pressures [de la Fuente et al. 2017] significantly influenced the carbonization process. The microwave plasma process successfully carbonized the asphaltene-derived carbon fibres at elevated temperatures, as observed from XRD and Raman patterns in Figure 5.4 and Figure 5.5, respectively. However, it also caused surface damage to the fibres due to the interaction of highly excited argon ions, as noticed in Figure 5.3. These surface damages, such as pits, pores and dents, are undesirable as they negatively affect the mechanical properties of the fibres. These interactions can change the fibre's crystalline structure and these surface defects can serve as stress concentrators, leading to a reduced tensile strength, as observed in our results shown in Figure 5.8.

## 5.7 Summary

The results and discussions presented in this study provide valuable insights into the chemical composition, morphology, crystalline structure, and mechanical properties of

microwave-plasma treated asphaltene carbon fibres. A comparative analysis was conducted between microwave-plasma treated fibres and conventional carbonized fibres. The investigation revealed that microwave plasma treatments are as effective as conventional carbonization by furnaces and significantly reduce the time and energy consumption required for the process. The XRD and Raman patterns of the microwave-plasma treated fibres exhibited similar characteristics to those of conventional carbonized fibres, indicating the formation of a higher graphitic structure and increased crystallinity within the fibres. As the duration of microwave-plasma treatment increased, an intensification in the formation of surface imperfections on the fibres was observed. This can be attributed to the reactivity of excited ions from argon in the plasma, which consequently impacted the mechanical properties of the fibres.

## CHAPTER 6. CONCLUSIONS

Carbon fibre is a high-demand material known for its lightweight nature, chemical resistance, thermal durability, and exceptional mechanical properties. However, the cost associated with carbon fibres limits their widespread adoption across various industries. A potential solution lies in utilizing AOA, a waste byproduct from the oil and gas industry. With its abundant availability, high carbon content, and aromatic structure, AOA stands as a promising precursor material for carbon fibres. This study focuses on the development of manufacturing process for carbon fibres utilizing AOA as a precursor material. The manufacturing process, including pre-processing, spinning, and post-processing, is detailed to achieve fibres with desired properties.

To address the issue of long processing times and high energy consumption in carbon fibre manufacturing, an alternative approach involving the use of microwave plasma technique is implemented. Microwave plasma technique proved to be effective in achieving higher temperatures as high as 1210 - 1302 °C, resulting in carbonization of asphaltene fibres which led to an increase in their carbon content and the development of a well-ordered crystalline structure.

The simulation of microwave plasma thermal treatment is conducted using COMSOL™ Multiphysics software which was instrumental in studying the plasma behaviour within the quartz tube. Numerous experiments and simulations are carried out to optimize the microwave plasma process. The evaluation of microwave plasma treatments on asphaltene-derived carbon fibres is performed through an analysis of morphological, chemical, crystalline, spectroscopic, and mechanical properties.

## 6.1 Novel Scientific Contributions

The Element analysis revealed the dynamic changes in the elemental composition of asphaltene-derived carbon fibres during microwave plasma treatments. The increasing carbon content observed with extended microwave plasma treatment duration indicates the efficacy of this method in advancing carbonization processes. While further optimization opportunities exist, these results emphasize the promising advantages of microwave plasma over traditional methods for achieving enhanced carbonization.

X-ray diffraction patterns provided a comparative analysis, underscoring the development of a layered graphite-like structure in both conventionally carbonized and microwave-plasma treated fibres. The progressive enhancement in crystallinity with prolonged microwave plasma treatment duration revealed a unique influence on the structural evolution, contributing to a more organized carbon matrix.

Raman spectroscopy provided the evolving graphitic structure of asphaltene-derived carbon fibres under varying microwave-plasma treatment times. The increasing intensity of the G peak indicated the progressive development of a higher graphitic structure, while the observed  $I_D/I_G$  ratios highlighted distinctions in structural characteristics.

Thermal analysis, supported by a fibre optic pyrometer, underscored the importance of microwave power in ensuring consistent and effective plasma generation. SEM analysis depicted morphological changes in asphaltene-derived fibres under various treatments. Conventional carbonization yielded minimal surface defects, while microwave plasma treatments, especially for extended durations, induced surface damage, pits, and striations.

Tensile testing of fibres, subjected to conventional and microwave plasma carbonization, revealed distinctive mechanical properties. Conventional carbonized fibres exhibited higher tensile



strength (590 MPa) compared to microwave-plasma treated fibres. The latter, treated for 5, 7, and 9 minutes, demonstrated varied strengths (92.5 MPa, 361.03 MPa, and 120 MPa, respectively). The presence of defects and surface damage in microwave-plasma treated fibres contributed to reduced tensile strength and modulus. Microwave plasma, generated at 1000 W with argon ionization, reached temperatures of approximately 1300 °C. While effective for carbonization, it led to surface damage due to the interaction of highly excited argon ions, emphasizing the importance of optimizing parameters.

## **6.2 Assumptions and Limitations**

In the manufacturing process, the utilization of AOA as a precursor material requires certain assumptions and limitations. Although AOA is valued for its high carbon content and aromatic properties, its precise structural characteristics remain unknown, which limits a comprehensive understanding of the material. Furthermore, while feedstocks from different batches may exhibit slight variations in characteristics, it is assumed that the precursor material remains relatively consistent in composition and structure for this study.

Assumptions include the effective and equal removal of impurities and light hydrocarbons from feedstocks through pre-treatment methods. During the spinning of the precursor in the twin-screw extruder, a consistent and constant temperature is assumed along the entire length of the melt pump and spinneret, along with uniform fibre diameter and consistent alignment of fibrillar structures within the fibres. The fibre diameter plays a significant role in determining the final mechanical properties. Smaller diameter fibres provide more uniform stability and have fewer defects compared to large diameter fibres, which often carry defects at thermal treatments. For the

purpose of this study, measurements have been focused on comparing fibres with similar diameters.

In the post-treatment processing, it is assumed that critical reactions during stabilization and carbonization occur uniformly throughout the precursor material. During the tensile testing of the fibre, the assumptions were made that the fibre had a circular, solid shape with a uniform diameter. Microwave plasma within the custom-designed quartz tube with argon flow has been modelled. Assumptions have been made regarding the properties of the quartz tube, including its negligible reflectance, heat capacity, thermal conductivity, and conductive heat transfer. Additionally, the composition of the gas flow is assumed to be pure and maintained at a constant pressure throughout. The propagation of microwaves is considered to be reflective, resulting in reduced power within the multi-modal cavity, with all microwave energy being fully utilized for plasma generation. It is also assumed that there are no surface reactions with the excited argon atoms in the plasma. These assumptions limit the clear and precise understanding of microwave plasma within the quartz tube setup.

### **6.3 Future Work**

The study of microwave plasma thermal treatments in asphaltene-derived carbon fibre manufacturing presents various challenges related to mechanical properties, fibre diameters, and the microwave plasma treatments. Overcoming these challenges is essential for producing cost-effective carbon fibres with enhanced properties while minimizing energy consumption. Carbon fibres are renowned for their exceptional mechanical properties. Further research aims to improve the mechanical properties of the fibres, with a specific focus on improving fibre diameter [Sieira et al. 2021] and reducing sulfur content present in the fibres [Bisheh & Abdin 2023].

In order to enhance the processability of the precursor and reduce the diameter of the fibre, it is necessary to improve its viscosity and spinnability. This can be achieved by blending polymers with high aromaticity together with asphaltenes, which enhance their melt spinnability and stretching capacity. In the study conducted by Zhu et al., It was reported that the use of polymers in bitumen can lead to improved properties such as increased stiffness at higher temperatures, enhanced crack resistance at low temperatures, better moisture resistance, and longer fatigue life. The final properties of polymer modified bitumen are determined by factors such as the characteristics of the bitumen itself, the content and type of polymer used, and the manufacturing process [Zhu et al. 2014]. Various types of polymers including polyethylene, polypropylene, ethylene-vinyl-acetate (EVA), styrene-butadiene-styrene (SBS), and styrene-ethylene-butadiene-styrene (SEBS) have been investigated for their potential use [Zhu et al. 2014]. In addition to these polymer modifications, researchers have also explored the use of organoclays to improve the dispersion of polymers in bitumen and influence its final rheological properties [Sureshkumar et al. 2010].

To improve the properties of asphaltene-derived carbon fibres, it is crucial to enhance the pre-processing of asphaltene precursors by reducing heteroatom content, particularly sulfur. Future work will focus on expanding current solvent-based pre-treatment methods for AOA. Additionally, thermal treatment [Zuo et al. 2021], as well as acid or catalyst-based pre-treatment of AOA precursors, will be investigated to extract and process asphaltene precursors more efficiently.

To achieve improved performance, better microstructures, and enhanced mechanical or electrical properties in carbon fibres, a graphitization process at higher temperatures is necessary [Wei et al. 2022]. The current microwave plasma setup, equipped with vacuum controllers, can effectively achieve higher temperatures for the graphitization process. Graphitization is typically

an energy intensive procedure. However, using microwave plasma makes it more energy-efficient and reduces the processing time.

Previous work by Lee et al. has examined the use of plasma-assisted stabilization, which has shown promising results in stabilizing PAN fibres more efficiently compared to traditional methods. This advancement can potentially reduce both cost and time associated with precursor fibre stabilization, thus facilitating the development of low-cost carbon fibres. In this particular approach, precursor fibres are exposed to a radio-frequency capacitive plasma discharge that generates active species such as oxygen radicals, as shown in Figure 6.2 [Lee et al. 2013].

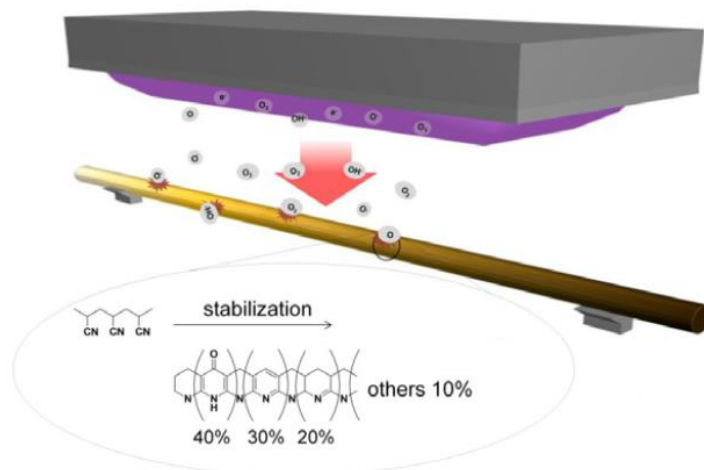


Figure 6.1: Schematic diagram of plasma assisted stabilization mechanism [Lee et al. 2013]

In the future, this method can also be applied to produce asphaltene-derived carbon fibres. By incorporating this method. The entire post-treatment process can become more cost effective, energy efficient and faster in duration. Future work aims to investigate the appropriate plasma parameters for producing asphaltene-based carbon fibres.

Microwave plasma treatment has introduced surface defects on the fibres. Future investigations will aim to fine-tune treatment parameters for more efficient processing of larger volumes of fibres within shorter time frames. Improving the mechanical properties of carbon fibres, such as addressing surface defects and enhancing performance, is a key focus for future research. These advancements aim to bring asphaltene-derived carbon fibres closer to commercial carbon fibres in terms of mechanical strength. This will create new possibilities for their utilization across various industries, including automotive and construction fields. Further investigation will also consider the sustainability aspect of this approach to align with the increasing demand for eco-friendly materials and processes in different sectors.

## References

- Alshareef, A. H. (2019). Asphaltenes: Definition, Properties, and Reactions of Model Compounds. *Energy & Fuels*, 34(1), 16–30.
- Alberta Innovates. (2018). *Oil sands – Overview* [Review of *Oil sands – Overview*].
- Arnold, U., De Palmenaer, A., Brück, T., & Kuse, K. (2018). Energy-Efficient Carbon Fibre Production with Concentrated Solar Power: Process Design and Techno-economic Analysis. *Industrial & Engineering Chemistry Research*, 57(23), 7934–7945.
- Baeva, M., Bösel, A., Ehlbeck, J., & Loffhagen, D. (2012). Modeling of microwave-induced plasma in argon at atmospheric pressure. *Physical Review E*, 85(5).
- Banerjee, C., Chandaliya, V. K., & Dash, P. S. (2021). Recent advancement in coal tar pitch-based carbon fibre precursor development and fibre manufacturing process. *Journal of Analytical and Applied Pyrolysis*, 158, 105272.
- Bhat, G. (2016). *Structure and Properties of High-Performance Fibres* (pp. 7–70). Woodhead Publishing.
- Bisheh, H., & Abdin, Y. (2023). *Carbon Fibres: From PAN to Asphaltene Precursors; A State-of-Art Review*. 19.
- Bohnert, G., Lula, J., & Bowen, III, Daniel E. (2012). *Carbonized asphaltene-based carbon-carbon fibre composites*.
- Bouherine, K., Tibouche, A., Ikhlef, N., & Leroy, O. (2016). 3-D Numerical Characterization of a Microwave Argon PECVD Plasma Reactor at Low Pressure. *IEEE Transactions on Plasma Science*, 44(12), 3409–3416.
- Breeze, P. (2018). Chapter 7 - Advanced Waste-to-Energy Technologies: Gasification, Pyrolysis, and Plasma Gasification. *Energy from Waste*, 65–75.
- Brown, K. R., Harrell, T. M., Skrzypczak, L., Scherschel, A., Wu, H. F., & Li, X. (2022). Carbon fibres derived from commodity polymers: A review. *Carbon*, 196, 422–439.
- Chao, H.-W., Hsu, H.-C., Chen, Y.-R., & Chang, T.-H. (2021). Characterizing the dielectric properties of carbon fiber at different processing stages. *Scientific Reports*, 11(1).
- Choi, D., Kil, H.-S., & Lee, S. (2019). Fabrication of low-cost carbon fibres using economical precursors and advanced processing technologies. *Carbon*, 142, 610–649.
- Chung, D. (2014). *Carbon Fibre Composites*. (pp. 17–64). Butterworth-Heineman.
- Cundy, C. S. (1998). Microwave Techniques in the Synthesis and Modification of Zeolite

- Catalysts. A Review. *Collection of Czechoslovak Chemical Communications*, 63(11), 1699–1723.
- Das, S. (2011). Life cycle assessment of carbon fiber-reinforced polymer composites. *The International Journal of Life Cycle Assessment*, 16(3), 268–282.
- de la Fuente, J. F., Kiss, A. A., Radoiu, M. T., & Stefanidis, G. D. (2017). Microwave plasma emerging technologies for chemical processes. *Journal of Chemical Technology & Biotechnology*, 92(10), 2495–2505.
- Delhaes, P. (2003). *Fibres and Composites* (pp. 3–20). CRC Press.
- Dielectric Constants of various materials*. (n.d.). [www.clippercontrols.com](http://www.clippercontrols.com).  
<https://www.clippercontrols.com/pages/Dielectric-Constant-Values.html#G>
- Donnet, J.-B., & Bansal, R. C. (1998). *Carbon fibres* (pp. 10–40). Marcel Dekker.
- Eddie, D. D. (1998). The effect of processing on the structure and properties of carbon fibres. *Carbon*, 36(4), 345–362.
- Eddie, D. D., & Dunham, M. G. (1989). Melt spinning pitch-based carbon fibers. *Carbon*, 27(5), 647–655.
- Farrow, G. J., & Jones, C. (1994). The Effect of Low Power Nitrogen Plasma Treatment of Carbon Fibres on the Interfacial Shear Strength of Carbon Fibre/Epoxy Composites. *The Journal of Adhesion*, 45(1-4), 29–42.
- Fitzer, E., & Manocha, L. M. (1998). Carbon Fibres. *Springer EBooks*, 3–69.
- Forintos, N., & Czigany, T. (2019). Multifunctional application of carbon fibre reinforced polymer composites: Electrical properties of the reinforcing carbon fibres – A short review. *Composites Part B: Engineering*, 162, 331–343.
- Frank, E., Ingildeev, D., & Buchmeiser, M. R. (2017). High-performance PAN-based carbon fibres and their performance requirements. *Structure and Properties of High-Performance Fibres*, 7–30.
- Frank, E., Steudle, L. M., Ingildeev, D., Spörl, J. M., & Buchmeiser, M. R. (2014). Carbon Fibres: Precursor Systems, Processing, Structure, and Properties. *Angewandte Chemie International Edition*, 53(21), 5262–5298.
- Fridman, A. A. (2012). *Plasma chemistry*. Cambridge University Press.
- Galos, J. (2020). Microwave processing of carbon fibre polymer composites: a review. *Polymers and Polymer Composites*, 096739112090389.

- Hao, Y., Shi, C., Bi, Z., Lai, Z., She, A., & Yao, W. (2023). *Recent Advances in Properties and Applications of Carbon Fibre-Reinforced Smart Cement-Based Composites*. 16(7), 2552–2552.
- Huang, X. (2009). Fabrication and Properties of Carbon Fibres. *Materials*, 2(4), 2369–2403.
- Issa, A. A., Al-Degs, Y. S., Mashal, K., & Al Bakain, R. Z. (2015). Fast activation of natural biomasses by microwave heating. *Journal of Industrial and Engineering Chemistry*, 21, 230–238.
- Jin, S., Guo, C., Lu, Y., Zhang, R., Wang, Z., & Mu, J. (2017). Comparison of microwave and conventional heating methods in carbonization of polyacrylonitrile-based stabilized fibres at different temperature measured by an in-situ process temperature control ring. *Polymer Degradation and Stability*, 140, 32–41.
- Kappe, C. O., Stadler, A., & Dallinger, D. (2013). *Microwaves in Organic and Medicinal Chemistry*. John Wiley & Sons.
- Kaur, J., Millington, K., & Smith, S. (2016). Producing high-quality precursor polymer and fibres to achieve theoretical strength in carbon fibres: A review. *Journal of Applied Polymer Science*, 133(38).
- Kaw, P. K., Valeo, E. J., & Dawson, J. M. (1970). Interpretation of an Experiment on the Anomalous Absorption of an Electromagnetic Wave in a Plasma. *Physical Review Letters*, 25(7), 430–433.
- Kawajiri, K., & Sakamoto, K. (2021). Environmental impact of carbon fibers fabricated by an innovative manufacturing process on life cycle greenhouse gas emissions. *Sustainable Materials and Technologies*, 31.
- Kim, M. S., Lee, D. H., Kim, C. H., Lee, Y. J., Hwang, J. Y., Yang, C.-M., Kim, Y. A., & Yang, K. S. (2015). Shell–core structured carbon fibres via melt spinning of petroleum- and wood-processing waste blends. *Carbon*, 85, 194–200.
- Kim, S.-Y., Kim, S. Y., Lee, S., Jo, S., Im, Y.-H., & Lee, H.-S. (2015). Microwave plasma carbonization for the fabrication of polyacrylonitrile-based carbon fibre. *Polymer*, 56, 590–595.
- Kim, Y., Desirée Leistenschneider, Arno de Klerk, & Chen, W. (2021). Rigorous Deasphalting, Autoxidation, and Bromination Pretreatment Methods for Oilsands Bitumen Derived Asphaltenes to Improve Carbon Fibre Production. *Energy & Fuels*, 35(21), 17463–17478.
- Kuptajit, P., & Sano, N. (2019). Application of microwave-induced plasma for extremely fast synthesis of large surface area activated carbon. *Applied Physics Express*, 12(8), 086001.



- Kushner, M. J. (2009). Hybrid modelling of low temperature plasmas for fundamental investigations and equipment design. *Journal of Physics D: Applied Physics*, 42(19), 194013.
- Langmuir, I. (1928). Oscillations in Ionized Gases. *Proceedings of the National Academy of Sciences*, 14(8), 627–637.
- Lee, S.-W., Lee, H.-Y., Jang, S.-Y., Jo, S., Lee, H.-S., Choe, W.-H., & Lee, S. (2013). Efficient preparation of carbon fibres using plasma assisted stabilization. *Carbon*, 55, 361–365.
- Leistenschneider, D., Abedi, Z., Ivey, D. G., & Chen, W. (2022). Coating of Low-Cost Asphaltenes-Derived Carbon Fibres with V<sub>2</sub>O<sub>5</sub> for Supercapacitor Application. *Energy & Fuels*, 36(6), 3328–3338.
- Leistenschneider, D., Zuo, P., Kim, Y., Abedi, Z., Ivey, D. G., de Klerk, A., Zhang, X., & Chen, W. (2021). A mechanism study of acid-assisted oxidative stabilization of asphaltene-derived carbon fibres. *Carbon Trends*, 5, 100090.
- Li, P., Liu, J., Liu, Y., Wang, Y., Li, Z., Wu, W., Wang, Y., Yin, L., Xie, H., Wu, M., He, X., & Qiu, J. (2015). Three-dimensional ZnMn<sub>2</sub>O<sub>4</sub>/porous carbon framework from petroleum asphalt for high performance lithium-ion battery. *Electrochimica Acta*, 180, 164–172.
- Li, Y., & Yang, W. (2008). Microwave synthesis of zeolite membranes: A review. *Journal of Membrane Science*, 316(1-2), 3–17.
- Liu, F., Wang, H., Xue, L., Fan, L., & Zhu, Z. (2008). Effect of microstructure on the mechanical properties of PAN-based carbon fibres during high-temperature graphitization. *Journal of Materials Science*, 43(12), 4316–4322.
- Liu, J., Xiao, S., Shen, Z., Xu, L., Zhang, L., & Peng, J. (2018). Study on the oxidative stabilization of polyacrylonitrile fibres by microwave heating. *Polymer Degradation and Stability*, 150, 86–91.
- Lu, S., Blanco, C., & Rand, B. (2002). Large diameter carbon fibres from mesophase pitch. *Carbon*, 40(12), 2109–2116.
- Mainka, H., Täger, O., Körner, E., Hilfert, L., Busse, S., Edelmann, F. T., & Herrmann, A. S. (2015). Lignin – an alternative precursor for sustainable and cost-effective automotive carbon fiber. *Journal of Materials Research and Technology*, 4(3), 283–296.
- Menéndez, J. A., Arenillas, A., Fidalgo, B., Fernández, Y., Zubizarreta, L., Calvo, E. G., & Bermúdez, J. M. (2010). Microwave heating processes involving carbon materials. *Fuel Processing Technology*, 91(1), 1–8.
- Mohsenian, S., Sheth, S., Bhatta, S., Nagassou, D., Sullivan, D., & Trelles, J. P. (2018). Design and characterization of an electromagnetic-resonant cavity microwave plasma reactor for atmospheric pressure carbon dioxide decomposition. *Plasma Processes and Polymers*,

16(2), 1800153.

Morgan, P. (2005). *Carbon Fibres and Their Composites*. CRC Press.

Mullins, O. C. (2010). The Modified Yen Model. *Energy & Fuels*, 24(4), 2179–2207.

Nabais, J. M. V., Carrott, P. J. M., Ribeiro Carrott, M. M. L., & Menéndez, J. A. (2004). Preparation and modification of activated carbon fibres by microwave heating. *Carbon*, 42(7), 1315–1320.

Ni, G., Qin, F., Guo, Z., Wang, J., & Shen, W. (2020). Nitrogen-doped asphaltene-based porous carbon fibres as supercapacitor electrode material with high specific capacitance. *Electrochimica Acta*, 330, 135270.

Ouyang, Z., Surla, V., Cho, T. S., & Ruzic, D. N. (2012). Characterization of an Atmospheric-Pressure Helium Plasma Generated by 2.45-GHz Microwave Power. *IEEE Transactions on Plasma Science*, 40(12), 3476–3481.

Paulauskas, F. L., Bigelow, T. S., Yarborough, K. A., & Meek, T. T. (2000). Manufacturing of Carbon Fibres Using Microwave-Assisted Plasma Technology. *SAE Technical Paper Series*.

Plasma Processing of Materials: Scientific Opportunities and Technological Challenges. (1991). In *National Academies Press*. National Academies Press.

Punase, A., & Hasçakir, B. (2016). Stability Determination of Asphaltenes through Dielectric Constant Measurements of Polar Oil Fractions. *Energy & Fuels*, 31(1), 65–72.

Rahaman, M. S. A., Ismail, A. F., & Mustafa, A. (2007). A review of heat treatment on polyacrylonitrile fibre. *Polymer Degradation and Stability*, 92(8), 1421–1432.

Rašković, V., & Marinković, S. (1978). Processes in sulfur dioxide treatment of PAN fibres. *Carbon*, 16(5), 351–357.

Riccardo d'Agostino, Favia, P., Oehr, C., & Wertheimer, M. R. (2005). Low-Temperature Plasma Processing of Materials: Past, Present, and Future. *Plasma Processes and Polymers*, 2(1), 7–15.

Riggs, D. M., Shuford, R. J., Lewis, R. W. (1982). Graphite Fibres and Composites. In: Lubin, G. (eds) *Handbook of Composites*. Springer, Boston, MA.

Ryu, Z., Rong, H., Zheng, J., Wang, M., & Zhang, B. (2002). Microstructure and chemical analysis of PAN-based activated carbon fibres prepared by different activation methods. *Carbon*, 40(7), 1144–1147.

- Saad, S., Ali Shayesteh Zeraati, Roy, S., Saadi, R., Radović, J. R., Ashna Rajeev, Miller, K. A., Bhattacharyya, S. P., Larter, S. R., Natale, G., Uttandaraman Sundararaj, Ajayan, P. M., Rahman, M. M., & Md Golam Kibria. (2022). *Transformation of petroleum asphaltenes to carbon fibres*. 190, 92–103.
- Saito, N., Aoki, K., Usui, Y., Shimizu, M., Hara, K., Narita, N., Ogihara, N., Nakamura, K., Ishigaki, N., Kato, H., Haniu, H., Taruta, S., Kim, Y. A., & Endo, M. (2011). Application of carbon fibres to biomaterials: a new era of nano-level control of carbon fibres after 30-years of development. *Chemical Society Reviews*, 40(7), 3824–3834.
- Salem, M. K. (2021). Simulation for a Plasma Discharge Model in Microwave Transmitter-Receiver Waveguide by COMSOL Multi Physics Software. *Hyperscience International Journals*, 1(1), 22–27.
- Shen, Q., Huang, R., Xu, Z., & Hua, W. (2020). Numerical 3D Modeling: Microwave Plasma Torch at Intermediate Pressure. *Applied Sciences*, 10(15), 5393.
- Shokrani Havigh, R., & Mahmoudi Chenari, H. (2022). A comprehensive study on the effect of carbonization temperature on the physical and chemical properties of carbon fibers. *Scientific Reports*, 12(1).
- Sieira, P., de Souza Mendes, P. R., de Castro, A., & Pradelle, F. (2021). Impact of spinning conditions on the diameter and tensile properties of mesophase petroleum pitch carbon fibres using design of experiments. *Materials Letters*, 285, 129110.
- Singer, L. S. (1981). Carbon fibres from mesophase pitch. *Fuel*, 60(9), 839–847.
- Singh, R. K., Kumar, R., Singh, D. P., Savu, R., & Moshkalev, S. A. (2019). Progress in microwave-assisted synthesis of quantum dots (graphene/carbon/semiconducting) for bioapplications: a review. *Materials Today Chemistry*, 12, 282–314.
- Soo-Jin Park. (2018). *Carbon Fibers*. (pp. 31–66). Springer.
- Bitumen Beyond Combustion – Phase 2, Stantec Consulting Ltd. (2018). Stantec-Bitumen-Beyond-Combustion-Phase-2-Report.pdf (albertainnovates.ca)
- Strausz, O. P., & Lown, E. M. (2003). *The chemistry of Alberta oil sands, bitumens and heavy oil*. Canada.
- Sureshkumar, M. S., Filippi, S., Polacco, G., Kazatchkov, I., Stastna, J., & Zanzotto, L. (2010). Internal structure and linear viscoelastic properties of EVA/asphalt nanocomposites. *European Polymer Journal*, 46(4), 621–633.
- Thirumdas, R., Sarangapani, C., & Annapure, U. S. (2014). Cold Plasma: A novel Non-Thermal Technology for Food Processing. *Food Biophysics*, 10(1), 1–11.

- Torres, D., Pinilla, J. L., & I. Suelves. (2017). Unzipping of multi-wall carbon nanotubes with different diameter distributions: Effect on few-layer graphene oxide obtention. *Applied Surface Science*, 424, 101–110.
- Trejo, F., Rana, M. S., & Ancheyta, J. (2010). Thermogravimetric determination of coke from asphaltenes, resins and sediments and coking kinetics of heavy crude asphaltenes. *Catalysis Today*, 150(3-4), 272–278.
- Wang, N., Tahmasebi, A., Yu, J., Xu, J., Huang, F., & Mamaeva, A. (2015). A Comparative study of microwave-induced pyrolysis of lignocellulosic and algal biomass. *Bioresource Technology*, 190, 89–96.
- Wyatt, L. M., Coveney, V., Riddiford, C., & Sharpe, R. (1994). *7 - Materials, properties and selection* (E. H. Smith, Ed.). ScienceDirect; Butterworth-Heinemann.
- Yadav, H. N. S., Kumar, M., Kumar, A., & Das, M. (2021). COMSOL simulation of microwave plasma polishing on different surfaces. *Materials Today: Proceedings*, 45, 4803–4809.
- Yang, S., Cheng, Y., Xiao, X., & Pang, H. (2020). Development and application of carbon fibre in batteries. *Chemical Engineering Journal*, 384, 123294.
- Yang, Y., Hua, W., & Guo, S. Y. (2014). Numerical study on microwave-sustained argon discharge under atmospheric pressure. *Physics of Plasmas*, 21(4), 040702.
- Yu, P. Y., & Cardona, M. (2010). *Fundamentals of semiconductors : physics and materials properties*. Springer.
- Yuan, L. Y., Chen, C. S., Shyu, S. S., & Lai, J. Y. (1992). Plasma surface treatment on carbon fibres. Part 1: Morphology and surface analysis of plasma etched fibres. *Composites Science and Technology*, 45(1), 1–7.
- Zaitsev, A., Moisan, S., & Poncin-Epaillard, F. (2021). Cellulose carbon fibre: plasma synthesis and characterization. *Cellulose*, 28(4), 1973–1988.
- Zhang, C., Liu, J., Guo, S., Xiao, S., Shen, Z., & Xu, L. (2018). Comparison of microwave and conventional heating methods for oxidative stabilization of polyacrylonitrile fibres at different holding time and heating rate. *Ceramics International*, 44(12), 14377–14385.
- Zhao, G., Zhang, C., Lv, L., Liu, J., & Guo, S. (2022). Research on dynamic microwave low-temperature carbonization of high-performance carbon fibre. *Diamond and Related Materials*, 125.
- Zhou, J., Bomben, P., Gray, M., & Helfenbaum, B. (2021). *BITUMEN BEYOND COMBUSTION*.
- Zhu, J., Birgisson, B., & Kringos, N. (2014). Polymer modification of bitumen: Advances and

challenges. *European Polymer Journal*, 54, 18–38.

Zuo, P., Desirée Leistenschneider, Kim, Y., Abedi, Z., Ivey, D. G., Zhang, X., & Chen, W. (2021). Asphaltene thermal treatment and optimization of oxidation conditions of low-cost asphaltene-derived carbon fibres. *Journal of Industrial and Engineering Chemistry*, 104, 427–436.

Zuo, P., Qu, S., & Shen, W. (2019). Asphaltenes: Separations, structural analysis and applications. *Journal of Energy Chemistry*, 34, 186–207.

## APPENDIX- A: REPRINT PERMISSIONS

Reprint permission for Figure 2.2 & 2.12 – [Frank et al. 2014]



This is a License Agreement between Sharath Krishna Chandra ("User") and Copyright Clearance Center, Inc. ("CCC") on behalf of the Rightsholder identified in the order details below. The license consists of the order details, the Marketplace Permissions General Terms and Conditions below, and any Rightsholder Terms and Conditions which are included below.

All payments must be made in full to CCC in accordance with the Marketplace Permissions General Terms and Conditions below.

Order Date	30-Nov-2023	Type of Use	Republish in a thesis/dissertation
Order License ID	1422093-1	Publisher	WILEY - V C H VERLAG
ISSN	1433-7851	Portion	GMBH & CO. KGAA
			Chart/graph/table/figure

### LICENSED CONTENT

Publication Title	Angewandte Chemie	Rightsholder	John Wiley & Sons - Books
Article Title	Carbon fibers: precursor systems, processing, structure, and properties.	Publication Type	Journal
Author/Editor	Gesellschaft Deutscher Chemiker.	Start Page	5262
Date	01/01/1962	End Page	5298
Language	English	Issue	21
Country	Germany	Volume	53

### REQUEST DETAILS

Portion Type	Chart/graph/table/figure	Distribution	Canada
Number of Charts / Graphs / Tables / Figures Requested	2	Translation	Original language of publication
Format (select all that apply)	Electronic	Copies for the Disabled?	No
Who Will Republish the Content?	Academic institution	Minor Editing Privileges?	Yes
Duration of Use	Life of current and all future editions	Incidental Promotional Use?	No
Lifetime Unit Quantity	Up to 499	Currency	CAD
Rights Requested	Main product		

### NEW WORK DETAILS

Title	Microwave-Plasma based Thermal Treatment of Asphaltene-derived Carbon Fibres	Institution Name	University of Calgary
Instructor Name	Dr. Simon Park	Expected Presentation Date	2023-12-04

### ADDITIONAL DETAILS

The Requesting Person / Organization to Appear on the License	Sharath Krishna Chandra
---	-------------------------

### REQUESTED CONTENT DETAILS

Title, Description or Numeric Reference of the Portion(s)	Fundamental reaction path for the carbonization of a polyaromatic mesophase pitch precursor.	Title of the Article / Chapter the Portion Is From	Carbon fibers: precursor systems, processing, structure, and properties.
Editor of Portion(s)	Dr. , Frank, Erik; Dipl.-Chem., Steudle, Lisa M.; Dr., Ingildeev, Denis; Dipl.-Chem., Spörl, Johanna M.; Prof., Buchmeiser, Michael R.	Author of Portion(s)	Dr. , Frank, Erik; Dipl.-Chem., Steudle, Lisa M.; Dr., Ingildeev, Denis; Dipl.-Chem., Spörl, Johanna M.; Prof., Buchmeiser, Michael R.
Volume / Edition	53 / International ed. in English.	Publication Date of Portion	2014-05-18
Page or Page Range of Portion	5262-5298		

## Reprint permission for Figure 2.3 – [Park 2018]



This is a License Agreement between Sharath Krishna Chandra ("User") and Copyright Clearance Center, Inc. ("CCC") on behalf of the Rightsholder identified in the order details below. The license consists of the order details, the Marketplace Permissions General Terms and Conditions below, and any Rightsholder Terms and Conditions which are included below.

All payments must be made in full to CCC in accordance with the Marketplace Permissions General Terms and Conditions below.

Order Date	30-Nov-2023	Type of Use	Republish in a thesis/dissertation
Order License ID	1422100-1	Publisher	Springer Singapore;
ISBN-13	9789811305375	Portion	Springer Singapore Image/photo/illustration

### LICENSED CONTENT

Publication Title	Carbon Fibers	Country	Singapore
Author/Editor	Park, Soo-Jin	Rightsholder	Springer
Date	01/30/2019	Publication Type	Book
Language	English		

### REQUEST DETAILS

Portion Type	Image/photo/illustration	Distribution	Canada
Number of Images / Photos / Illustrations	1	Translation	Original language of publication
Format (select all that apply)	Electronic	Copies for the Disabled?	No
Who Will Republish the Content?	Academic institution	Minor Editing Privileges?	Yes
Duration of Use	Life of current and all future editions	Incidental Promotional Use?	No
Lifetime Unit Quantity	Up to 499	Currency	CAD
Rights Requested	Main product		

### NEW WORK DETAILS

Title	Microwave-Plasma based Thermal Treatment of Asphaltene-derived Carbon Fibres	Institution Name	University of Calgary
Instructor Name	Dr. Simon Park	Expected Presentation Date	2023-12-04



### ADDITIONAL DETAILS

Order Reference Number	N/A	The Requesting Person / Organization to Appear on the License	Sharath Krishna Chandra
------------------------	-----	---	-------------------------


### REQUESTED CONTENT DETAILS

Title, Description or Numeric Reference of the Portion(s)	Chemical structure of cellulose polymer chain	Title of the Article / Chapter the Portion Is From	Chapter - 2
---	---	--	-------------

Reprint permission for Figure 2.4b – [Mullins 2010]



---



**The Modified Yen Model**  
Author: Oliver C. Mullins  
Publication: Energy & Fuels  
Publisher: American Chemical Society  
Date: Apr 1, 2010  
*Copyright © 2010, American Chemical Society*

**PERMISSION/LICENSE IS GRANTED FOR YOUR ORDER AT NO CHARGE**

This type of permission/license, instead of the standard Terms and Conditions, is sent to you because no fee is being charged for your order. Please note the following:

- Permission is granted for your request in both print and electronic formats, and translations.
- If figures and/or tables were requested, they may be adapted or used in part.
- Please print this page for your records and send a copy of it to your publisher/graduate school.
- Appropriate credit for the requested material should be given as follows: "Reprinted (adapted) with permission from {COMPLETE REFERENCE CITATION}. Copyright {YEAR} American Chemical Society." Insert appropriate information in place of the capitalized words.
- One-time permission is granted only for the use specified in your RightsLink request. No additional uses are granted (such as derivative works or other editions). For any uses, please submit a new request.

If credit is given to another source for the material you requested from RightsLink, permission must be obtained from that source.

[BACK](#) [CLOSE WINDOW](#)

© 2023 Copyright - All Rights Reserved | [Copyright Clearance Center, Inc.](#) | [Privacy statement](#) | [Data Security and Privacy](#)  
| [For California Residents](#) | [Terms and Conditions](#) Comments? We would like to hear from you. E-mail us at [customercare@copyright.com](mailto:customercare@copyright.com)



Reprint permission for Figure 2.7 – [Delhaes 2003]



This is a License Agreement between Sharath Krishna Chandra ("User") and Copyright Clearance Center, Inc. ("CCC") on behalf of the Rightsholder identified in the order details below. The license consists of the order details, the Marketplace Permissions General Terms and Conditions below, and any Rightsholder Terms and Conditions which are included below.

All payments must be made in full to CCC in accordance with the Marketplace Permissions General Terms and Conditions below.

Order Date	04-Dec-2023	Type of Use	Republish in a
Order License ID	1423170-1		thesis/dissertation
ISBN-13	978-0-203-16678-9	Publisher Portion	Taylor & Francis
			Image/photo/illustration

#### LICENSED CONTENT

Publication Title	Fibers and composites	Country	United Kingdom of Great Britain and Northern Ireland
Author/Editor	Delhaes, Pierre.		
Date	05/15/2003	Rightsholder	Taylor & Francis Informa UK Ltd - Books
Language	English	Publication Type	Book

#### REQUEST DETAILS

Portion Type	Image/photo/illustration	Distribution	Canada
Number of Images / Photos / Illustrations	1	Translation	Original language of publication
Format (select all that apply)	Electronic	Copies for the Disabled?	No
Who Will Republish the Content?	Academic institution	Minor Editing Privileges?	Yes
Duration of Use	Life of current edition	Incidental Promotional Use?	No
Lifetime Unit Quantity	Up to 499	Currency	CAD
Rights Requested	Main product		

#### NEW WORK DETAILS

Title	Microwave-Plasma based Thermal Treatment of Asphaltene-derived Carbon Fibres	Institution Name	University of Calgary
		Expected Presentation Date	2023-12-04
Instructor Name	Dr. Simon Park		

#### ADDITIONAL DETAILS

Order Reference Number	N/A	The Requesting Person / Organization to Appear on the License	Sharath Krishna Chandra
------------------------	-----	---	-------------------------

Reprint permission for Figure 2.8 – [Bhat 2016]



This is a License Agreement between Sharath Krishna Chandra ("User") and Copyright Clearance Center, Inc. ("CCC") on behalf of the Rightsholder identified in the order details below. The license consists of the order details, the Marketplace Permissions General Terms and Conditions below, and any Rightsholder Terms and Conditions which are included below.

All payments must be made in full to CCC in accordance with the Marketplace Permissions General Terms and Conditions below.

Order Date	30-Nov-2023	Type of Use	Republish in a thesis/dissertation
Order License ID	1422146-1	Publisher	Elsevier Science
ISBN-13	9780081005507	Portion	Image/photo/illustration

#### LICENSED CONTENT

Publication Title	Structure and Properties of High-Performance Fibers	Country	United Kingdom of Great Britain and Northern Ireland
Date	09/27/2016	Rightsholder	Elsevier Science & Technology Journals
Language	English	Publication Type	Book

#### REQUEST DETAILS

Portion Type	Image/photo/illustration	Distribution	Canada
Number of Images / Photos / Illustrations	1	Translation	Original language of publication
Format (select all that apply)	Electronic	Copies for the Disabled?	No
Who Will Republish the Content?	Academic institution	Minor Editing Privileges?	Yes
Duration of Use	Life of current edition	Incidental Promotional Use?	No
Lifetime Unit Quantity	Up to 499	Currency	CAD
Rights Requested	Main product		

#### NEW WORK DETAILS

Title	Microwave-Plasma based Thermal Treatment of Asphaltene-derived Carbon Fibres	Institution Name	University of Calgary
Instructor Name	Dr. Simon Park	Expected Presentation Date	2023-12-04

#### ADDITIONAL DETAILS

Order Reference Number	N/A	The Requesting Person / Organization to Appear on the License	Sharath Krishna Chandra
------------------------	-----	---	-------------------------

#### REQUESTED CONTENT DETAILS

Title, Description or Numeric Reference of the Portion(s)	Different die designs and the effect on resultant fibre structure and properties	Title of the Article / Chapter the Portion Is From	N/A
---	--	--	-----

Reprint permission for Figure 2.9 & 2.11 – [Frank et al. 2017]



This is a License Agreement between Sharath Krishna Chandra ("User") and Copyright Clearance Center, Inc. ("CCC") on behalf of the Rightsholder identified in the order details below. The license consists of the order details, the Marketplace Permissions General Terms and Conditions below, and any Rightsholder Terms and Conditions which are included below.

All payments must be made in full to CCC in accordance with the Marketplace Permissions General Terms and Conditions below.

Order Date	30-Nov-2023	Type of Use	Republish in a
Order License ID	1422094-1		thesis/dissertation
ISBN-13	9780081005507	Publisher Portion	Elsevier Science
			Chart/graph/table/figure

## LICENSED CONTENT

Publication Title	Structure and Properties of High-Performance Fibers	Rightsholder	Elsevier Science & Technology Journals
Article Title	High-performance PAN-based carbon fibers and their performance requirements	Publication Type	Book
		Start Page	7
		End Page	30
		Volume	53
Date	09/27/2016		
Language	English		
Country	United Kingdom of Great Britain and Northern Ireland		

## REQUEST DETAILS

Portion Type	Chart/graph/table/figure	Distribution	Canada
Number of Charts / Graphs / Tables / Figures Requested	1	Translation	Original language of publication
Format (select all that apply)	Electronic	Copies for the Disabled?	No
Who Will Republish the Content?	Academic institution	Minor Editing Privileges?	Yes
Duration of Use	Life of current edition	Incidental Promotional Use?	No
Lifetime Unit Quantity	Up to 499	Currency	CAD
Rights Requested	Main product		

## NEW WORK DETAILS

Title	Microwave-Plasma based Thermal Treatment of Asphaltene-derived Carbon Fibres	Institution Name	University of Calgary
		Expected Presentation Date	2023-12-04
Instructor Name	Sharath Krishna Chandra		

## ADDITIONAL DETAILS

Order Reference Number	N/A	The Requesting Person / Organization to Appear on the License	Sharath Krishna Chandra
------------------------	-----	---	-------------------------

Reprint permission for 2.10 – [Wyatt et al. 1994]



This is a License Agreement between Sharath Krishna Chandra ("User") and Copyright Clearance Center, Inc. ("CCC") on behalf of the Rightsholder identified in the order details below. The license consists of the order details, the Marketplace Permissions General Terms and Conditions below, and any Rightsholder Terms and Conditions which are included below.

All payments must be made in full to CCC in accordance with the Marketplace Permissions General Terms and Conditions below.

Order Date	30-Nov-2023	Type of Use	Republish in a thesis/dissertation
Order License ID	1422147-1	Publisher	Elsevier Science
ISBN-13	9780750611541	Portion	Image/photo/illustration

## LICENSED CONTENT

Publication Title	Manufacturing Engineer's Reference Book	Country	United Kingdom of Great Britain and Northern Ireland
Article Title	1 - Materials Properties and Selection	Rightsholder	Elsevier Science & Technology Journals
Author/Editor	KOSHAL, D.	Publication Type	Book
Date	10/18/1993	Start Page	1/1
Language	English	End Page	1/119

## REQUEST DETAILS

Portion Type	Image/photo/illustration	Distribution	Canada
Number of Images / Photos / Illustrations	1	Translation	Original language of publication
Format (select all that apply)	Electronic	Copies for the Disabled?	No
Who Will Republish the Content?	Academic institution	Minor Editing Privileges?	Yes
Duration of Use	Life of current edition	Incidental Promotional Use?	No
Lifetime Unit Quantity	Up to 499	Currency	CAD
Rights Requested	Main product		

## NEW WORK DETAILS

Title	Microwave-Plasma based Thermal Treatment of Asphaltene-derived Carbon Fibres	Institution Name	University of Calgary
Instructor Name	Dr. Simon Park	Expected Presentation Date	2023-12-04

## ADDITIONAL DETAILS

Order Reference Number	N/A	The Requesting Person / Organization to Appear on the License	Sharath Krishna Chandra
------------------------	-----	---	-------------------------

Reprint permission for Figure 2.13 – [Liu et al. 2008]



This is a License Agreement between Sharath Krishna Chandra ("User") and Copyright Clearance Center, Inc. ("CCC") on behalf of the Rightsholder identified in the order details below. The license consists of the order details, the Marketplace Permissions General Terms and Conditions below, and any Rightsholder Terms and Conditions which are included below.

All payments must be made in full to CCC in accordance with the Marketplace Permissions General Terms and Conditions below.

Order Date	30-Nov-2023	Type of Use	Republish in a
Order License ID	1422148-1	Publisher	thesis/dissertation
ISSN	1573-4803	Portion	KLUWER ACADEMIC PUBLISHERS (BOSTON)
			Chart/graph/table/figure

#### LICENSED CONTENT

Publication Title	Journal of materials science	Publication Type	e-Journal
Article Title	Effect of microstructure on the mechanical properties of PAN-based carbon fibers during high-temperature graphitization	Start Page	4316
		End Page	4322
		Issue	12
		Volume	43
		URL	<a href="http://www.springerlink.com/content/100181/">http://www.springerlink.com/content/100181/</a>
Date	01/01/1966		
Language	English		
Country	United States of America		
Rightsholder	Springer Nature BV		

#### REQUEST DETAILS

Portion Type	Chart/graph/table/figure	Distribution	Canada
Number of Charts / Graphs / Tables / Figures Requested	1	Translation	Original language of publication
Format (select all that apply)	Electronic	Copies for the Disabled?	No
Who Will Republish the Content?	Academic institution	Minor Editing Privileges?	Yes
Duration of Use	Life of current edition	Incidental Promotional Use?	No
Lifetime Unit Quantity	Up to 499	Currency	CAD
Rights Requested	Main product		

#### NEW WORK DETAILS

Title	Microwave-Plasma based Thermal Treatment of Asphaltene-derived Carbon Fibres	Institution Name	University of Calgary
		Expected Presentation Date	2023-12-04
Instructor Name	Dr. Simon Park		

The Requesting Person / Organization to Appear on the License

Sharath Krishna Chandra

#### REQUESTED CONTENT DETAILS

Title, Description or Numeric Reference of the Portion(s)	Raman spectra taken from the surface of PAN-based carbon fibers as a function of heat-treatment temperature from 1,800 to 2,800 C	Title of the Article / Chapter the Portion Is From	Effect of microstructure on the mechanical properties of PAN-based carbon fibers during high-temperature graphitization
Editor of Portion(s)	Fujie, Liu; Haojing, Wang; Linbing, Xue; Lidong, Fan; Zhenping, Zhu	Author of Portion(s)	Fujie, Liu; Haojing, Wang; Linbing, Xue; Lidong, Fan; Zhenping, Zhu
Volume / Edition	43	Publication Date of Portion	2008-05-31
Page or Page Range of Portion	4316-4322		

Reprint permission for Figure 2.14 – [Kappe et al. 2013]



This is a License Agreement between Sharath Krishna Chandra ("User") and Copyright Clearance Center, Inc. ("CCC") on behalf of the Rightsholder identified in the order details below. The license consists of the order details, the Marketplace Permissions General Terms and Conditions below, and any Rightsholder Terms and Conditions which are included below.

All payments must be made in full to CCC in accordance with the Marketplace Permissions General Terms and Conditions below.

Order Date	30-Nov-2023	Type of Use	Republish in a
Order License ID	1422149-1		thesis/dissertation
ISBN-13	9783527647842	Publisher Portion	Wiley
			Chart/graph/table/figure

#### LICENSED CONTENT

Publication Title	Microwaves in Organic and Medicinal Chemistry	Country	Germany
Author/Editor	Kappe, C. Oliver, Stadler, Alexander, Dallinger, Doris	Rightsholder	John Wiley & Sons - Books
Date	03/19/2013	Publication Type	e-Book
Language	English		

#### REQUEST DETAILS

Portion Type	Chart/graph/table/figure	Distribution	Canada
Number of Charts / Graphs / Tables / Figures Requested	1	Translation	Original language of publication
Format (select all that apply)	Electronic	Copies for the Disabled?	No
Who Will Republish the Content?	Academic institution	Minor Editing Privileges?	Yes
Duration of Use	Life of current edition	Incidental Promotional Use?	No
Lifetime Unit Quantity	Up to 499	Currency	CAD
Rights Requested	Main product		

#### NEW WORK DETAILS

Title	Microwave-Plasma based Thermal Treatment of Asphaltene-derived Carbon Fibres	Institution Name	University of Calgary
		Expected Presentation Date	2023-12-04
Instructor Name	Dr. Simon Park		

#### ADDITIONAL DETAILS

The Requesting Person / Organization to Appear on the License	Sharath Krishna Chandra
---	-------------------------

Title, Description or Numeric Reference of the Portion(s)	Electric and magnetic field components in microwaves.	Title of the Article / Chapter the Portion Is From	N/A
Editor of Portion(s)	N/A	Author of Portion(s)	Kappe, C. Oliver; Stadler, Alexander; Dallinger, Doris
Volume / Edition	2; 2nd, Completely Revised and Enlarged Edition	Publication Date of Portion	2013-03-18
Page or Page Range of Portion	11		



Reprint permission for Figure 2.17 – [Kim et al. 2015]



Marketplace

This is a License Agreement between Sharath Krishna Chandra ("User") and Copyright Clearance Center, Inc. ("CCC") on behalf of the Rightsholder identified in the order details below. The license consists of the order details, the Marketplace Permissions General Terms and Conditions below, and any Rightsholder Terms and Conditions which are included below.

All payments must be made in full to CCC in accordance with the Marketplace Permissions General Terms and Conditions below.

Order Date	30-Nov-2023	Type of Use	Republish in a thesis/dissertation
Order License ID	1422154-1	Publisher Portion	ELSEVIER LTD.
ISSN	0032-3861		Chart/graph/table/figure

#### LICENSED CONTENT

Publication Title	Polymer	Rightsholder	Elsevier Science & Technology Journals
Article Title	Microwave plasma carbonization for the fabrication of polyacrylonitrile-based carbon fiber	Publication Type	Journal
		Start Page	590
		End Page	595
Date	01/01/1992	Volume	56
Language	English		
Country	United Kingdom of Great Britain and Northern Ireland		

#### REQUEST DETAILS

Portion Type	Chart/graph/table/figure	Distribution	Canada
Number of Charts / Graphs / Tables / Figures Requested	1	Translation	Original language of publication
Format (select all that apply)	Electronic	Copies for the Disabled?	No
Who Will Republish the Content?	Academic institution	Minor Editing Privileges?	No
Duration of Use	Life of current edition	Incidental Promotional Use?	No
Lifetime Unit Quantity	Up to 499	Currency	CAD
Rights Requested	Main product		

#### NEW WORK DETAILS

Title	Microwave-Plasma based Thermal Treatment of Asphaltene-derived Carbon Fibres	Institution Name	University of Calgary
		Expected Presentation Date	2023-12-04
Instructor Name	Dr. Simon Park		

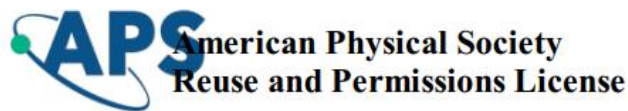
#### ADDITIONAL DETAILS

Order Reference Number	N/A	The Requesting Person / Organization to Appear on the License	Sharath Krishna Chandra
------------------------	-----	---	-------------------------

#### REQUESTED CONTENT DETAILS

Title, Description or Numeric Reference of the Portion(s)	. A schematic of the microwave plasma system for the carbonization process.	Title of the Article / Chapter the Portion Is From	Microwave plasma carbonization for the fabrication of polyacrylonitrile-based carbon fiber
Editor of Portion(s)	Kim, So-Young; Kim, Seong Yun; Lee, Sungho; Jo, Sungmu; Im, Yeon-Ho; Lee, Hun-Su	Author of Portion(s)	Kim, So-Young; Kim, Seong Yun; Lee, Sungho; Jo, Sungmu; Im, Yeon-Ho; Lee, Hun-Su
Volume / Edition	56	Issue, if Republishing an Article From a Serial	N/A
Page or Page Range of Portion	590-595	Publication Date of Portion	2015-01-14

Reprint permission for Figure 2.18 – [Baeva et al. 2012]



30-Nov-2023

This license agreement between the American Physical Society ("APS") and Sharath Krishna Chandra ("You") consists of your license details and the terms and conditions provided by the American Physical Society and SciPris.

#### Licensed Content Information

<b>License Number:</b>	RNP/23/NOV/072535
<b>License date:</b>	30-Nov-2023
<b>DOI:</b>	10.1103/PhysRevE.85.056404
<b>Title:</b>	Modeling of microwave-induced plasma in argon at atmospheric pressure
<b>Author:</b>	M. Baeva et al.
<b>Publication:</b>	Physical Review E
<b>Publisher:</b>	American Physical Society
<b>Cost:</b>	USD \$ 0.00

#### Request Details

<b>Does your reuse require significant modifications:</b>	No
<b>Specify intended distribution locations:</b>	United States, Canada
<b>Reuse Category:</b>	Reuse in a thesis/dissertation
<b>Requestor Type:</b>	Student
<b>Items for Reuse:</b>	Figures/Tables
<b>Number of Figure/Tables:</b>	1
<b>Figure/Tables Details:</b>	Axial flow velocity $V_z$ (dashed) and gas temperature $T$ (solid) along the $z$ axis, and (b) 2D plot of the gas temperature distribution at a gas flow rate of 200 ml/min and absorbed microwave power
<b>Format for Reuse:</b>	Electronic

#### Information about New Publication:

<b>University/Publisher:</b>	University of Calgary
<b>Title of dissertation/thesis:</b>	Microwave-Plasma based Thermal Treatment of Asphaltene-derived Carbon Fibres
<b>Author(s):</b>	Sharath Krishna Chandra
<b>Expected completion date:</b>	Dec. 2023

#### License Requestor Information

<b>Name:</b>	Sharath Krishna Chandra
<b>Affiliation:</b>	Individual
<b>Email Id:</b>	sharath.chandra@ucalgary.ca
<b>Country:</b>	Canada



## Reprint permissions for Figure 5.9 & 5.10 – [Liu et al. 2018]



This is a License Agreement between Sharath Krishna Chandra ("User") and Copyright Clearance Center, Inc. ("CCC") on behalf of the Rightsholder identified in the order details below. The license consists of the order details, the Marketplace Permissions General Terms and Conditions below, and any Rightsholder Terms and Conditions which are included below.

All payments must be made in full to CCC in accordance with the Marketplace Permissions General Terms and Conditions below.

Order Date	30-Nov-2023	Type of Use	Republish in a
Order License ID	1422160-1	Publisher	thesis/dissertation
ISSN	0141-3910	Portion	ELSEVIER LTD. Chart/graph/table/figure

### LICENSED CONTENT

Publication Title	Polymer degradation and stability	Rightsholder	Elsevier Science & Technology Journals
Article Title	Study on the oxidative stabilization of polyacrylonitrile fibers by microwave heating	Publication Type	Journal
Date	01/01/1979	Start Page	86
Language	English	End Page	91
Country	United Kingdom of Great Britain and Northern Ireland	Volume	150

### REQUEST DETAILS

Portion Type	Chart/graph/table/figure	Distribution	Canada
Number of Charts / Graphs / Tables / Figures Requested	2	Translation	Original language of publication
Format (select all that apply)	Electronic	Copies for the Disabled?	No
Who Will Republish the Content?	Academic institution	Minor Editing Privileges?	Yes
Duration of Use	Life of current edition	Incidental Promotional Use?	No
Lifetime Unit Quantity	Up to 499	Currency	CAD
Rights Requested	Main product		

### NEW WORK DETAILS

Title	Microwave-Plasma based Thermal Treatment of Asphaltene-derived Carbon Fibres	Institution Name	University of Calgary
Instructor Name	Dr. Simon Park	Expected Presentation Date	2023-12-04

### ADDITIONAL DETAILS

Order Reference Number	N/A	The Requesting Person / Organization to Appear on the License	Sharath Krishna Chandra
------------------------	-----	---	-------------------------

### REQUESTED CONTENT DETAILS

Title, Description or Numeric Reference of the Portion(s)	Elemental mapping of the fiber cross section of the MSFs and CSFs. Schematic diagram of polyacrylonitrile fibers stabilized by conventional heating and microwave heating.	Title of the Article / Chapter the Portion Is From	Study on the oxidative stabilization of polyacrylonitrile fibers by microwave heating
Editor of Portion(s)	Liu, Jianhua; Peng, Jinhui; Shen, Zhigang; Xiao, Shijie; Xu, Lei; Zhang, Libo	Author of Portion(s)	Liu, Jianhua; Peng, Jinhui; Shen, Zhigang; Xiao, Shijie; Xu, Lei; Zhang, Libo
Volume / Edition	150	Issue, if Republishing an Article From a Serial	N/A
Page or Page Range of Portion	86-91	Publication Date of Portion	2018-03-31

## APPENDIX B: CHARACTERIZATION DATA

### Element Analysis (CHNS)

Results were obtained using the Elementer Unicube analyzer for each sample, with an approximate weight ranging from 2-3 grams.

#### Furnace Stabilized:

C (wt.%)	H (wt.%)	N (wt.%)	S (wt.%)
76.91	3.87	1.02	6.78
76.65	4.00	1.00	6.78
77.39	4.34	0.98	6.98
76.27	3.91	1.25	7.18

#### Furnace Carbonized:

C (wt.%)	H (wt.%)	N (wt.%)	S (wt.%)
86.97	0.54	0.61	5.48
87.31	0.49	0.63	5.34
87.46	0.51	0.59	5.59
87.38	0.49	0.60	5.38

#### Microwave Plasma (MWP) – 5min:

C (wt.%)	H (wt.%)	N (wt.%)	S (wt.%)
82.73	1.76	0.73	6.15

82.59	1.84	0.76	6.39
82.47	1.79	0.71	6.41
82.64	1.75	0.74	6.40

Microwave Plasma (MWP) – 7 min:

C (wt.%)	H (wt.%)	N (wt.%)	S (wt.%)
83.44	1.55	0.77	6.57
83.61	1.57	0.78	6.61
83.59	1.55	0.76	6.54
83.65	1.57	0.78	6.59

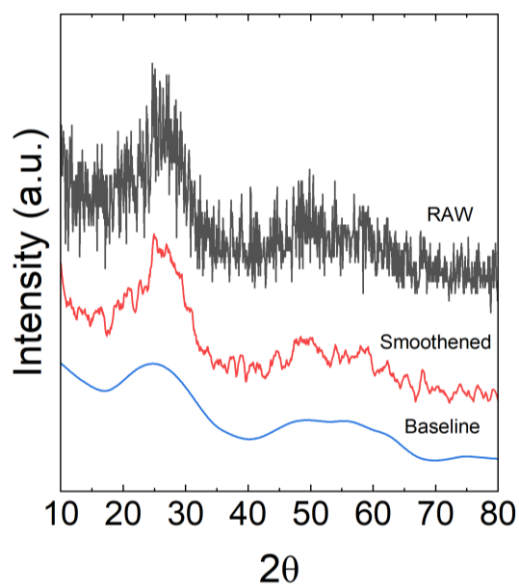
Microwave Plasma (MWP) – 9 min:

C (wt.%)	H (wt.%)	N (wt.%)	S (wt.%)
87.54	0.40	0.64	5.49
87.49	0.45	0.67	5.60
86.97	0.42	0.65	5.54
87.32	0.40	0.68	5.37

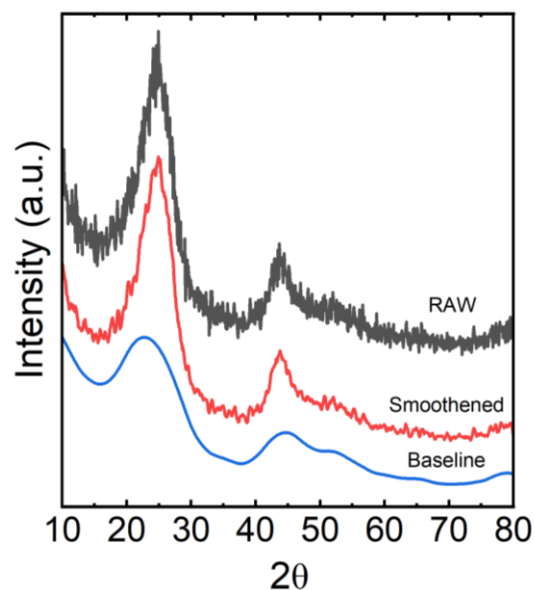
## X-ray Diffraction

The XRD analysis was performed with the Bruker D8 Advance, and the raw data were processed using Origin software to establish a baseline and smooth the datasets.

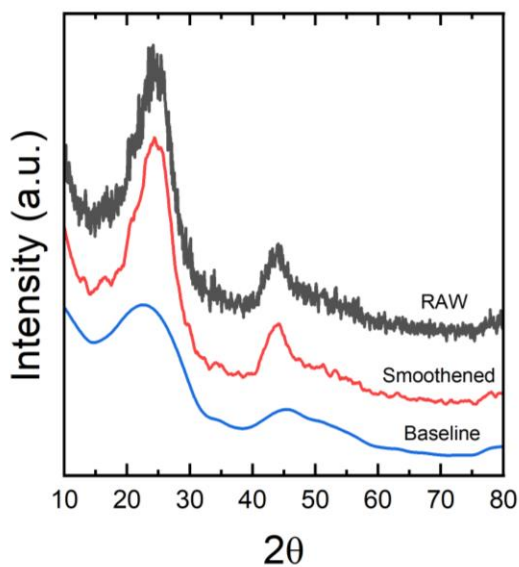
Furnace Stabilized:



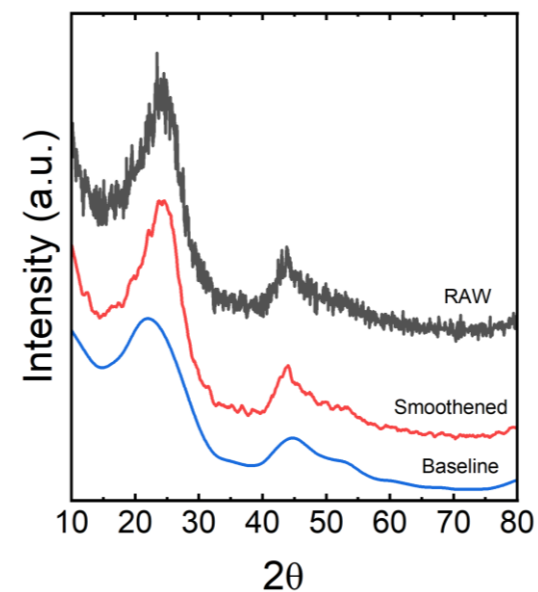
Furnace Carbonized:



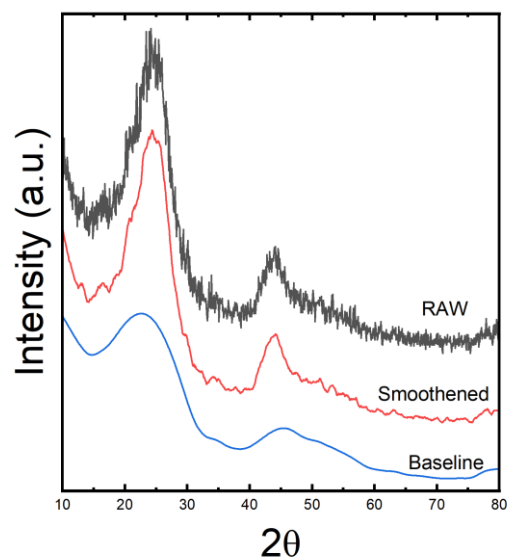
Microwave Plasma (MWP) – 5 min:



Microwave Plasma (MWP) – 7 min:



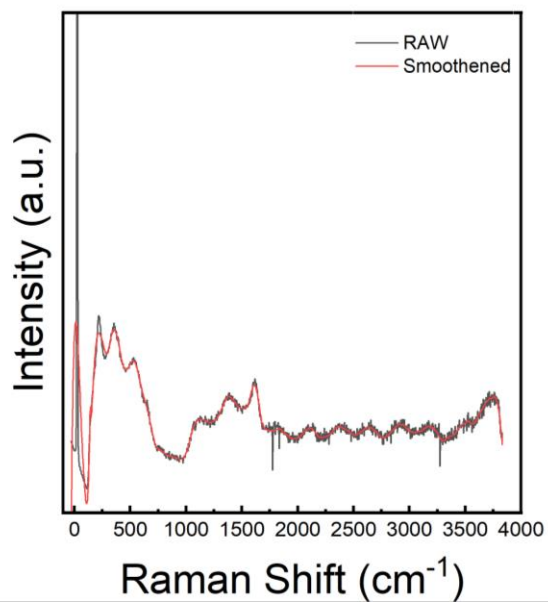
Microwave Plasma (MWP) – 9 min:



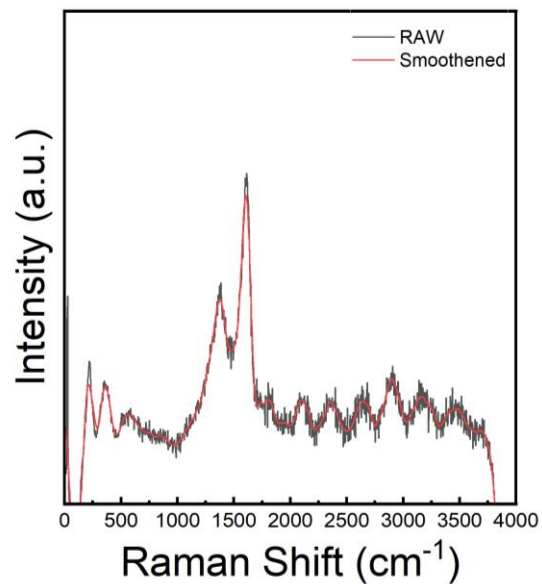
### Raman Spectroscopy

Raman spectroscopy was executed employing the Teledyne Princeton Instruments Isoplane 81 Raman Spectrometer, utilizing a PSU-H-LED 532 nm laser source, and the acquired data were processed using Origin software.

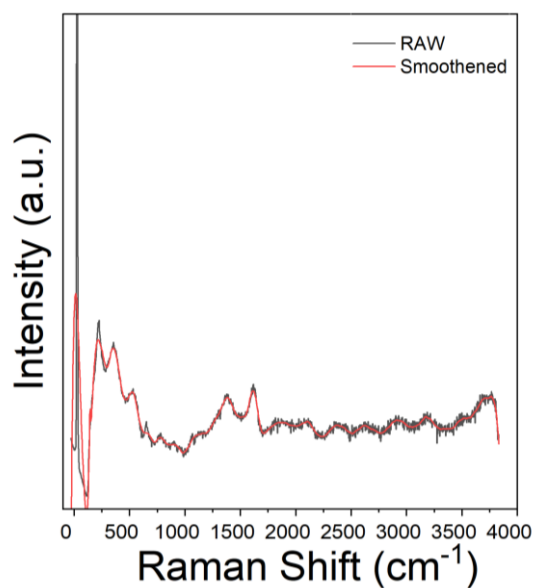
Furnace Stabilized:



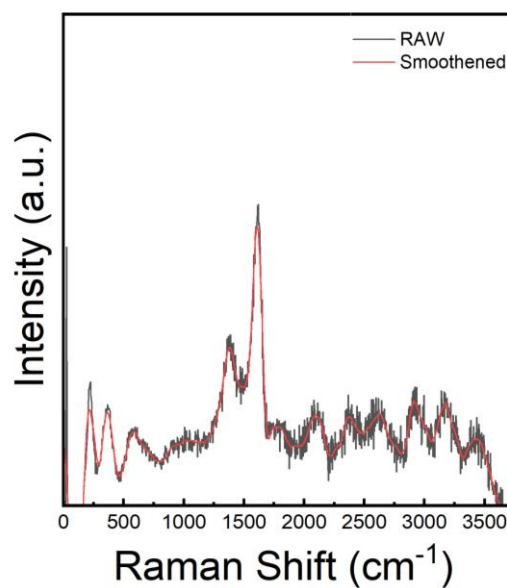
Furnace Carbonized:



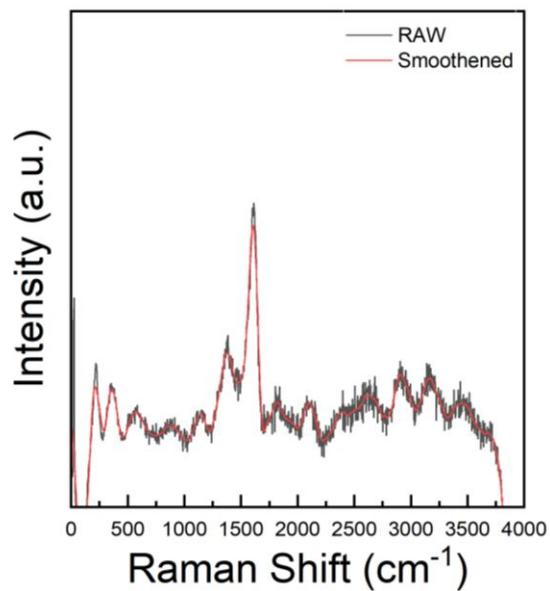
Microwave Plasma (MWP) – 5 min:



Microwave Plasma (MWP) – 7 min:



Microwave Plasma (MWP) – 9 min:

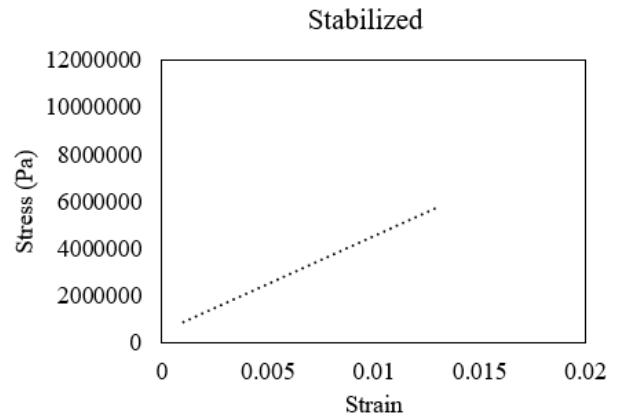
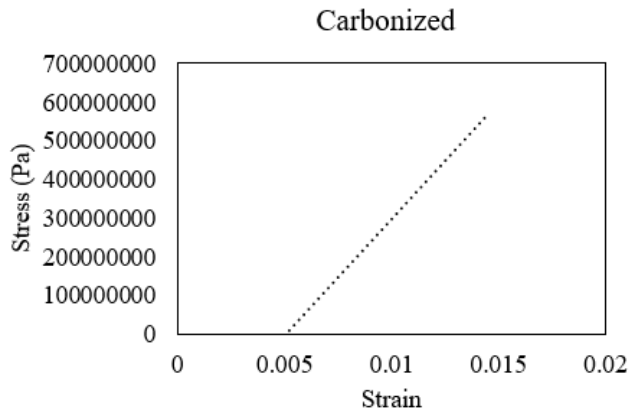


### **Mechanical Properties:**

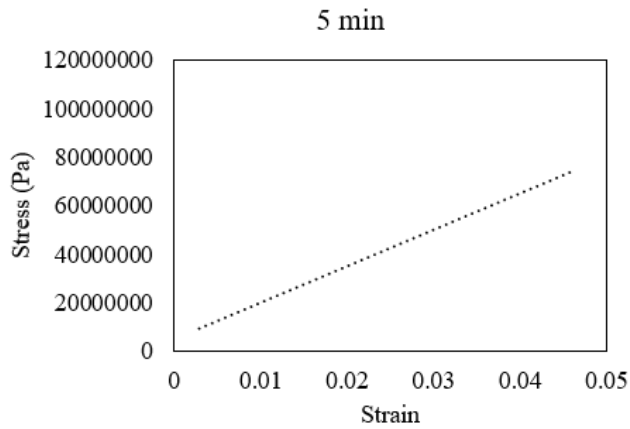
The tensile test was conducted using a Mark – 10 ESM Motorized Force Tester equipped with an M5-05 force guage in accordance with ASTM D3822/D3822M-14 standards. Normalized stress-strain graphs from different samples are provided below.

## Furnace Stabilized

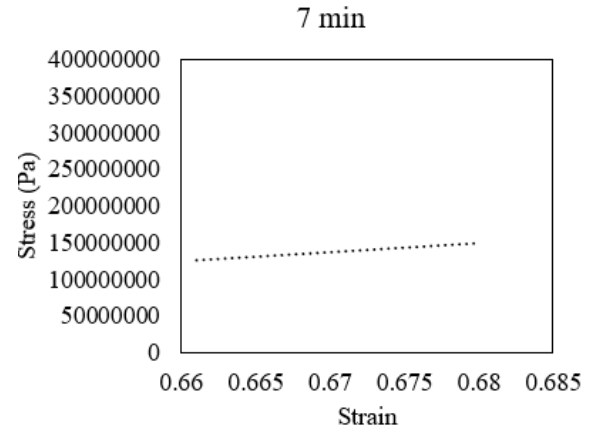
## Furnace Carbonized



## Microwave Plasma (MWP) – 5 min



## Microwave Plasma (MWP) – 7 min



## Microwave Plasma (MWP) – 9 min

